1986

Thermodynamics for Zeolite Heat Pump and Refrigeration Systems

J. A. Roux

J. A. Lou

Open-File Report 86-1S

Thermodynamics for Zeolite Heat Pump and Refrigeration Systems

J. A. Roux and J. H. Lou

August, 1986

The Mississippi Mineral Resources Institute
University, Mississippi 38677

THERMODYNAMICS FOR ZEOLITE HEAT PUMP AND REFRIGERATION SYSTEMS

BY

J. A. Roux and J. H. Lou

A Report Submitted to
Mississippi Mineral Resources Institute
in Partial Fulfillment of Grant No. MMRI 86-1 S

The University of Mississippi
August, 1986

ABSTRACT

This work is associated with the use of solar energy to operate an absorption heat pump and refrigeration system. A zeolite-water pair is proposed as the working matter. The slope of the constant water mass lines on the graph of log P_v versus $1/T_Z$ for zeolite determines the heat of absorption value for the zeolite-water system. A thermodynamic analysis was performed for both the refrigeration and heat pump systems. Computer simulation for the effects of various design parameters and different types of solar collectors was performed to determine the optimum operating conditions for the system. Comparisons of system performance for different zeolites-water and LiBr-water are presented. Also, the use of waste heat as a driving energy source is discussed. The intermittent cycle for a zeolite-water system shows good potential for a residential heating and cooling system.

TABLE OF CONTENTS

List of Table

Table page

List of Figures

NOMENCLATURE

a = End point of absorption process in absorption cycle

b = Starting point of desorption process in absorption cycle

c = End point of desorption process in absorption cycle

C = Constant

C_{α} = Constant for solar collector efficiency, Eq.(31)

Cp_z = Specific heat of zeolite

Cptb = Specific heat of copper

Cptk = Specific heat of steel

Cw = Constant

Cz = Constant for zeolite-water property, Eq.(l6)

COPhp = Coefficient of performance for heat pump

COP_r = Coefficient of performance for refrigeration

CPhpa = Heat pump system performance based on absorption cycle

CP_{hpc} = Heat pump system performance based on Carnot cycle limited by the ambient and heat source temperatures

CP_{hpca} = Heat pump system performance based on Carnot cycle according t absorption cycle temperature

CP_{hpi} = Instantaneous heat pump system performance

CP_{hpm1} = Mean heat pump system performance without considering the heat capacity losses

CP_{hpm2} = Mean heat pump system performance accounting for the heat capacity losses

CP_{ra} = Refrigeration system performance based on refrigeration cycle

CP_{pc} = Refrigeration system performance based on Carnot cycle limited the ambient and heat source temperatures

CP_{rca} = Refrigeration system perfer mance based on Carnot cycle according to absorption cycle temperature

CPri = Instantaneous refrigeration system performance

CP ,, = Mean refrigeration system performance without considering the heat capacity losses

CP ^2 = Mean refrigeration system performance accounting for the heat capacity losses

d = Starting point of absorption process in absorption cycle

E = Ln P / Log P

h = Enthalpy of water vapor (kj/kg)

ΔH = Heat of absorption (kj/kg)

Kt = Constant

L = Latent heat of vaporization (kj/kg)

m_{co} = Slope of solar collector efficiency line, Eq.(31)

m_z = Slope of constant mass line on log P_v versus $1/T_Z$ plot(1/K)

M = Mass (kg)

P = Pressure (bar)

Q = Heat (kj)

R = Water vapor gas constant (kj/kg, K)

S = Entropy (kj/kg)

T = Temperature

T_a = Absorption temperature

Tg = Desorption temperature

T_{Za} = Temperature at end of absorption process (K)

T_zb = Temperature at beginning of desorption (K)

T_{zc} = Temperature at end of desorption process (K)

T_{2d} = Temperature at beginning of absorption (K)

U = Net work input to heat pump cycle (kJ)

V = Specific volume (m^3/kg)

X(= Weight ratio of absorbed water to dry solid zeolite

Subscript s

a = absorption

ab = absorber

c = condenser, Carnot cycle

ca = absorption temperatures based on Carnot cycle

co = collector

e = evaporator

f = liquid state, final state

g = generator, gas

hp = heat pump

i = Instantaneous, initial state

Ĺ = counter index

p = power cycle

r = refrigeration

tb = tube

tk = tank

v = vapor

w = water

z = zeolite

Greek Symboles

Л = efficiency

^{00} = ambient

Φ = dimensionless absorbent slope

χ = constants

CHAPTER I

INTRODUCTION

Oil, gas, and coal have been used to provide most of our energy. Since the fuel shortage, the so-called energy crisis in the early 1 970's, people have become aware that the finite amount of fossil fuel is no longer an inexhaustible energy source. Presently, energy is obtained from four primary sources: petroleum, liquid natural gas, coal and nuclear fuel. Current energy probi ans occur due to the supply and demand of these sources. Moreover, environmental consequences associated with energy production are also of great concern. Also, the pollution resulting fram these four sources becomes an additional problem requiring solution. So, an inexhaustible, longer-term, pollution-less energy source is desired. Solar energy is a promising energy source that could be used to economically supply some of man's increasing demand. In addition, there will be no significantly harmful environmental effects from its use.

The Solar Energy Panel of NSF/NASA[1] has recommended investigations of the following concepts for solar energy conversion:

1) Thermal conversion
2) Photovoltaic conversion

3) Biological conversion

4) Wind power

5) Solar energy conversion by ocean

For operation of a thermal heat pump and refrigeration system, the thermal conversion method utilizes heat radiated directly fram the sun ana thus has less energy loss than otner solar conversion methods. Owing to the low operating temperatures and pressures of the thermal conversion process, this approach requires simple materials and hardwares. Therefore, the equipment cost is modest for the tnermal conversion approach.

Energy for space heating, air conditioning, and water heating accounts for 25 percent of the total energy consumption in tne U.S., according to the Standford Research Institute^]. With tne application of th enmody namie principles, solar energy can be used to heat or cool buildings. Due to the low operating temperatures and equipment cost, solar energy is a premising alternative to the conventional fuel-supplied neat pump system. However, solar energy is available only during day light hours and periods when the sun is not significantly obscured by clouds. It must be converted to heat and stored before it can be used in a practical heating or cooling system. A means to provide heat continuously and store heat on a intermittent basis is necessary.

Heat pumping and refrigeration can be accomplished by several thermal processes. Presently, the most common type of heat pumping and

refrigeration is based on the vapor-compression cycle. Here, the refrigerant is a condensable vapor, and the heat exchanger conditions are chosen so that liquid refrigerant is boiled in a lew-temper ature evaporator, gaining latent heat of vaporization. The vapor is condensed in the condenser, thus releasing the heat again, together with any heat that may have been added during the heat pumping and refrigeration process. A power cycle is required to generate a net mechanical work to raise the pressure from evaporation to condensation in the vapor-compression cycle.

Solar powered systems can be divided into the mechanical powered and non-me ch ani cal powered types. In mechanical powered systems, like the solar Rankine cycle[3] and Stirling system, the work input to the heat pump and refrigeration cycle is done through a compressor. Due to friction and pressure losses in mechanical movement, high pressures and temperatures are always required in this system. On the other hand, the non-mechani cal solar powered systems may suffer from fluid friction and irreversible heat transfer losses[4].

Absorption refrigeration systems operate on cycles in which the primary fluid, a gaseous refrigerant, has been vaporized in an evaporator, and is absorbed by a second absorbent. This cycle can be viewed thermodynamically as a combination of a power cycle and a vapor-com pression cycle, which are two components of the mechanical heat pump and refrigeration systems. With lew-velocity and small irreversible heat

transfer losses under low temperature conditions, the no n-mech ani cal absorption solar system has a power cycle efficiency close to that of the Carnot power cycle.

Much research interest have been attracted by the lew temperature and low pressure absorption solar system[5,6 ,7 ,8 ,9]. These works can be classified into two groups: continuous[5,6 ,7] and intermittent[8,91 cycles. The continuous cycle has a better power efficiency than the intermittent cycle because the continuously circulating working fluid receives and rejects heat in a nearly reversible process. Nevertheless, S. C. Chang[10] has pointed out that heat can not be easily rejected by an air cooler for the continuous cycle. Compared to the continuous cycle, an intermittent cycle has a lower power efficiency because of the heat capacity losses of the alternative cooling and reheating processes. With a wider heat rejection temperature range, which is broadened by lower night time temperatures, the intermittent absorption cycle is favorable for solar heating and cooling systems.

Methods to store thermal energy can be by sensible heat storage (storage in a material by virture of a temperature rise) and latent heat storage . Rock beds and water have been the two most widely used means of sensible heat storage. The former is used with air-cooled solar conversion devices. However, when air is used as the cooling fluid, the losses of available energy will raise the collector temperature, and thus lower the collector efficiency. A large temperature difference is

required in this kind of beat storage method. The latent heat storage method is associated with the phase change of a material. Such materials are capable of larger energy-storage per unit volume than are sensible heat storage materials. Presently, phase change materials have shown unacceptable reliability in repeated freeze-thaw cycles [21].

The absorber used in an intermittent absorption cycle can be either solid or liquid. Presently, two types of sorbent-sorbate combinations are widely used: LiBr-water and water-ammonia. Of these two combinations, LiBr-water is simpler to handle since a rectifying separator is not necessary, while in the water-ammonia system a rectifying separator is required to assure that there is no water vapor mixed with ammonia in the evaporator. In addition, the water-ammonia system requires higher generator temperatures (120 to 150 C) than a flat-plate solar collector can usually provide without special techniques. The required generator temperature range for a LiBr-water system is about 87-93 C, which is achieveable with a flat-plate collector. Moreover, the LiBr-water system has a larger CP than the water-ammonia system. However, LiBr-water systems may stop functioning due to the crystallization problem which occurs when operating outside of the above mentioned temperature range. The small operating temperature range limits the use of the LiBr-water system.

According to Shigheishi, Lanford, and Hollebone [11], zeolites show a favorable thermal capacity in comparison with the energy stored by

sensible heat storage materials and a reliable system performance compared to latent heat storage material. Figure 1 snows that the absorption isotherms for zeolite have a very weak pressure dependence. Due to this property, zeolites absorption has a high heat of absorption, ana hence a high absorption capacity. Zeolites are capable of absorbing large quantities of a variety of refrigerant gases, ranging from water vapor and ammonia to carbon oxide and freon. Since water has a higner latent heat of vaporation and condensation than other common refrigerants, the zeolite-water combination can provide the best performance and also requires the smallest quantities of zeolite. Some further advantages pointed by D. I. Tchernev [12] are low cost, non-toxic, ease of hanaling, and a convenient boiling point for absorption and desorption.

From an economics point of view, the cost of a solar energy system is determined mainly by the cost of the system components, such as the conaenser, heat exchanger, absorber, and refrigerant. In a zeolite-water solar intermittent system, a low-cost air cooler can be used for heat rejection and no rectifying separator is needed. Therefore, the zeolite-water intermittent system has potentially a low cost and good system performance.

Dubinin ana Astakhov[13] developed an approximate description for absorption equilibria of water vapor with zeolite over a wide temperature range by the theory for volume filling of micropores. Ronald and Langford[l4j have discussed the use of the heat of absorption for water

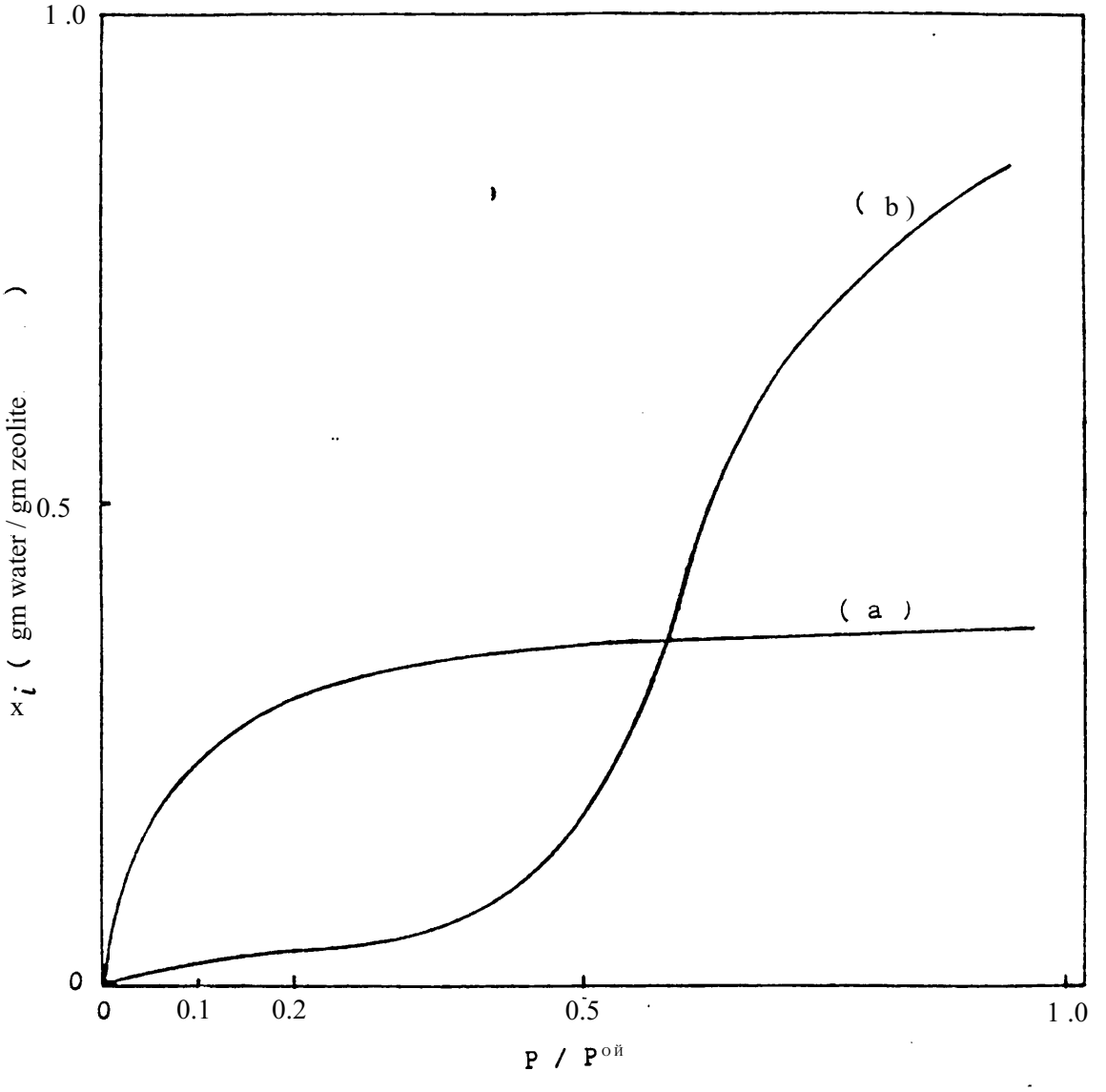

Fig. 1 Absorbed mass versus the relative pressure.

(a) microporous absorbent s(zeolite, some carbons)

lb) carbon, silica gel, etc...

« P is the pressure above absorber fluid.

P° is the saturated pressure corrsponding to temperature ;

of absorption.

with zeolite molecular sieves. Zeolite 13X was shown to have a higher energy density than other materials like: alumina gel, charcoal, and silica gel. Tchernev showed that zeolites have a very weak pressure dependence, which is important for solar heat pump and refrigeration systems. He also discussed several refrigerants which can be used in zeolite systems. Since water has the highest heat of vaporization, a zeolite-water system was adopted in his experiment. Also, different types of zeolite, 3A and 5A, were utilized to predict to performance of the zeolite heat pump and refrigeration systems in his work.

A mathematical model was first proposed by Meunier and Mischi er[15]. They treated the latent heat of condensation and evaporation as a constant and acquired a thermal CP greater than 0 .5 and a solar CP around 0.17. Chang[10] showed that the heat of absorption of zeolites was determined by the slope of the constant water mass lines on a graph of log P_v versus $1/T_Z$. He found four factors which can influence the performance of zeolite systems: (1) the slope of the constant mass lines on a log P_v versus $1/T_Z$ graph, (2) the evaporation and condensation temperatures, (3) the ambient temperature, and (4) the solar collector efficiency.

In addition to the heat of absorption, the initial desorption temperature is also important to overall system performance. Since the generator temperature influences the solar collector efficiency, a low desorption initiation temperature is preferable. A T_v versus T_2 graph

was developed for the desorption properties of different zeolites from the log P,, versus 1/T,, graphs (Fig. 2) . The desorption initiation temperature is directly related to the condensation temperature. The higher the condensation temperature, the higher the initiation desorption temperature. The high desorption initiation temperature in turn yields a lower solar collector efficiency and hence a lower system CP. The evaporation temperature does not affect the desorption initiation temperature, but does influence the overall system CP . The desorption initiation temperature will be different for various types of zeolites. Therefore, the heat of absorption will be different for different zeolites types (Fig. 3) .

Little research has been performed associated with a zeolite heat pumping concept. In the present work emphasis has been placed on thermodynamic analysis of a zeolite heat pump system. The overall heat pump CP also was found to be determined by the slope of the constant water mass lines on a log P_v versus $1/T_Z$ graph, the indoor and outdoor temperatures, ana solar collector type. A mathematical model was derived for computing heat pump performance with consideration of the sensible heat losses for the system equipment.

The above works are primarily concerned with the utilization of solar heat as the driving energy source for both the heat pump and refrigeration systems. The efficiency of the solar collector is important for determining the performance of the entire system. A high gener-

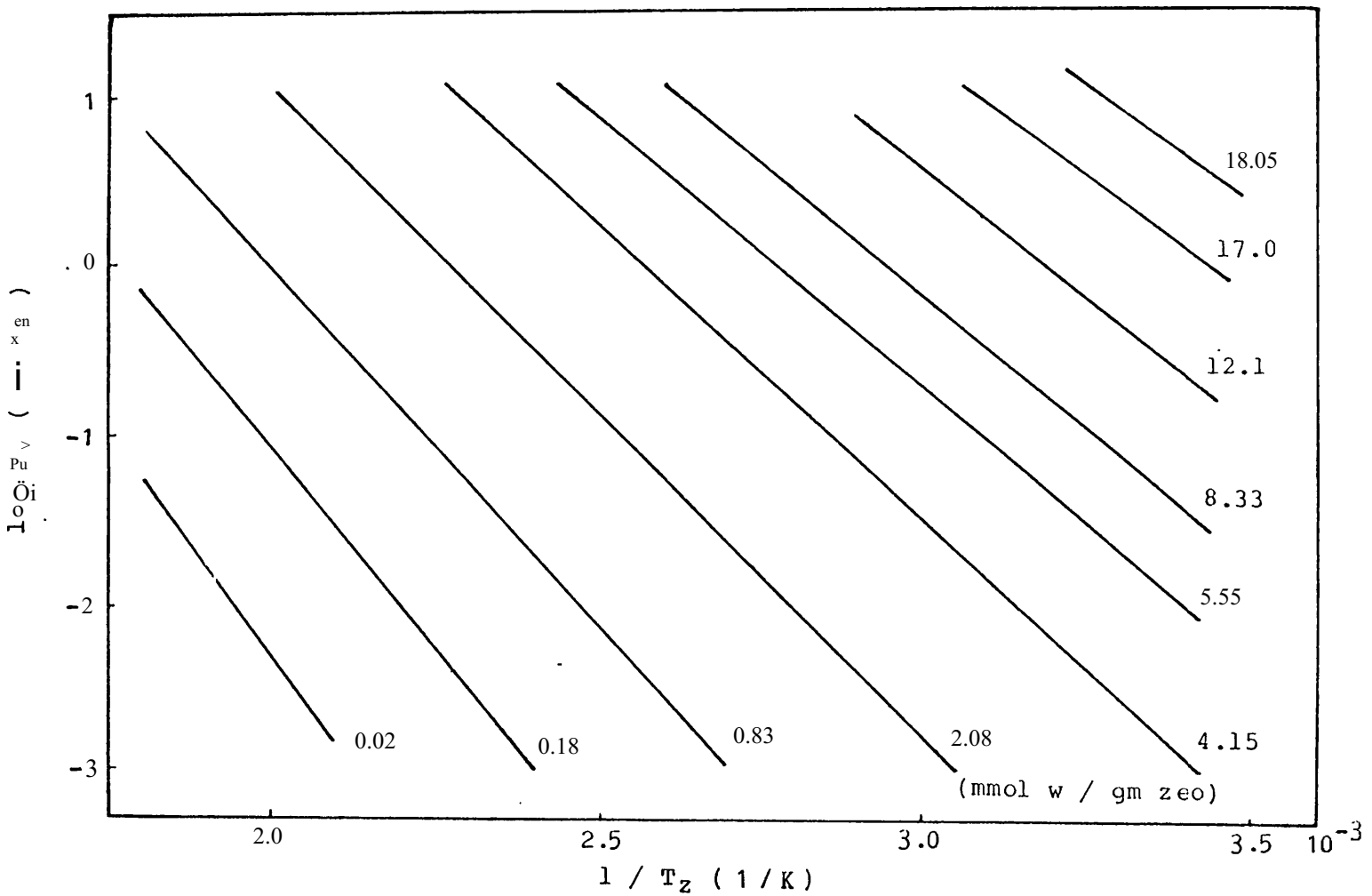

Fig. 2 The log P_v versus $1/T_Z$ plot for zeolite Z13-water pair from experimental data[8]

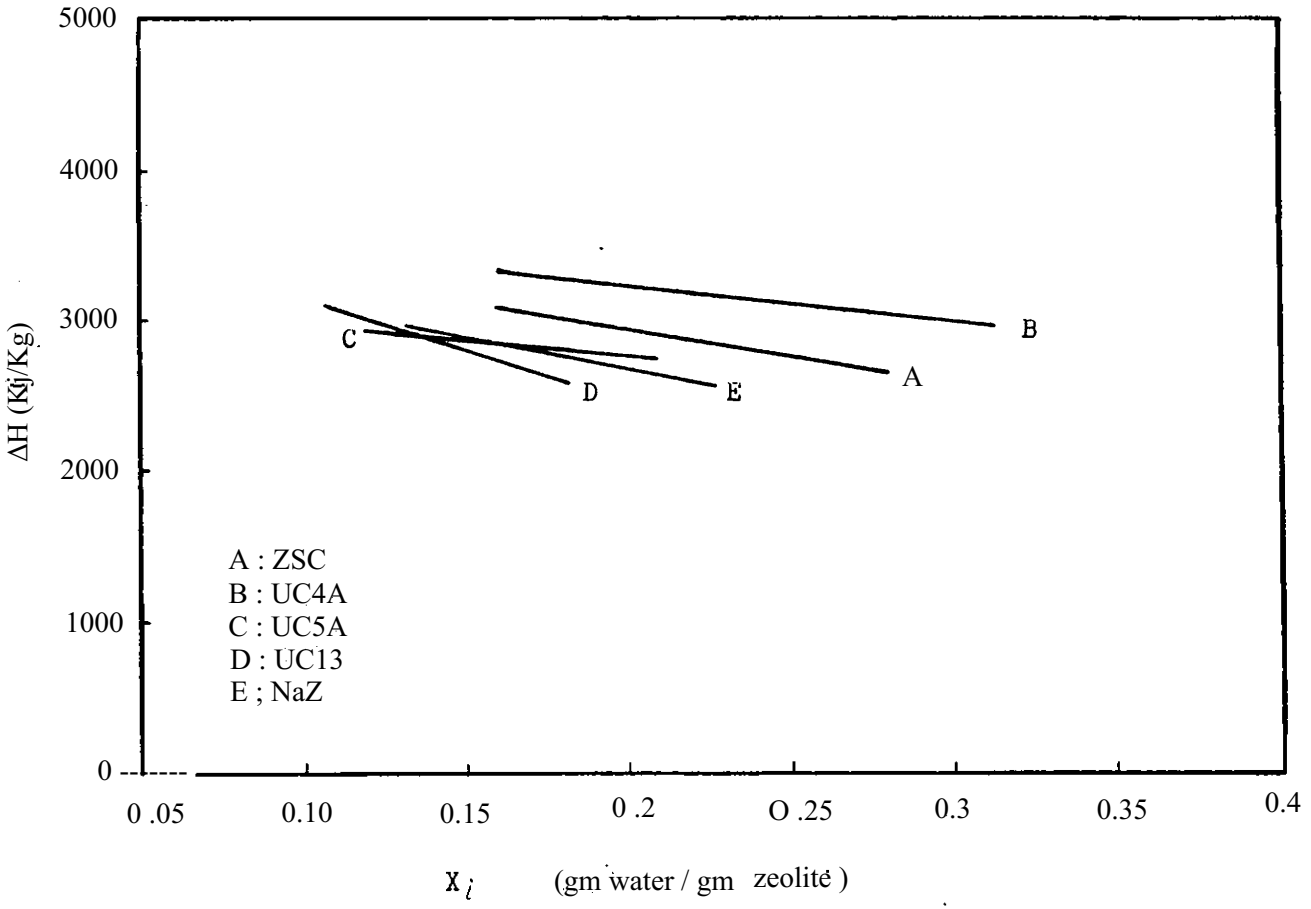

Fig. 3 The heat of absorption, ДН, as a function of the equilibrium amount of absorbed water for different zeolite types.

ator temperature implies a low solar collector efficiency. The use of industrial waste heat can be viewed as a solar collector with an efficiency of unity (typically 0.95-0.99)· Therefore the overall CP of a waste heat driven zeolite system is always higher than that of a solar heat driven zeolite system.

The following chapters will show the operation and the thermodynamic analysis of a solar zeolite system. A schematic flow chart for the solar heat pump will be presented in next chapter. Also, the operation principles will be briefly described. A mathematical model for both the adsorption and desorption processes of a zeolite system will be derived in Chapter 3· Chapter 4 will illustrate the influence of different operating parameters, including ambient temperature, types of solar collector, and varieties of zeolite.

CHAPTER II

STATEMENT OF PROBLEM

Zeolites are natural minerals resulting fron the reaction of salt-water with volcanic ash; also zeolites can be synthetically produced. The main constituents of zeolites are silica and alumina. Zeolites are characterized by an aluminosilicate tetrahedral framework, ion-exchangeable cation, and loosely held water molecules permitting reversible dehydration. The large cation and tunnel of the zeolite crystal structure permits the selective passage of organic molecules. Zeolites have been extensively studied fran the theoretical and technical standpoints because of their potential and actual use as "molecular sieves". The pores and inner cavities of zeolites run throughout the composition with pore diameters ranging form 3 angstroms to about 10 angstroms that allow the mineral to absorb large quantities of water, which has a molecular diameter of 2.65 angstroms. Zeolites carry a net charge which can attract polar compounds. At low temperatures, zeolites absorb large quantities of vapor into its pores. Once the zeolite has been activated by heating, it releases the vapor and some of its inner cavities are emptied. Based on this phenomenon, zeolites can be regarded as a solid absorbent. Moreover, operating over a large temperature range, zeolite can either absorb or desorb vapors without any structural damage. The

resulting effect is that zeolites act as a non-mech ani cal compressor for use in a heat pump or refrigeration system.

The entire zeolite heat pump system includes two main loops: a heat collecting cycle and a heat pump cycle (see Fig. 4). These two cycles are linked by a generator zeolite tank which contains the zeolite absorbent. The left-side loop has a heat collector (which may be a solar collector or a waste heat collector), a pump, an auxiliary heat exchanger, and a heat exchanger coil surrounded by the zeolite. The left-side loop is operating at almost atmospheric pressure. The right-side loop is composed of a condenser , a water reservoir, an evaporator, and a sealed generator tank which is filled with zeolite. Water vapor is circulated within this cycle intermittently.

The system starts to function when heat is received by the collector. The circulating fluid in the left-side loop carries the absorbed heat form the collector to the zeolite tank. Activated by the heat, the zeolite desorbs water vapor to the condensor. Since the right-side loop is totally sealed, the vapor pressure now increases. The temperature of the vapor increases as the vapor pressure increases. When the temperature of the vapor is higher than ambient temperature, the vapor starts to condense and releases its latent heat to the ambient. The vapor then drains into the water reservoir. Here, the heat pump effect is partially accomplished by condensing the water vapor in the condenser .

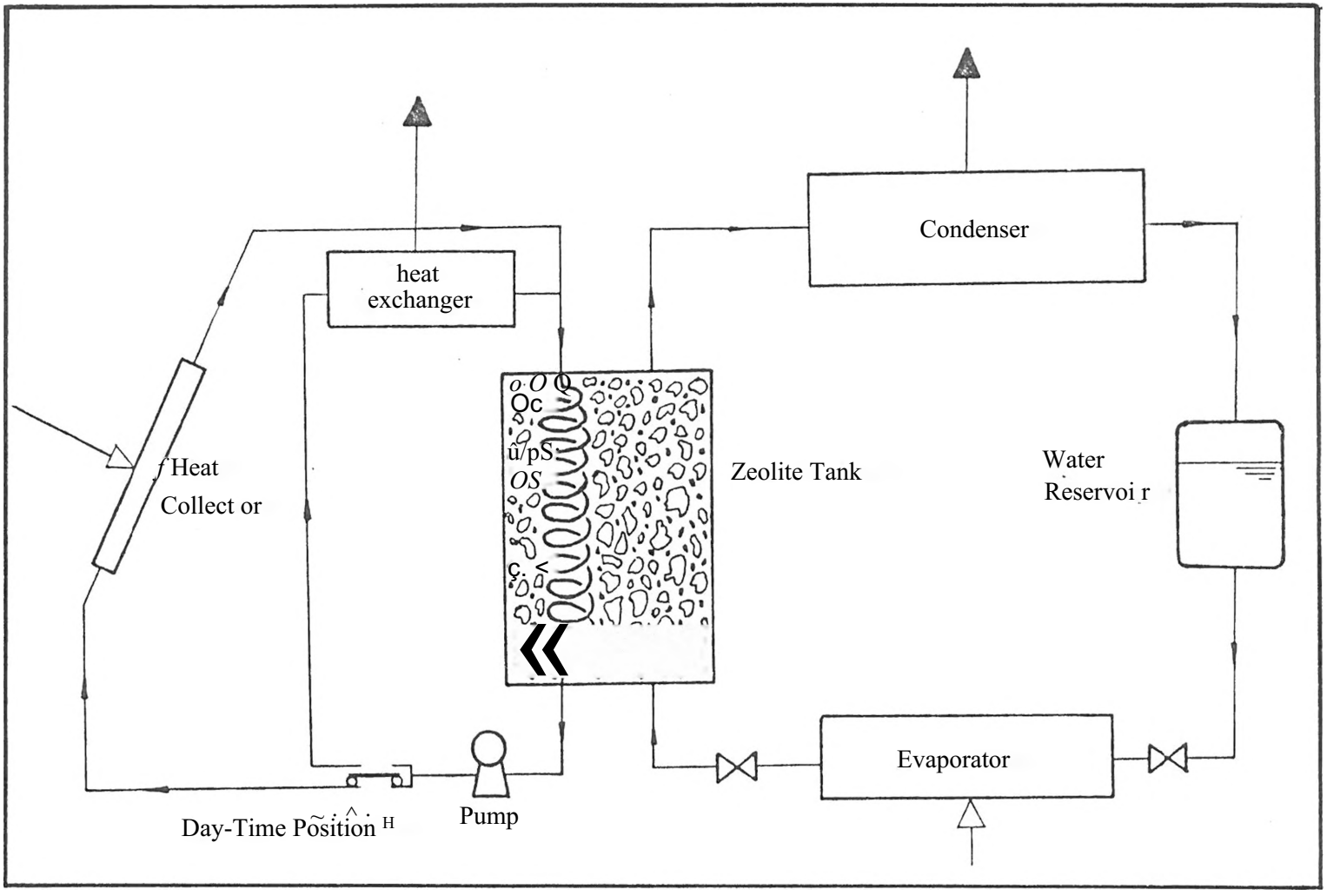

Fig. 4 Schematic for the zeolite heat pump and refrigeration systems.

During the period when the heat source is not available, the zeolite will be cooled. By opening the valves between the evaporator and water reservoir and between the evaporator and zeolite tank, the zeolite in the tank can absorb vapor fron the evaporator. Now the pressure of the vapor will decrease. The water in the evaporator will vaporize when the vapor pressure is reduced to about 5mm Hg. The vapor then returns to the zeolite tank with the heat absorbed fron the ambient environment. Again the zeolite tank receives heat. By changing the switch position (see Fig. 4) to the left-side loop, the circulating fluid in the copper coil will carry heat fran the zeolite tank and again release heat to the conditioned space. The heat pump effect is now completed at this stage.

A more complicated system may be expected in the actual operation of a zeolite heat pump system. Since the heat supply is not always available on consecutive days, the capability of the zeolite system to handle the heating load for several days is important in designing this system. Also, the operating conditions, such as indoor and outdoor temperatures will have a great influence on the overall heat pump CP. A thermodynamic math anati cal model for determining the system performance for different values of the governing parameters will be presented in the next chapter.

CHAPTER III

MATHEMATICAL ANALYSIS

3.0 Derivation of Heat Pump Equations

In this chapter, the performance of the zeolite heat pump and refrigeration systems will be modeled. According to the second law of thermodynamics, energy losses will occur in the various steps of energy conversion. For the solar absorption heat pump and refrigeration systems, the overall instantaneous system CP can be expressed as

$$CP_{hp} = (\quad \eta_p \quad (\quad \quad \eta_{co} \qquad 11>$$

$$cp_r = (cop_r) (n_p) \eta_{oo} \qquad u;$$

where CPhp and CP_r are defined as the ratio of heating load and cooling load to total received energy. COP^p anű COP_r are the coefficients of performance for the heat pump and refrigeration, respectively. η_ρ is the efficiency of the power cycle in an absorption system and is the η_{co} efficiency of the solar collector.

3.1 Heat Pump Based on Carnot Cycle

The ideal efficiency associated with energy losses for energy conversion can be calculated fron the Carnot cycle operating between tne two given temperature limits for the heat pump. They are given by

$$\eta_{\rho} = (T_{H} - T_{L}) / T_{H} \qquad (3a)$$

$$c°p_{hp=} T_{H} \cdot / \quad (\quad T_{H} - \quad T_{L} \quad) \qquad Gb)$$

In Eq.(3a) the high working temperature, T_H, will be the generator (zeolite) temperature, Tg, and the lew working temperature, T^, will be the indoor ambient temperature To1 . In Eq.(3b), the condenser temperature $T_{Д}$, and evaporator temperature, T^, for heat pump cycle will be the indoor temperature, T^, and outdoor temperature, TQ^, respectively. By substituting Eqs.(3a) and (3b), Eq.(1) can be rewritten as

$$CP_{npc} = \left(\frac{Tg. - Tco1}{rp} \right) \left(\frac{Tod}{mm} \right) \eta_{co} \qquad (4\}$$

Tne T-S diagram related to Eq. (4) is shown in Fig. 5. If can be seen that the high generator temperature will result in high power cycle efficiency, thus yielding high system performance. Since there is no work input to and output from the system, the work output from the power cycle will be equal to the work input to heat pump cycle.

3 .2 The Absorption Heat Pump Cycle

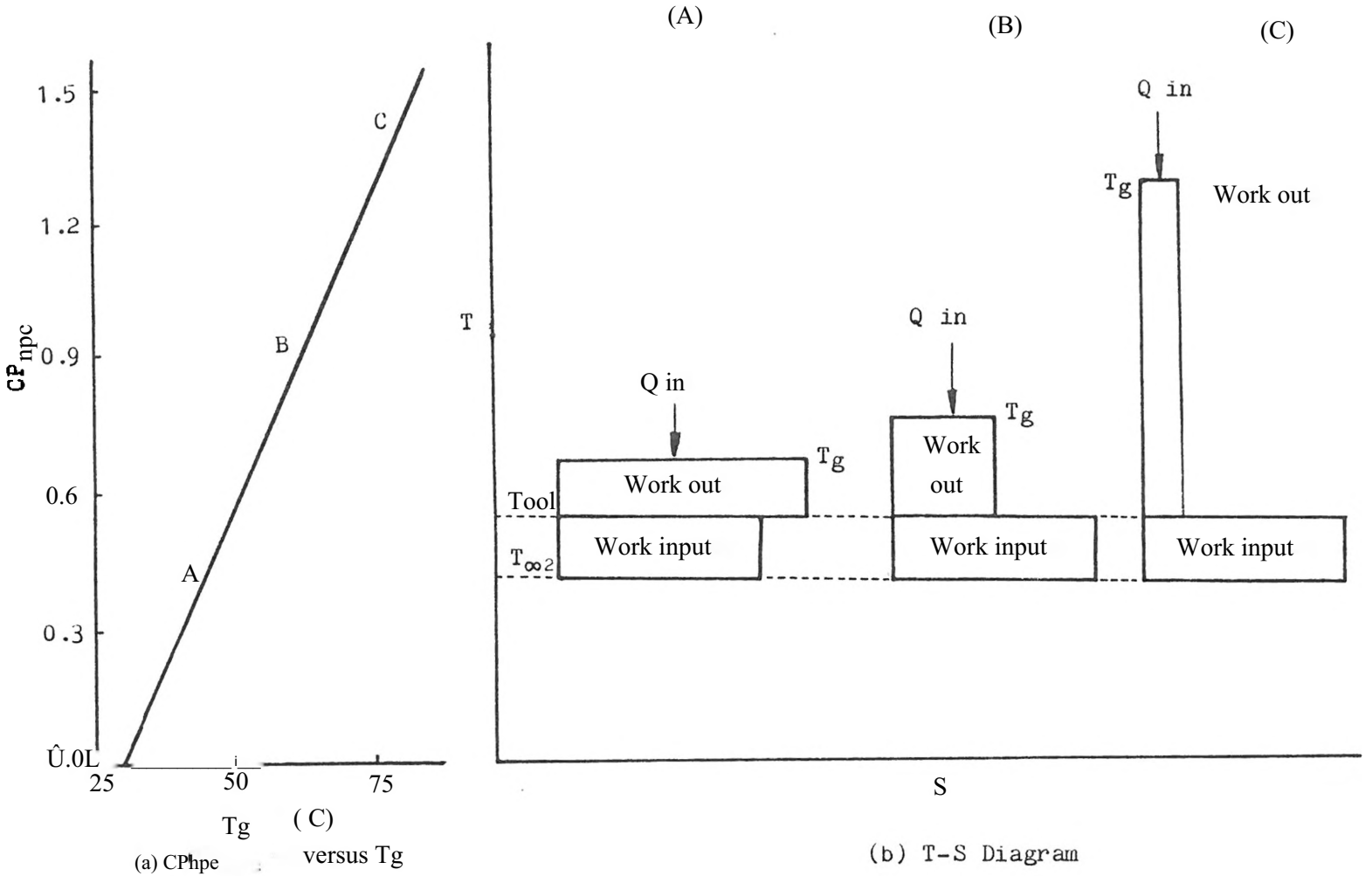

Fig. 5 T-3 diagram demonstrating tne CP_{hpc} as a function of generator temperaure, Tg.

As mentioned before, the working fluid of the absorption system is the vapor desorbed fram the sorbent zeolite. The working temperature range or the power cycle in an absorption heat pump cycle corresponds to the absorption and desorption temperatures. In a zeolite absorption system, the absorption and desorption temperatures are determined by the instantaneous mass concentration X¿.(gm water/gm zeolite). Figure 6 shows the relationship between mass concentration and the many pairs of absorption and desorption temperatures. As seen, the absorption temperature, $T_{я}$, and desorption temperature, T_o, must increase or decrease simultaneously with the change of mass concentration, X/ . The instantaneous neat pump system performance for the Carnot cycle based on the absorption and desorption temperatures can be expressed as

$$CP_{hpca} = \left(\frac{T_g - T_a}{T_g}\right)\left(\frac{T_c}{T_c - T_e}\right)\eta_{co} \qquad (5)$$

Considering the phase transformation involved in the absorption/desorption process of the absorption heat pump and refrigeration system, a more realistic expression for heat pump system performance can be derived by use of the Clausi us-Clapeyron relation. According to the definition of OPhp and Лp, Eq.(1) can be rewritten as

$$CP_{hpi} = \left(\frac{\text{Heating Load}}{\text{Work In}}\right)\left(\frac{\text{Work Out}}{Qi_n}\right)\eta_{oo} \qquad (6a)$$

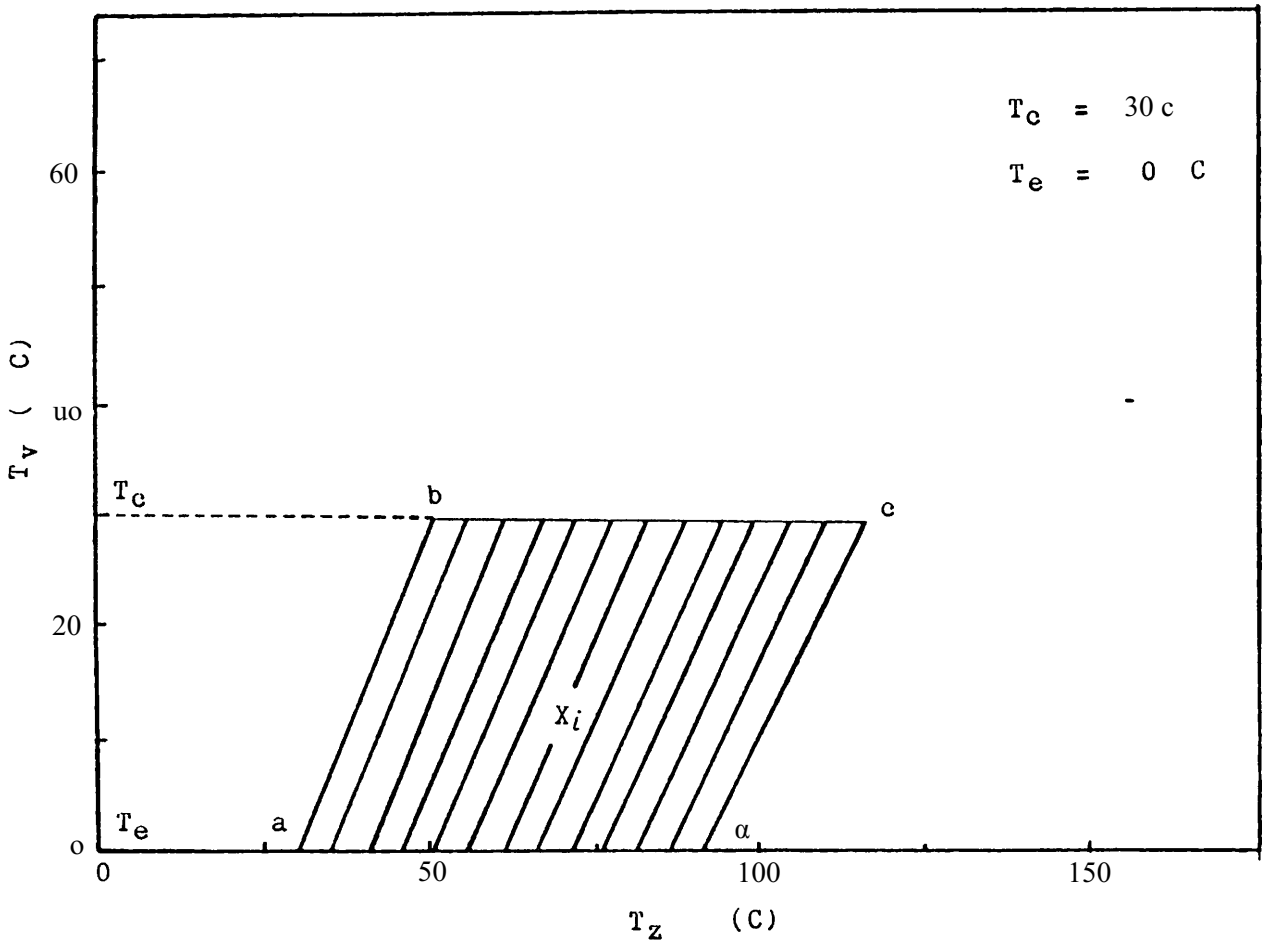

Fig. 6 The relationship between the absroption and desorption temperatures, T_a and Tg, with respect to the vapor temperautre, T_v.

Since there is no work output from the system, the work input to the heat pump cycle will be equal to the work output from the absorption power cycle. Thus, Eq. (6a) becomes

$$CP_{h}pr \left(\frac{\text{Heating load}}{Q\ in} \right) > \eta_{co} \qquad (6b)$$

where the heating load will be equal to the sum of the net work input to heat pmp cycle, U, and the heat of vaporization, L, in heat pump cycle. Q_{in} is equal to ΔH, the heat of absorption. Rewriting Eq. (bb) gives

$$^{CP}\text{hpr} \left(\frac{U}{\Delta H} + \frac{L}{H} \right) \eta\ co \qquad 17)$$

Since the work input to heat pump cycle is assumed to be equal to the work output from the power cycle, the $U/\Delta H$ term in Eq. (7) can be seen as the efficiency of power cycle. By the second law of thermodynamics, the net work output from the Carnot power cycle should be the net decrease of the input heat. However, the power cycle receives and rejects heat at the same values of heat of absorption and desorption. This implies, according to the first law of thermodynamics, that there will be no work output from power cycle. Fortunately, the absorption ana desorption temperatures are higner than the ambient temperature. Therefore, the theoretical maximum net work output from power cycle will be the availability between the heat of absorption and heat of desorp-

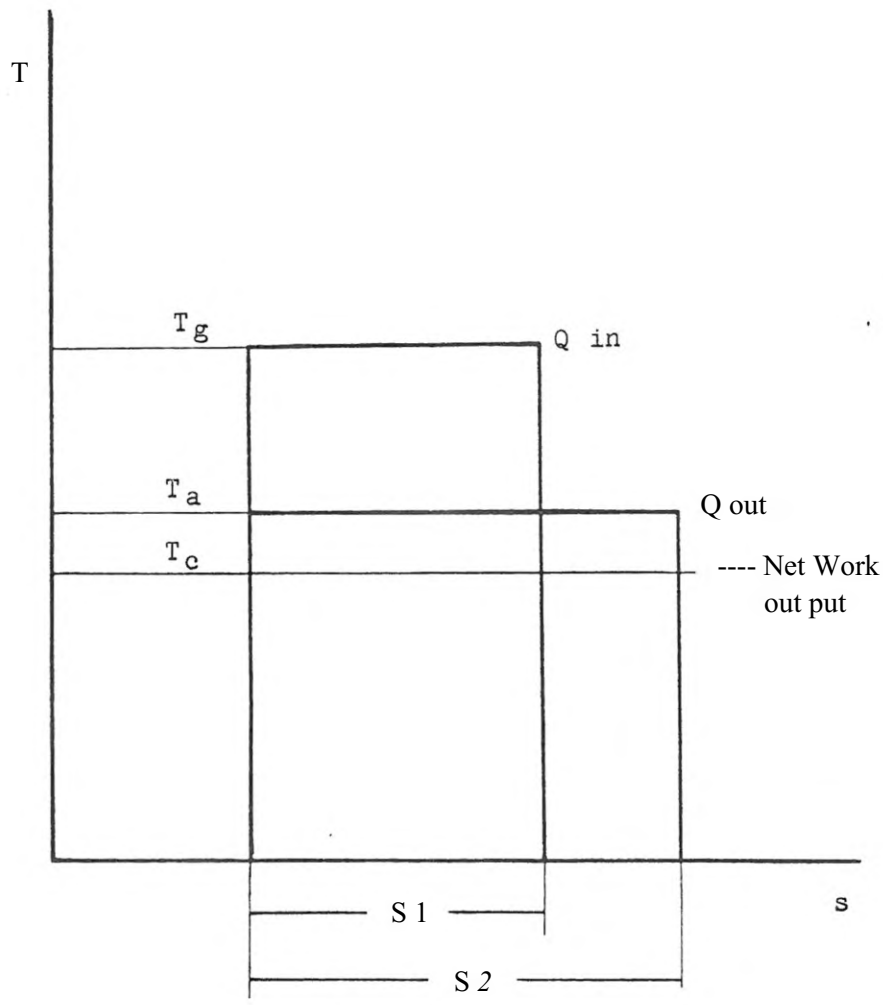

Fig. 7 T-s diagram demonstrating the availability between the desorption temperature, Tg, ana the absorption temperature, $T_{a>}$

tion at T_a and T_g, respectively(see Fig. 7). The efficiency for the power cycle, therefore, can be expressed as

$$\eta = \frac{\text{Net Work}}{\text{«in}} = \frac{T_c (\Delta S_2 - \Delta S_1)}{T_g \Delta S_1} \quad (8a)$$

The neat of absorption is equal to the heat of desorption, which gives

$$T_a \Delta S_2 = T_g \Delta S_1 \quad (8b)$$

Combining Eqs. (8b) and (8a) yields

$$\frac{U}{\Delta H} = \frac{T_c}{T_a} \left(1 - \frac{T_a}{T_g} \right) \quad 18c)$$

To determine the ΔH in Eq.(7), the heat of absorption, the Clausius-Clapeyron equation is employed. The heat absorption process occurs between the evaporation pressure, P_e, and the condensation pressure, P_c. The vapor-solid phase transformation for absorption and desorption can be expressed by

$$\frac{d (\ln P_v)}{d T} = \frac{\Delta H}{R T^2} \quad (9)$$

Int ergrating Eq. (9) yields

$$\ln\left(\frac{P_c}{P_e}\right) = \int_{T_a}^{T_{es}} \left(\frac{\Delta H}{R\,T_z^2}\right) d\,T_z \qquad \text{UO)}$$

Using the Clausi us-Cl ape yr on equation, the liqui d-vapor transformation in the evaporator can be expressed as

$$\frac{d\,(\ln P_v)\,L}{d\,T_v} = \frac{}{R\,T\gamma^2} \qquad (11)$$

Integrating Eq. (11) gives ’

$$\ln\left(\frac{P_Q}{P_e\,A_e}\right) = \int^{T_Q} \left(\frac{L}{R\,T_V^2}\right) d\,T_v \qquad (12a)$$

Combining Eqs. (10) and (12a) yields

$$\int_{P_e}^{P_{oc}} L\,d\left(\frac{i}{T_v\,A_a}\right) = \Delta H\,d\left(\frac{1}{T_z}\right) \qquad (12b)$$

Assuming L and ΔH as constants gives

$$L\left(\frac{11}{T_e\,T_c}\right) = \Delta H\left(\frac{11}{T_a\,T_g}\right) \qquad (13)$$

Rearranging Eq. (13) and combining with Eqs. (7) and (8c) gives the result

$$^{CP}hpa = \left(1 + \frac{Te}{T_c - T_e}\right)\left(\frac{Tg - T_a\, T_G}{Tg - T_a}\right)\eta_{co} \qquad (14)$$

Equation 14; is an expression for the zeolite heat pump system based on the absorption cycle. It is found tnat Eq. (14) is very close to Eq. (5) when T_a is close to T_G . This means the absorption cycle efficiency tends to be identical to the ideal Carnot cycle efficiency when the absorption temperature is close to condenser temperature. A comparison can be made between the system performance for the overcall Carnot cycle, Eq.(5), and the absorption cycle, Eq.(14), which gives

$$\frac{^{cp}hpa}{^{CP}hpca} = \frac{^{T}c}{^{T}a} \qquad (15a)$$

The power cycle efficiency is mainly determined by the desorption and absorption temperatures. Yet, tne condenser temperature will affect the absorption power cycle efficiency when the absorption temperature is far higher than the condenser temperaure. Tne power cycle efficiency ratio for the overall Carnot cycle can be expressed as

$$n_G = 1 - \frac{T}{Tg} \qquad (15b)$$

Combining Eqs. (15b) and (8c) yielas

$$\eta_a = \Pi_{ca} \frac{T_c}{T_a} < 15\alpha J$$

Eq.(15c) is similar to Eq.(15a). This implies the absorption power cycle efficiency determines the instantaneous system performance for heat pump at constant condensation and evaporation temperatures. Figure 8 shows the T-S diagram for the absorption cycle. The absorption and desorption temperarur es, T_o and T_{-d} will change at each mass concentration, thus changing the power cycle efficiency. Therefore, an instantaneous system performance for the absorption heat pump cycle can be obtained from Eq. (14). However, the working temperatures, $T_я$ and T_σ, of the power cycle require measurements for each mass concern-ration to determine the instantaneous system performance. The following sections will illustrate the absorption properities of zeolite.

3 -3 Absorbent Properties Equation

To calculate CPhpi in Eq. (7) the heat of absorption, ΔH, must be known. An absorption equation for zeolites can be used to evaluate the heat of absorption. According to the theory of volume filling of micro-porous absorbent (such as zeolite, charcoal) the mass concentration lines can be viewed as linear in the absorption process. Figure 2 snows the linearity of mass concentration lines in the coordinates of log P_v versus $1/T_Z$. Based on the linearity assumption of zeolite absorption, the absorbent equation can be given as

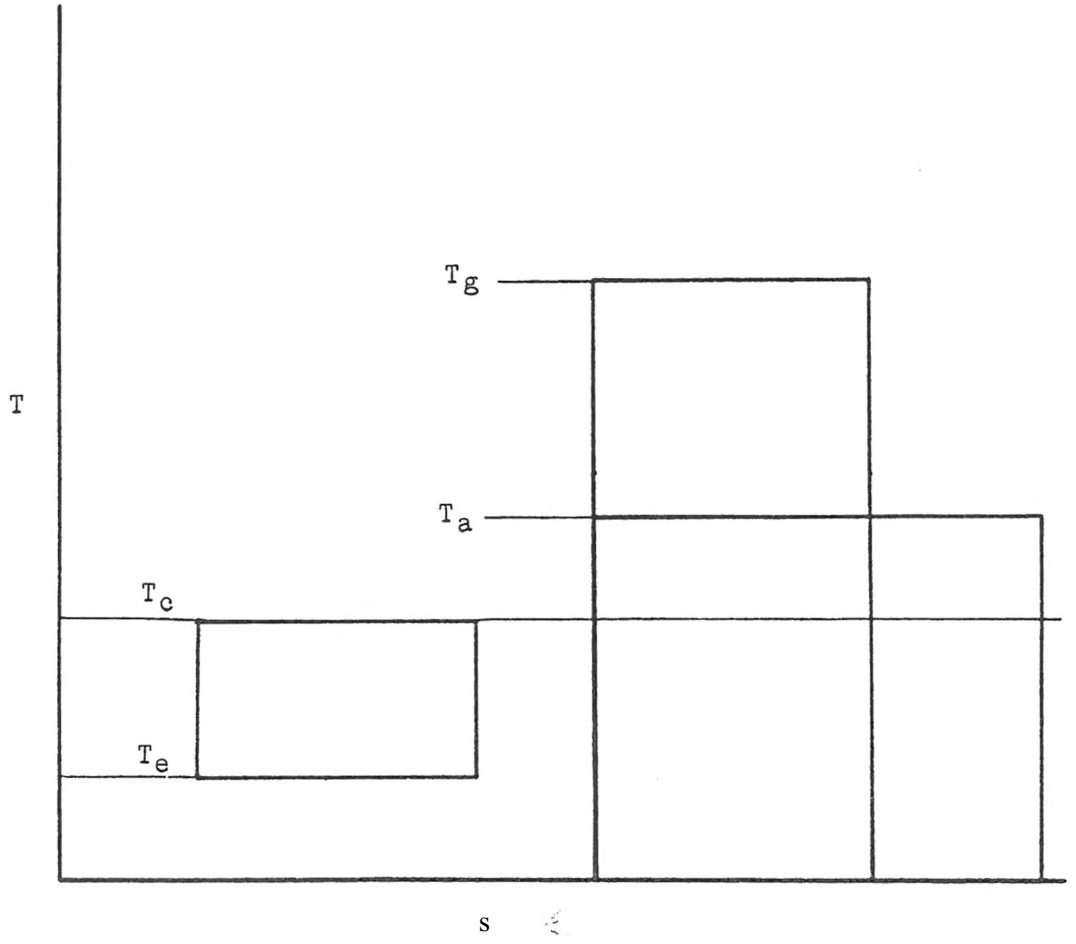

Fig. 8 T-s diagram illustrating tne absorption cycle

$$\log P_v = m_z \left(\frac{1}{-T_z} \right) + C_z \qquad (16a)$$

or

$$\ln P_v = E\, m_z \left(\frac{1}{-T_z} \right) + C_z E \qquad (16b)$$

where E is equal to (In P_v) / (log P_v) = 2.302581 . To acquire the value of the heat of absorption, Eq.(l6a) is rewritten as a differential expr es sion

$$m_z = \frac{- d \log P_v}{d (1/T_Z)} \qquad (17a)$$

Equation(9), thus, can be rewritten as

$$\Delta H = (R T_z) L^2 \frac{- d \log P_v}{T_z^2 \, d (1/T_Z)} J \left(\frac{d \ln P_v}{d \log P_v} \right) \qquad (17b)$$

Substituting Eq.(17a) into Eq.(17b) yields

$$\Delta H = R E m_7 \qquad (18)$$

It can be seen that the heat of absorption, ΔH, is only dependent of the slope, m_z, of tne mass concentration lines in a log P_y versus $1/T_Z$ plot. In addition, the points along a certain mass concentration line will have the same value of heat of absorption.

3.4 Sorbent and Sorbate Temperatures in Absorption Process

Equation(16a) reveals the relationship between the equilibrium sorbate (water) pressure and the sorbent (zeolite) temperature. The sorbate temperature can be acquired by employing the Clapeyron equation

$$\frac{dP_Y}{dT_v} = \frac{L}{\cdot Ty\,(V_v - V_f)} \quad (19)$$

Since $V_v >> V p$, V £ can be viewed as negligilible. Using the ideal gas equation of state(P V = R T) yields

$$\frac{dP_v}{P_v} = L\left(\frac{dTy}{R\,Ty^2}\right) \quad (20)$$

Rewriting Eq. (9) gives

$$\Delta H = B\,į\left(\frac{d\,In\,P_\gamma}{d\,T_z}\right) \quad (21)$$

Using the ideal gas equation of state again, Eq. (21) can be written as

$$\Delta H = R\,T_z\left(\frac{2}{P_\gamma}\right)\left(\frac{d\,P_V}{d\,T\,2}\right) \quad (22)$$

Substituting Eq. (20) into Eq. (22) yields

$$\Delta H = T\,2\,L\left(\frac{d\,T_v}{Ty^2}\right)\left(\frac{1}{dT_z}\right) = REm_z \quad (23)$$

Rearranging and separating the variables of Eq. (23) gives the result

$$-\frac{dT_y}{T_y^2} = \left(\frac{R E \text{ш} 2}{L}\right)\left(\frac{dT2}{T_z^2}\right) \quad (24)$$

Taking the heat of evaporation, L, as constant and integrating Eq.(24) yields

$$T_v = \frac{1}{\left(\frac{R E m_z 1}{L}\right)\left(\frac{}{T_z}\right) + C} \quad (25)$$

where C is the integration constant. The value for the integration constant will be shown in the next section. Equation(25) provides a clear relationship between the sorbate temperature, T_y, and tne sorbent temperature, T . However, the determination of sorbent and sorbate temperatures still requires the relationship between the absorption properties of zeolite and the sorbent and sorbate temperatures. This relationship will be derived next.

3.5 Sor bent 3jnd_ Jtør ba^e_Xej^^ Referring _tA Abs.orbent Properties

Considering the properties of absobent, the sorbent and sorbate temperatures can be expressed as a function of the straight line which is characteristic of tne mass concentration line on log P_γ versus $1/T_Z$

graph. Assuming the heat of evaporation, L, as constant and integrating Eq. (20) gives

$$\ln P_v = -\left(\frac{L}{E}\right)\left(\frac{1}{\tau_v}\right) + C_w \qquad \text{к 26)}$$

where is equal to 14.2(bar) when T_y varies fron 0 to 30 C. Combining Eqs. (26) and (16b) yields

$$\frac{E\, m_2}{-T_z} + E\, C_z = C_w - \left(\frac{L}{R}\right)\left(\frac{1}{T_v}\right) \qquad (27a)$$

The integration constant in Eq. (25) can be acquired by rearranging Eq. (27a), which gives

$$c = \frac{fi\,(C_w - E\,C\,2)}{L} \qquad (27P)$$

Equa tions (27 a) and (27b) are based on constant heat of evaporation, L. A more complicated expression for the relationship between the sorbent and sorbate temperatures can be obtained by letting tne heat of evaporation vary as a function of vapor temperature. However, computations have shown that this is not necessary to achieve accuracyi 10J .

An absórbate temperature, T , versus absorbent temperature, T , plot can be established based upon Eq.(2Ṭa). Figure 6 shows the isosters (constant X¿ lines) of T_v versus T_2 in the absoption process of zeolite. Rearranging Eq.(27) to explicitly determine T_z gives

$$T_z = \frac{-\ m_z E}{C_w \dfrac{L}{R\,T_v} - E\,C_2} \qquad (.28)$$

where G_z is the constant (see Eq.(l6a)) for the mass concentration line of zeolite on the log P_v versus 1/T plot. For any constant mass concentration, the T_v versus T_z lines can be acquired by utilizing Eq. (28). The temperature of the absorbent, T ·, in absorption process for each mass concentration line on T_y versus T_z plot will be located along the line corresponding to the evaporation temperature, T_e(see Fig. 6) . Similarly, the temperature of the absorbent in the desorption process for each mass concentration line will be located along the line corresponding to the condensation temperature, T_c(see Fig. 6) . Equation(28) can be rewritten for the absorption temperature, T„, and the desorption temperature, T_g, as follows

$$T_{gL} = \frac{-\ m_z' E}{{}^{c}w - \dfrac{L}{R\,T_G} - E\,{}^{c}{}_{z}¿} \qquad (.29)$$

$$T_{aL}' = \frac{-\ m_z \dot{\iota} E}{Cw - \frac{L}{R\ T_e} - E\ C_z} \quad (30)$$

3.6 Effect of Solar Collector Efficiency

Presently, several solar collector types are available, For convenience, let the P-type solar collector be a single-glass glazing flat-plate collector, the S-type, a double-glass glazing flat-plate collector, and the V-type, an evacuated flat-plate collector, respectively. The efficiency of these three types of solar collectors are nearly a linear function of collector temperature which can be expressed as

$$\eta_{co} = \text{”}^{m}\ co\ Tco^{+\tilde{C}}\ co \quad (3D$$

Figure 9 shows the linear properties of the solar collector efficiency with respect to the collector temperature. To simplify tne problon, the collector temperature will be assumed to be equal to the zeolite temperature; this implies that the efficiency of the heat exchanger is equal to unity. The water mass concentration will remain constant as the vapor temperature in Fig. 6 is increased fron point a to point b. During the heating fron point a to point b in Fig. 6, the water vapor will be held in the zeolite absorbent. Since tnere is no water vapor desorbed frem the zeolite at this stage, it is important to

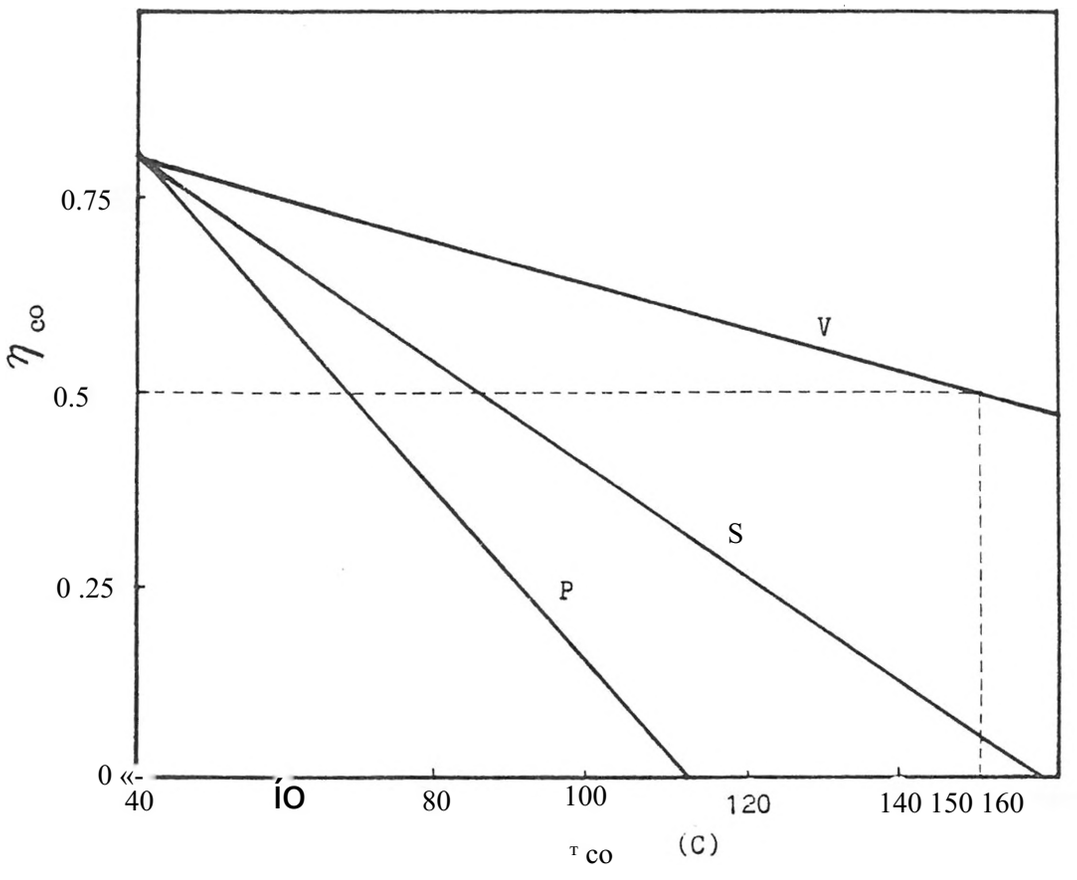

Fig. 9 Linear properties for different types of solar collector.

notice that there is no fluid circulating in the heat pump cycle before the zeolite reaches the initiation desorption temperature (point b in Fig. 6) . Therefore, the overall system performance for the heat pump is equal to zero before the desorption process begins. After reaching the initiation desorption temperature, the system performance will increase gradually. From point b to c, the zeolite temperature is equal to the desorption temperature. Inserting Eq. (29) into Eq. (3D with T . = giv es

$$\eta_{co} = \left(\frac{\text{“ } E\, m z_i\, m_{co}}{L} + \text{co} \right) \Big/ \left(C_w - \frac{}{R\, T_c} - E\, C_{z\,i} \right) \qquad (32)$$

Equation(32) shows that the collector efficiency is affected by tne type of solar collector and absorption properties of tne zeolite system.

3.7 Instantaneous CP for Zeolite Heat Pump System

In a solar zeolite system, the total heat -of absorption will depend on the heat received by the solar collector. Considering the efficiency of the solar collector, Eq. (7) can be rewritten as

$$\%_{pi_P} = \left(la^* — \frac{L}{\Delta H} \right) \qquad (33a)$$

An instantaneous system performance for the heat pimp can be derived by combining Eqs. (18), (32) and (33a). This result can be expressed as

$$ {}^{CP}h_{Pl} = \left(\eta a + \frac{L}{R E m_{\zeta i}} \right) \left(\frac{- E 4; {}^{m}eo}{\frac{L}{Gw \text{“} \frac{}{R T_c} \text{“} G_{Z\zeta}^{E}}} + C co \right) \qquad (33b) $$

Equation(33b) shows that the overall system performance for the heat pump is a function of the zeolite properties, the type of solar collector, and the ambient temperature.

3.8 Mean CP for Zeolite Heat Pump System

To consider the actual operation of a zeolite heat pump system, the mass of the working fluid is a critical factor. Due to the sensible heat losses in an absorption and desorption processes, the practical system performance will be reduced. The mean system performance for tne zeolite heat pump system can be defined as

$$ {}^{CP}Ьp_{ш1} = \frac{W_{zj} \int_{D}^{re} \Delta H \, d X;_{L} + W L \, d X; \int_{b}^{c}}{w_z \int_{,b}^{} \frac{\text{í°}\Delta H}{\eta \circ\circ} d X_i} \qquad (34a) $$

where b and c denote the beginning and the end of the desorption process(see Fig. 6) , respectively. W_z is the weight of the zeolite. Numerical evaluation can be performed by rewriting Eq.(34a) as

$$CP_{\text{max}} = \frac{\sum_{i=b}^{c} \left[\left(X_{i-1} - X_{i-1} \right) \frac{(\Delta H_{\gamma} + \Delta H_{O})_{c}}{2} \right] + 2LL(X_{i} - X_{i-1}) \sum_{i=b}^{c}}{\sum_{i=b}^{c} \left[\left(X_{i} - X_{i-1} \right) \frac{(\Delta H_{i} + \Delta H_{i-1})_{\rho}}{2 \Pi_{co}} \right]} \quad (34b)$$

The symbol X_i is the sorbate mass concentration of the zeolite at the Z-th mass concentration line. Π_{eo} is the solar collector efficiency for Tgi at mass concentration X/. Equation(34b) does not account for the capacity heat losses. Nevertheless, it reveals a simple expression for calculating the maximum CP value for the zeolite heat pump system.

The influence of thermal capacity losses may result frem the sorbent, sorbate, and thermal equipment (heat exchanger tube and zeolite tank). An overall system performance considering heat losses during the desorption process can be given as

$$CP_{hpm2} = \frac{(h_{L+D} - h_1) - Q_1}{D_{h2} + Q_2 + Q_3 + Q_4 + Q_5} \quad (35)$$

where is the total heat taken into the evaporator fran the ambient air. The expression for $L_{\wedge}$. can be given as

$$L_h = \sum_{\dot{L}=b}^{c} L(Xi - {}^{x}l\text{-}1)\, b\, W_z\, J \qquad (3Ö)$$

Dh1 is the heat condensed in the condenser, which can be expressed as

$$D_{hl} = \Sigma I \underset{í=b}{\overset{o}{(}} X; - X_{¿\_,}) \frac{(\ \Delta H_{\_\_}. + н\ \blacksquare_{ł})}{2_{1}}\ W_z\, J \qquad (.37)$$

D^2 is the heat absorbed by the water in the desorption process of the zeolite. The expression of Dh2 can be given by

$$^{D}h2 = \Sigma \underset{¿=b}{\overset{c}{L}} (X; - X\cdot{}^{\wedge}) \frac{(\ \ + \Delta H/)}{2\ Лco^{\wedge}}\ W_z\ ] \qquad <38J$$

Q1 is the heat required to cool the sorbate (water) from the condensation temperature, T_, to the evaporation temperature, T_. Q1 can be expressed as

$$QI = \sum_{\dot{L}=0}^{c} C\,(X/ - X¿\text{-}1)\,(h_c - h_e)\,W_z\,] \qquad (39a)$$

where h is the enthalpy of the water. Q2 is the heat needed to heat the sorbate fram the beginning of the desorption process to the end of the process (see Fig. 6) . Q2 can be given by

$$Q2 = \Sigma_{¿=a}\left[\frac{b\ Xi\ (h\text{-} - h^{\wedge}p}{\%O¿}\ W_z\right] + \Sigma_{\dot{L}=b} L\ \frac{c\ X\ ¿\ (h'¿ - h^{\wedge\wedge}p}{\eta\ CO\ ¿}\ W_z] \qquad (39b)$$

Q3 is the heat required to raise the temperature of the sorbent framn the beginning of the desorption process to the end of the process (see Fig. 6). The specific heat of zeolite is given as 0 .953(Kj/Kg-K). Q3 can be expressed as

$$03 = \Sigma\ \acute{\imath} \left[\frac{c\ {}^{c}Pz\ (\ {}^{T}z_{\text{¿}} - {}^{T}z_{\text{¿}-1}\ )}{\text{^co¿}}\ W_{z}\ \right] \qquad 139c)$$

Q4 is the heat required to raise the temperature of the zeolite tank from the temperature at the beginning of desorption process to the temperature at the end of the desorption process. Cp , is the specific heat of the tank material. Q4 can be expressed as

$$Q4 = \sum_{i=a}^{c} \left[\frac{Cp_{tk}\ (\ T_{z} - T_{z\,i-1}\ )}{\eta_{co\,i}}\ W_{tk}\ \right] \qquad (39a)$$

05 is heat required to raise the temperature of heat exchanger tube from the beginning of desorption process to the end of process. Tne specific heat of tube material is given by Cp . 05 can be expressed as

$$05 = \Sigma_{\text{¿}=a}^{c} \left[\frac{{}^{Cp}tb\ (\ {}^{T}zi\ \text{“}\ {}^{T}Z_{\text{¿}\_-|}\ J}{\eta_{co\,L}}\ {}^{W}tbJ \right] \qquad (39e)$$

3.9 Optimum Slope for Heat Pump System

As mentioned before, a change of the slope of a mass concentration line on the graph of log P_y versus $1/T_Z$ can affect the value of generator temperature(or desorption temperature). Since the efficiency of the solar collector is a function of generator temperature, Eq. (7) can be optimized by considering the system performance to be a function of the slope(m_z) of the mass concentration line only. Assuming the heat of evaporation, L, to be constant and combining Eqs. (7), (8c), and (31) gives

$$CP_{hpi} = \left(\frac{T_c}{T_o - Te}\right)\left(\frac{Tg - Ta}{Tg}\right)\left(\frac{Tc}{Ta}\right)(\text{“Tg } m_{co} + C_{co}) \qquad (40\text{ a})$$

Letti ng $K_t = (T_c/(T_c - T_e \Pi (T_o / T_a>$ and rearranging Eq.(40a) gives

$$CP_{hpi} = K_t\left(Tamco+Cco - mcoTg - \frac{TaCco}{T8}\right) \qquad (40b)$$

To simplify the derivation, let $\phi = (RSn_z)/L$ and $(1/T_e - 1/T_C)$ in $\lambda =$ Eq.(13). Substituting Eq.(13) into Eq.(40b) yields

$$CP_{hpi} = K_t\, t\, T_a m_{co}\, C_{co} \text{"} \pm \frac{m_{co}}{\frac{1\lambda}{Ta\,\Phi} - \frac{}{}} + T_a c_{co}\left(\frac{1\lambda}{Ta\,\Phi}\right) J\, J \qquad (41)$$

To optimize CP ^in Eq.(41), differentiating Eq.(41) with respect to ϕ yields

$$\frac{d\,CPhpi}{d\,\Phi} = \left[\frac{{}^{m}co/\,\phi^{2}}{(l/Ta-\lambda/\varphi)^{2}\,\Phi} \quad \frac{T_a C_{co}}{2}\right] K_t \tag{42}$$

Let $\frac{d\,CPhpi}{d\,\phi} = 0$ and solve for ϕ, which yields

$$\varphi = \frac{C\,co\,\lambda + \underline{Vmco}\,T_a\,C\,co\,X^2}{(Cco/\,T_a - m_{co}} \tag{43}$$

Equation(43) expresses the optimum slope of the mass concentration lines with respect to the instantaneous system performance for each absorption temperature. As seen, the determination of the instantaneous optimum slope can be influenced by the type of solar collector, condensation temperature, evaporation temperature, and the absorption temperature.

To determine the optimum absorbent slope for the mean heat pump system performance, the water mass concentration, X¿, musu be considered. As seen in Eq.(35), the amount of the water mass absorbed is related to the heat of absorption and the heat of rejection. To simplify the problem, the absorbent slope is assumed to be constant. The optimum uniform absorbent slope for the mean heat pump system performance, CP^p_{m2} can be obtained by differentiating Eq.(35). Due to the

complicated mathematical expressions involved in the derivation, the optimum absorbent slope for the mean heat pump system performance was acquired numerically. A maximum mean heat pump system performance was obtained for each value of the absorbent slope. Therefore, by varying the value of the uniform absorbent slope, the relationship between the maximum mean heat pump system performance and the absorbent slope can be determined.

3.10 -0 Derivation for Refrigeration Equations

The derivation of the governing equations for a solar zeolite refrigeration system is similar to that of the heat pump. Here, the refrigeration cycle will replace the heat pump cycle in the operation of the zeolite system. As mentioned earlier, energy losses occur at the various steps of conversion. Equation(2) is the basic expression for the overall system performance for refrigeration. Details of the derivation for the governing equations for refrigeration will be presented below.

3.10 Refrigeration CP Based on Carnot Cycle

The ideal efficiency for energy conversion in an absorption refrigeration system is based on Carnot cycle within two operating temperature limits and can be expressed as

$$\Pi o = (T_H - T_L) / T_H \quad (44a)$$

$$COP_r = T_L / (T_H - T_L) \quad (44b)$$

In Eq.(44a), the high working temperature will be the generator temperatur e(or the desorption temperature) and the low working temperature will be the ambient temperature, T_x . In Eq.(44b), the hign and low working temperatures will be the ambient temperature, TQQ , and evaporation temperatures, T_e, respectively. Substituting Eqs. (44a) and (44b) into Eq. (2) yields

$$CP_{rc} = \left(\frac{Tg - Too}{Tg} \right) \left(\frac{Te}{Tco - T_e} \right) \eta_{co} \quad (45)$$

The T-S diagram corresponding to Eq. (45) is shewn in Fig. 10. Similar to Fig. 5, the high generator temperature will produce hign power cycle efficiency. Therefore, the system performance for *ref* rigeration will increase with increasing generator temperature. The cooling effect will remain constant, while the power cycle efficiency will be changed.

3.11 The Absorption Refrigeration Cycle

In an absorption system, the temperature limits for the power cycle efficiency can be influenced by the absorption temperature, T_a, and desorption temperature, T_σ, of the system. The high and lew working

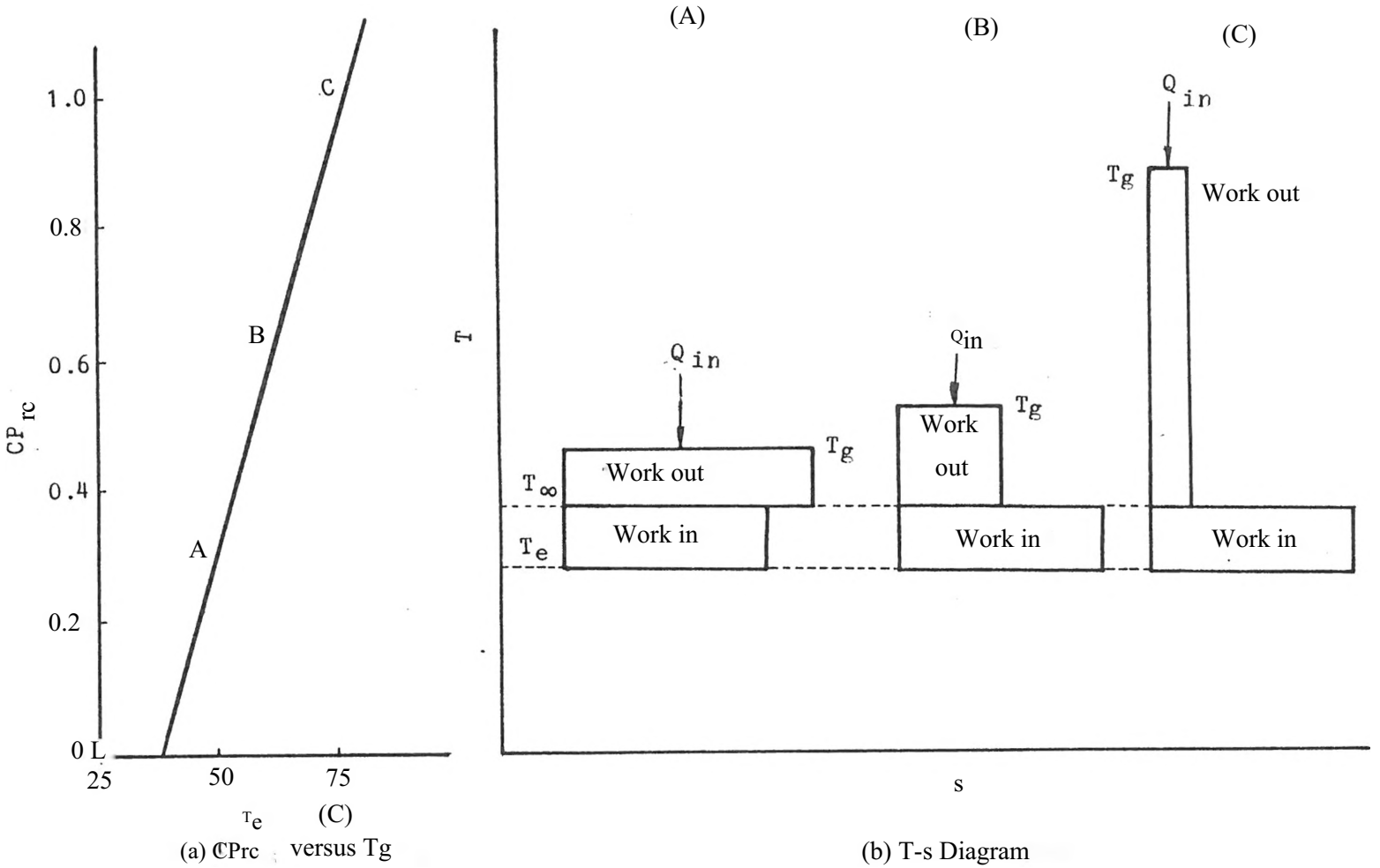

(a) CPrc versus Tg (b) T-s Diagram

Fig. 10 T-s diagram demonstrating CP_{rc} as a function of generator-temperature, T_{σ}

temperatures for the power cycle efficiency will be determined by the instantaneous water mass concentration of the zeolite. Thus, rewriting Eq.(45) gives

$$CP_{rea} = \left(\frac{Tg - Ta}{Tg} \right) \left(\frac{T_e}{T_c - Te} \right) \eta_{co} \qquad (46)$$

Equation(46) is for the Carnot cycle system performance based on absorption and desorption temperatures, T_a and T_g. Considering the the phase transformation in the absorption-desorption process, the Clausi-us-Clapeyron relation can be employed. By the definition for COP_r and hp, Eq. (2) can be expressed as

$$CP_{r-1} = \left(\frac{\text{Cooling Load Work Out}}{\text{Work In}} \right) \left(\frac{\text{Work Out}}{Q_{in}} \right) n_{co} \qquad (47)$$

The work input to the refrigeration cycle is equal to the work output from Lhe absorption power cycle. Rearranging Eq.(47) gives

$$CP_{ri} = \left(\frac{\text{Cooling load}}{Q_{in}} \right) \eta_{co} \qquad (48)$$

The cooling load of Eq. (48) is the heat of vaporization, L, in the evaporator and the Q. is the heat of absorption. Therefore, Eq. (48) becomes

$$CP_{ri} = \left(\frac{L}{\Delta H}\right) \eta_{co} \quad (49)$$

Substituting Eq.(13) into Eq.(49) gives

$$CP_{ra} = \left(\frac{T_g - T_a}{T_g}\right)\left(\frac{T_e}{T_c - T_e}\right)\left(\frac{T_c}{Ta}\right) \eta c© \quad (50)$$

Equation(50) can be seen to be very close to Eq. (46) when the absorption temperature, T_a, is close ¿o the condensation temperature, T_G. A comparison can be made between the system performance based on the absorption cycle , Eq.(50), and overall Carnot cycle, Eq.(46), which gives

$$\frac{CP_{ra}}{CP_{rea}} = \frac{T_e}{T_a} \quad 151)$$

The T-S diagram for absorption cycle is illustrated in Fig. 8. Further proof can be made by use of the availability derivation. The theoretical maximum net work output frem power cycle will be the availability between the heat of absorption and heat of desorption at T_a and Tg, respectively (see Fig. 7) . The efficiency for the absorption power cycle, thus, can be expressed identically as Eq. (8c). By combining Eqs. (2), (8c) ana (47), the result is the same as Eq. (50). Therefore, the instantaneous system performance for refrigeration will be deter-

mined by the absorption power cycle efficiency at constant condensation and evaporation temperatures.

3.12 Instantaneous CP for Zeolite Refrigeration System

The instantaneous system performance for refrigeration can be obtained fram the absorption properties mentioned previously. Combining Eqs.(18) , (32), and (49) yields

$$CP_{ri} = \frac{L}{RE\, m_{z\zeta}} \left(\frac{-E\, m_{\sim\zeta} \cdot m_{pz}}{L} + Cco \right) \qquad (52)$$

$$C_w - \frac{}{RT_C} - E\, C_{2\zeta} \cdot$$

Equation(52) is an expression for the instantaneous system performance refrigeration. It does not account for the amount of the working fluid in the absorption and desorption processes, but only tne properties of the working fluid. A realistic expression for system CP will be derived next.

3.13 Mean CP for Zeolite Refrigeration System

To consider the actual operation of the refrigeration system, the amount of refrigerant in the refrigeration cycle is important to the heat of vaporization and the heat of absorption. By tne definition of Eq. (49), the mean system CP for refrigeration can be expressed as

$$CP_{\pi\eta 1} = \frac{W_z \int_b^c L \, dX,}{W_z \int_{jbco}^{\circ} \frac{\Delta H}{\eta} \, d x_{¿}} \qquad (53)$$

Numerically evaluating Eq. (53) gives

$$CP_{rm1} = \frac{\sum_{¿=b}^{c} 2_u [L 1 X_{;} - X_{;-2})]}{\sum_{¿=b}^{c} Ĺ (X / - X_{¿\_1})} \cdot \frac{(ÁH_{¿} + \Delta H \cdot_{¿1})}{2 \eta_{co} \cdot_{¿}} \; J \qquad (54;$$

Equation(54; is an expression for the mean refrigeration system performance without considering the sensible heat losses in the absorption and desorption processes. A realistic expression accounting for the sensible heat losses will reduce the system performance given by Eq. (49), which can be expressed as

$$CP_{rm2} = \frac{Eh - Q1}{{}^{D}h2^{+} 02 + 03 + 04 + 05} \qquad (55;$$

where Lh, Dh2, 0Ъ Q2, Q3, Q4, and Q5 are defined identically to tnose in Eq.(35).

3.14 Optimum Slope for Refrigeration System

Tne optimum slope of the mass concentration lines for instantaneous refrigeration performance can be acquired by expressing tne system CP as a function of the slope only. Assuming the heat of vaporization to be constant and combining Eqs.(13) and (44j gives

$$CP_{ri} = \frac{Ь}{Я\ E\ m\text{-}_{\Delta}1}\left(\frac{\text{“ m co}}{\frac{L\ 1}{Ta\ REm_z}\left(\frac{1}{T_e\ T_c}\right)} + C_{oo}\right) \qquad < 56\ J$$

To simplify the equation, let ϕ = (Rßn$_z$)/L and X= (1/T $_e$- 1/T) . Rearranging Eq. (56) yields

$$CP_{ri} = \frac{\text{“ m co}}{\frac{\Phi}{Ta^{*}}\ \lambda} + \frac{C\ co}{\phi} \qquad (57\ J$$

Letting T$_a$ and λ be constants and differentiating Eq. (57) gives

$$\frac{d\ CPri\ ^{m}co^{Z}\ T_a}{d\ \varphi\ (\ \varphi\ /\ T_a\ -\ )\ )\ \varphi} = \frac{C_c\ o}{} \qquad (58j$$

To optimize CPriin Eq.(58j , let Eq.(58) (d CP^^/ α φ) equal zero and solve for φ, which yields

$$\phi = \frac{\sqrt{C_{co}\lambda + \Theta_o C_{co}\lambda^2}}{C_{co}/\tau_a - \tau_{co}} \quad \text{к 59 J}$$

It can be found that the Eq.(54) is identical to Eq.(39). This indicates the instantaneous optimum slope is tne same for both the heat pump and the refrigeration systems. Moreover, it implies tnat the zeolite can be utilized without considering the use for heat pump or tne refrigeration.

The derivation of the optimum slope for the refrigeration system performance will be neglected due to the complicated implicit matnematical expressions involved. Eased on Eq. (55), the maximum ref irgeration system performance can be numerically found for eacn value of the absorbent slope. Therefore, the relationship between the maximum refrigeration system performance and the slope can be acquired.

CHAPTER IV

RESULTS AND DISCUSSION

4.0 Zeolite Heat Pump System

Expressions for the thermodynamic properties of the solar zeolite heat pump and refrigeration system were developed in the previous chapter. In this present chapter, the various governing parameters which describe the heat pump and refrigeration system performances were studied for various zeolite types. The ideal zeolite properties for optimum system performance were also explored.

4.1 Absorption and Desorption Temperatures

The absorption and desorption temperatures of each zeolite were determined from the zeolite properties and the condenser and evaporator temperatures. As mentioned before, the zeolite properties, m_z and C_z, are related to the constant water-mass concentration lines on a log P_Y versus $1/T_2$ graph for each zeolite.

In the present work, various zeolites were used to describe the zeolite heat pump and refrigeration systems as shewn in Table 1 .

Table 1 Properties for various zeolites

Zeolite	Slope, mz (1/K)	$x_{¿}$	Origin
ZSC	25OO-29OO	0.28-0.16	S. C. CHANG [10]
UCA	2500-2800	0 .20-0.12	Union Carbide [22]
UC5A	2400-2900	0.18-0.11	Union Carbide [22]
UCI3	2400-2800	0.22-0.13	Union Carbide [22]
NaZ	2700-3200	0.31-0.16	M. M. Dubinin [8]

Figure 11a shows the log P_v versus $1/T_Z$ graph for zeolite ZSC, which was acquired form S. C. Chang[10]. Figures 11b to 11d are for zeolites UCAA, UC5A, and UC13, which are obtained form Union Carbide Corp.[22], while a similar figure for zeolite NaZ fron M. M. Dubinin[8] is shown in Fig. 11 e. Moreover, it should be noted from Tchernev [] 4] that natural zeolites were found to have heat of absorption, ΔH, values around 2650 Kj/Kg (1200 Btu/lbm) , while synthetic zeolites have ΔH values around 3980 Kj/Kg (1800 Btu/lbm) .

Since pairs of absorption and desorption temperatures can be obtained using Eqs. (28) and (29), a T_v versus T_z plot can be established for each zeolite type. Figures 12a, 12b, 12c, 12d and 12e illustrate the relationship between the vapor temperature, T_v, and the zeolite temperature, T_z, for zeolites ZSC, UCAA, UCA, UC13, and NaZ, respectively. These zeolite characteristics will be used in the following sections to compute the system performances corresponding to the various zeolites.

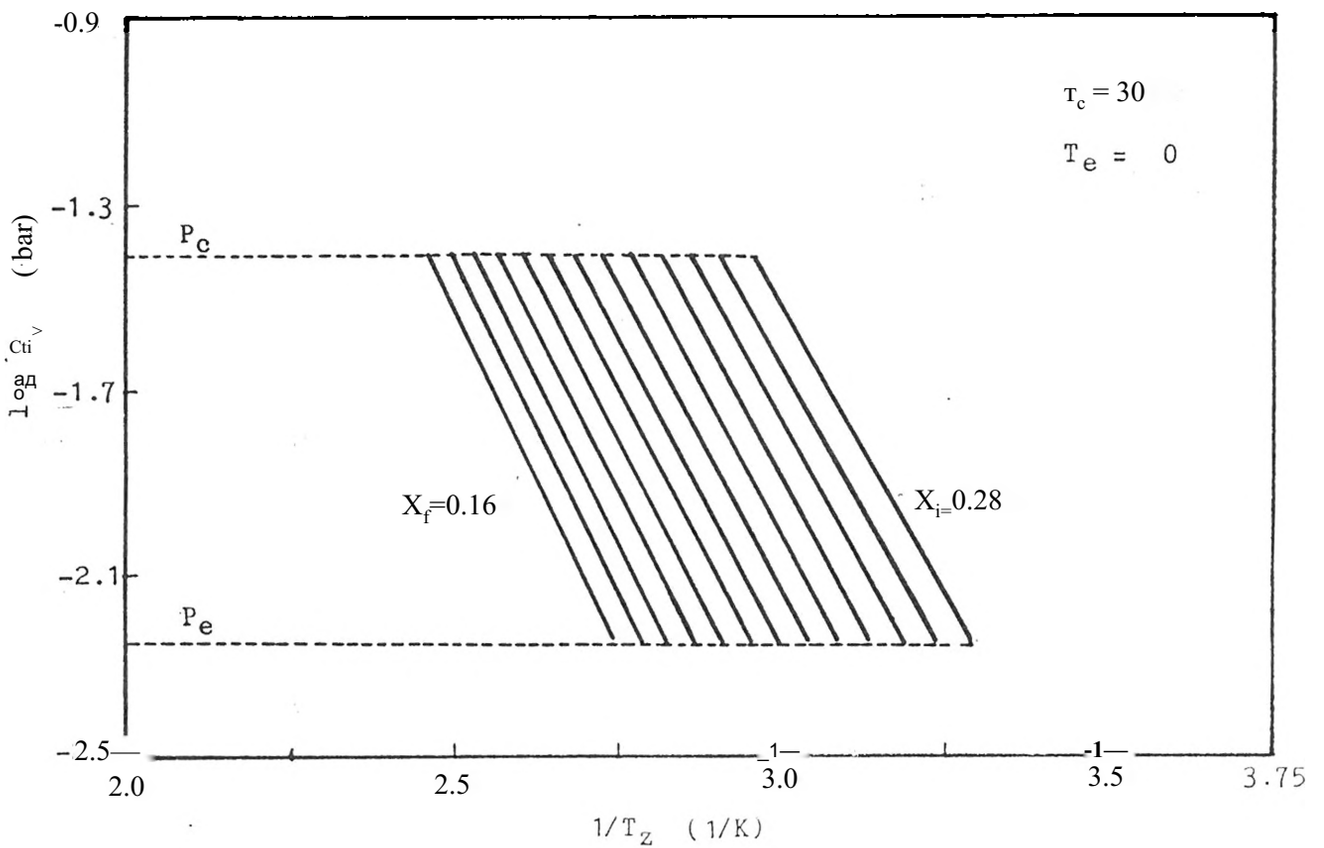

Fig. 11a The log P_v versus $1/T_z$ graph for zeolite ZSC.

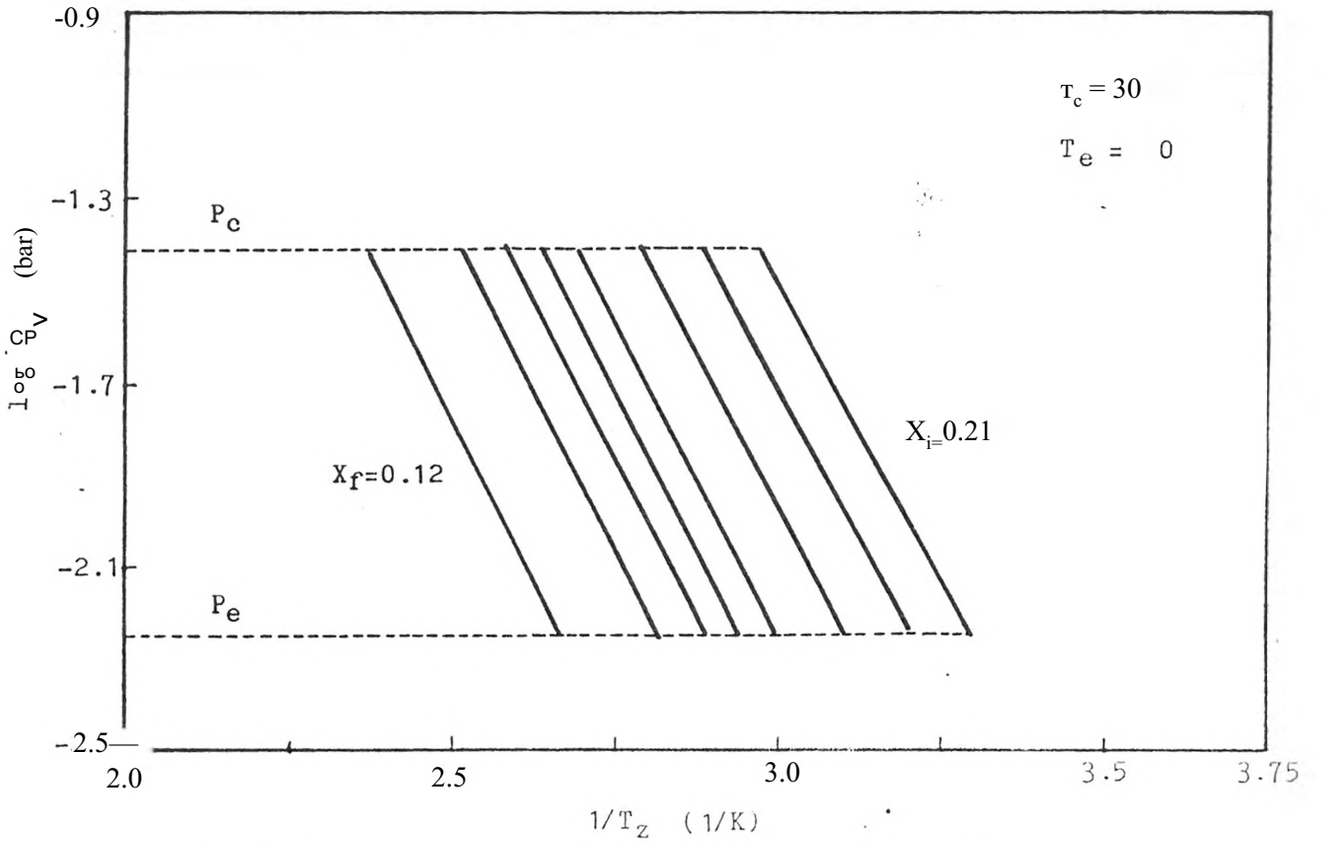

Fig. 11b The log P_v versus $1/T_z$ graph for zeolite UC4A.

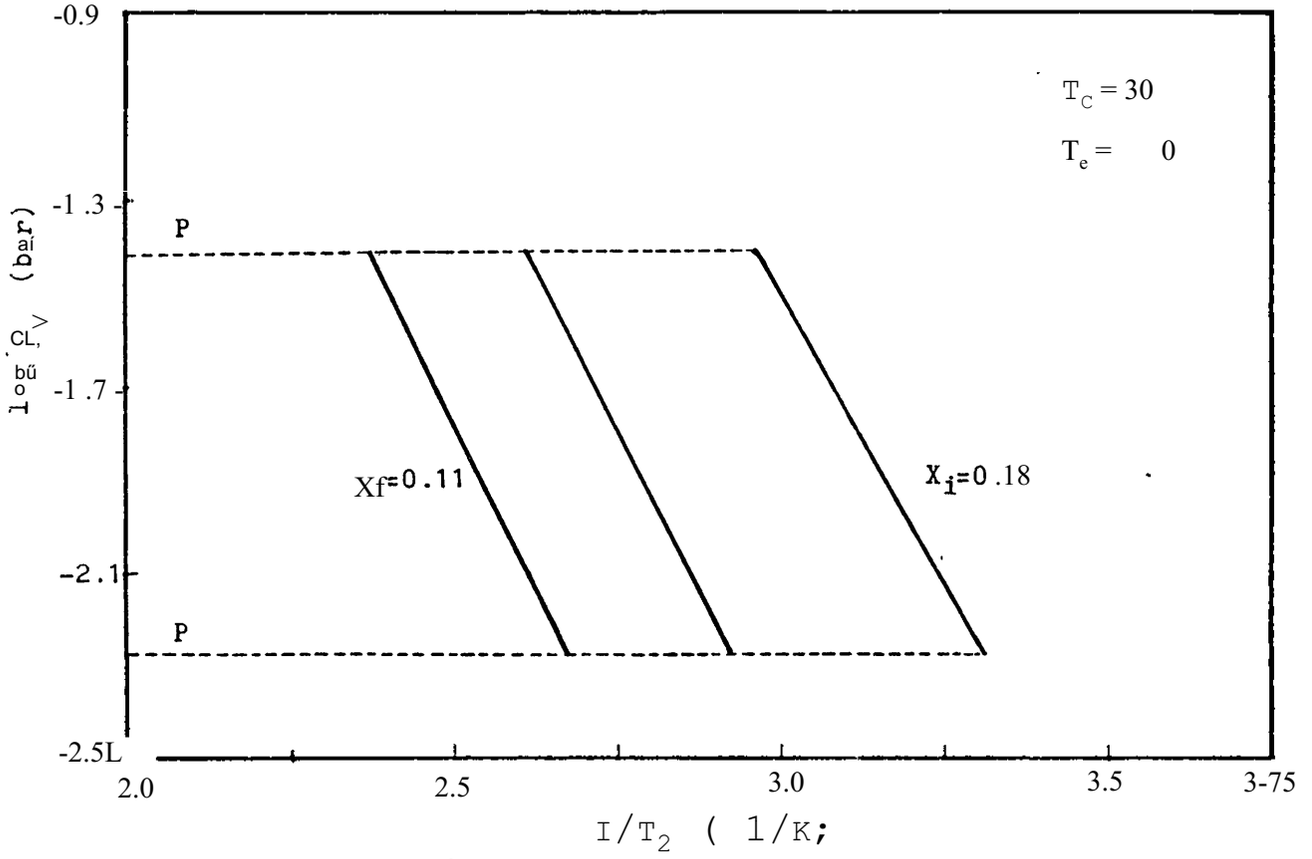

Fig. 11c The log P_y versus 1/T graph for zeolite UCA.

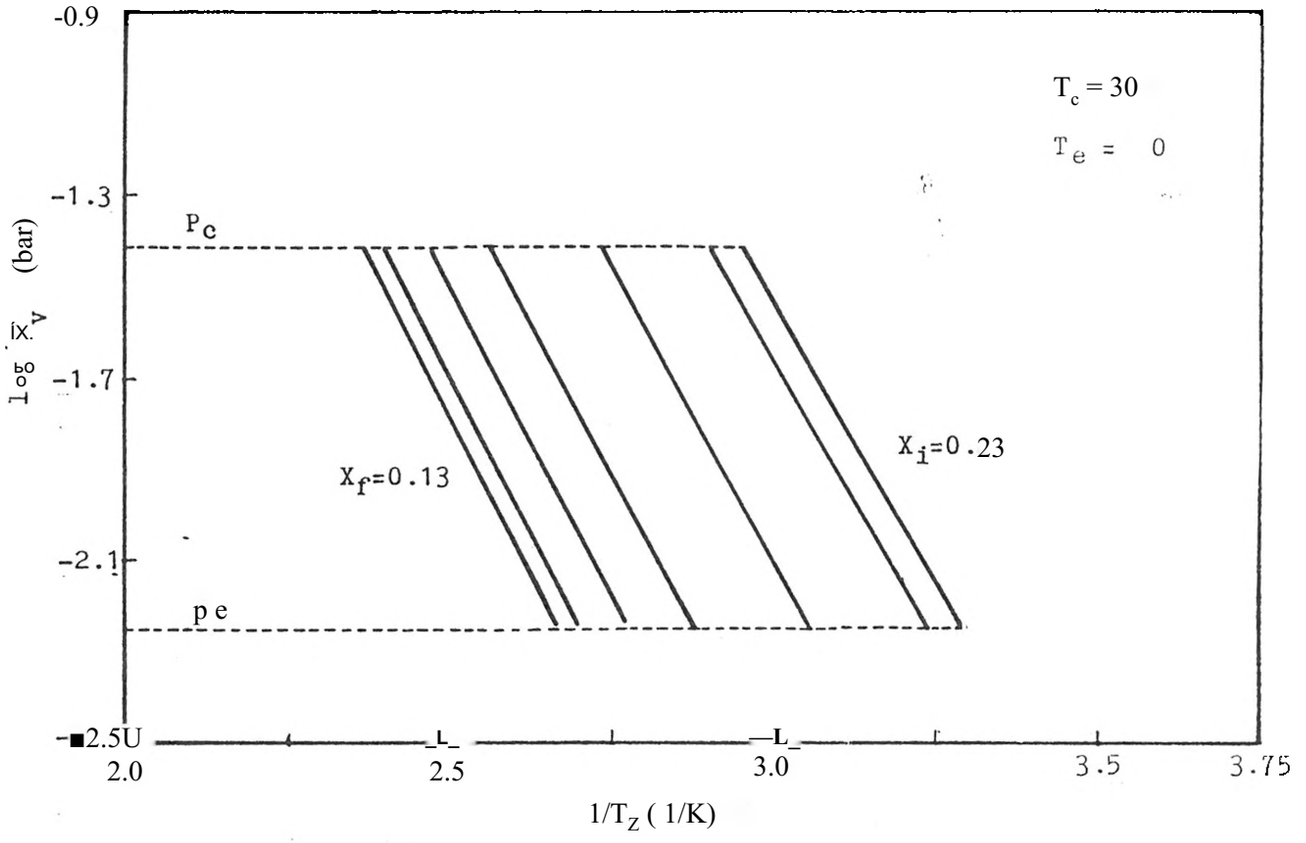

Fig. 11d The log P_y versus $1/T_z$ graph for zeolite UC13.

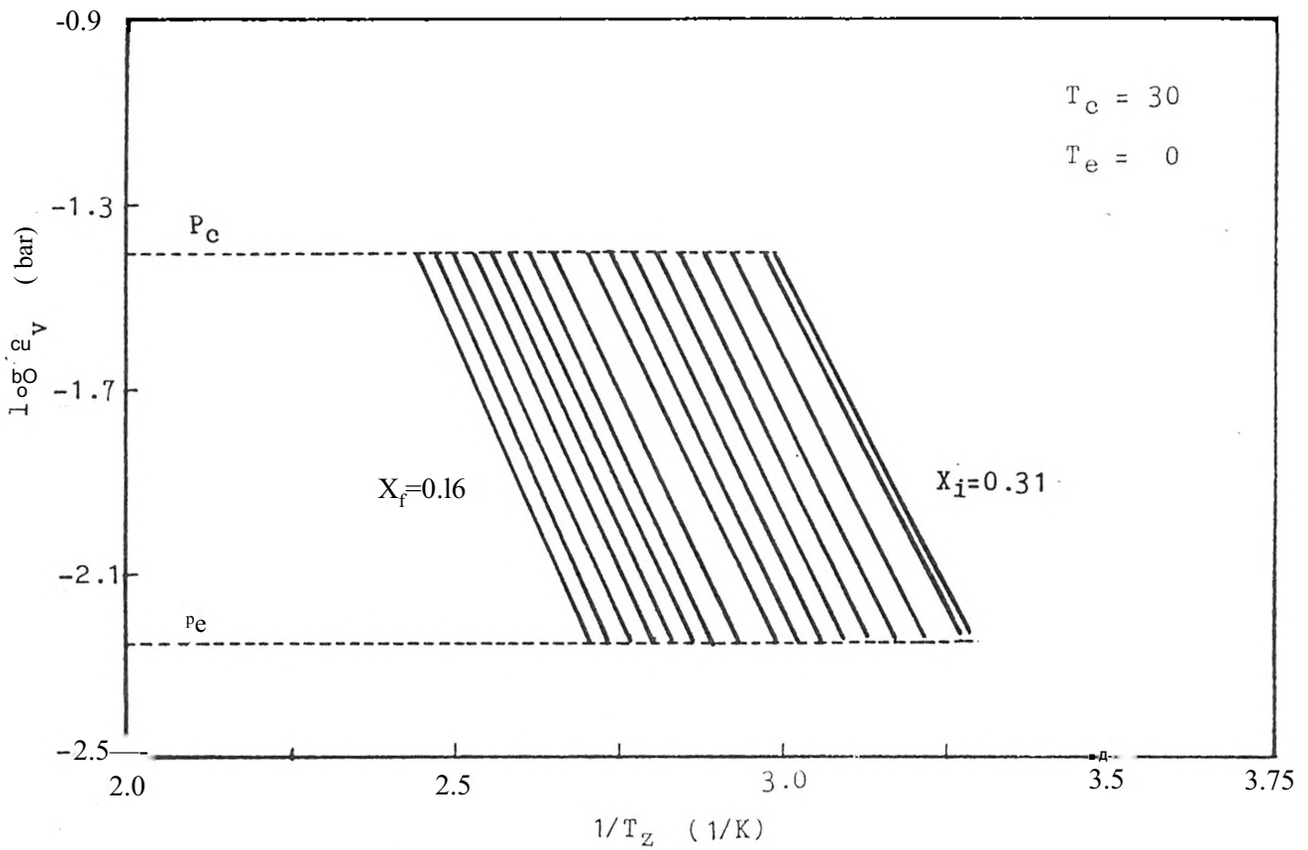

Big. 11e The log P_y versus 1/T graph for zeolite NaZ
z

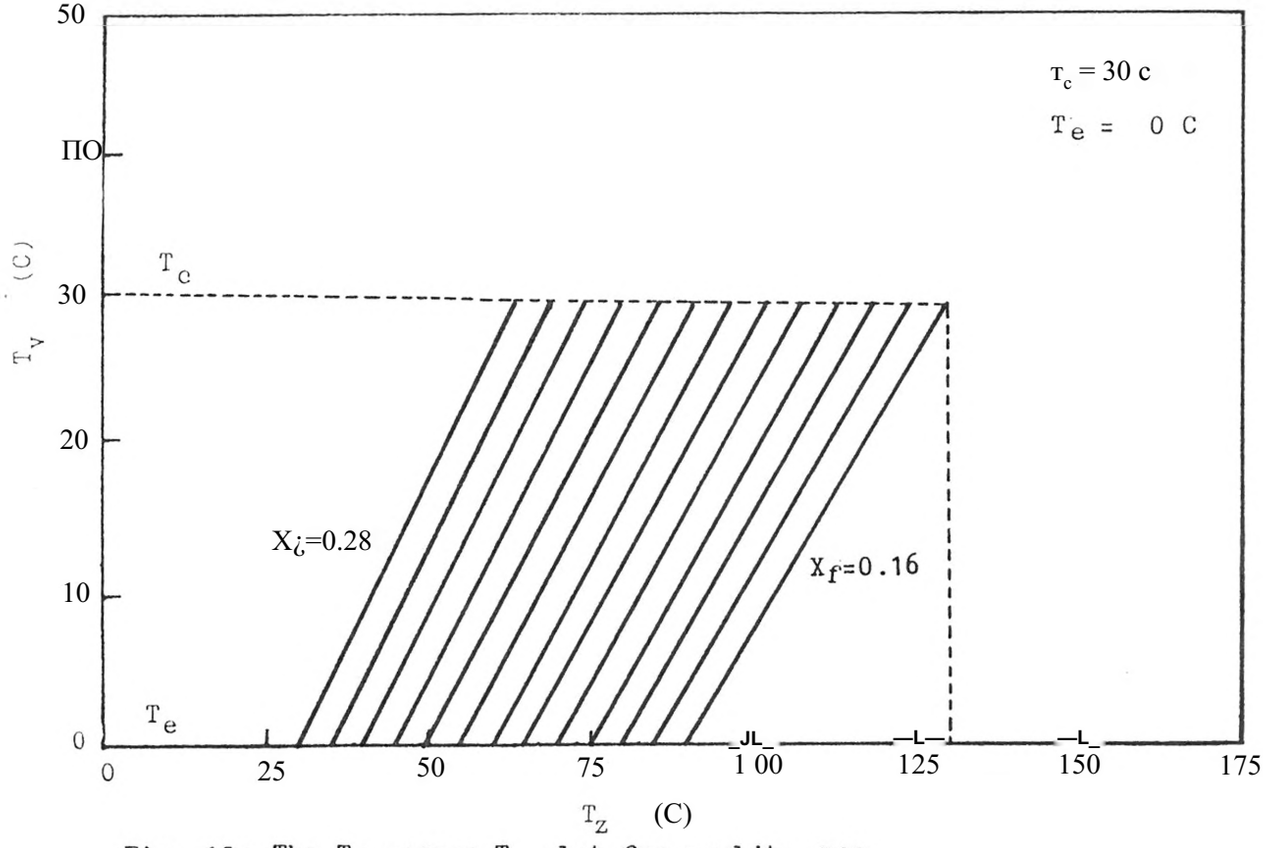

Fig. 12a The T_v versus T_z plot for zeolite ZSC.

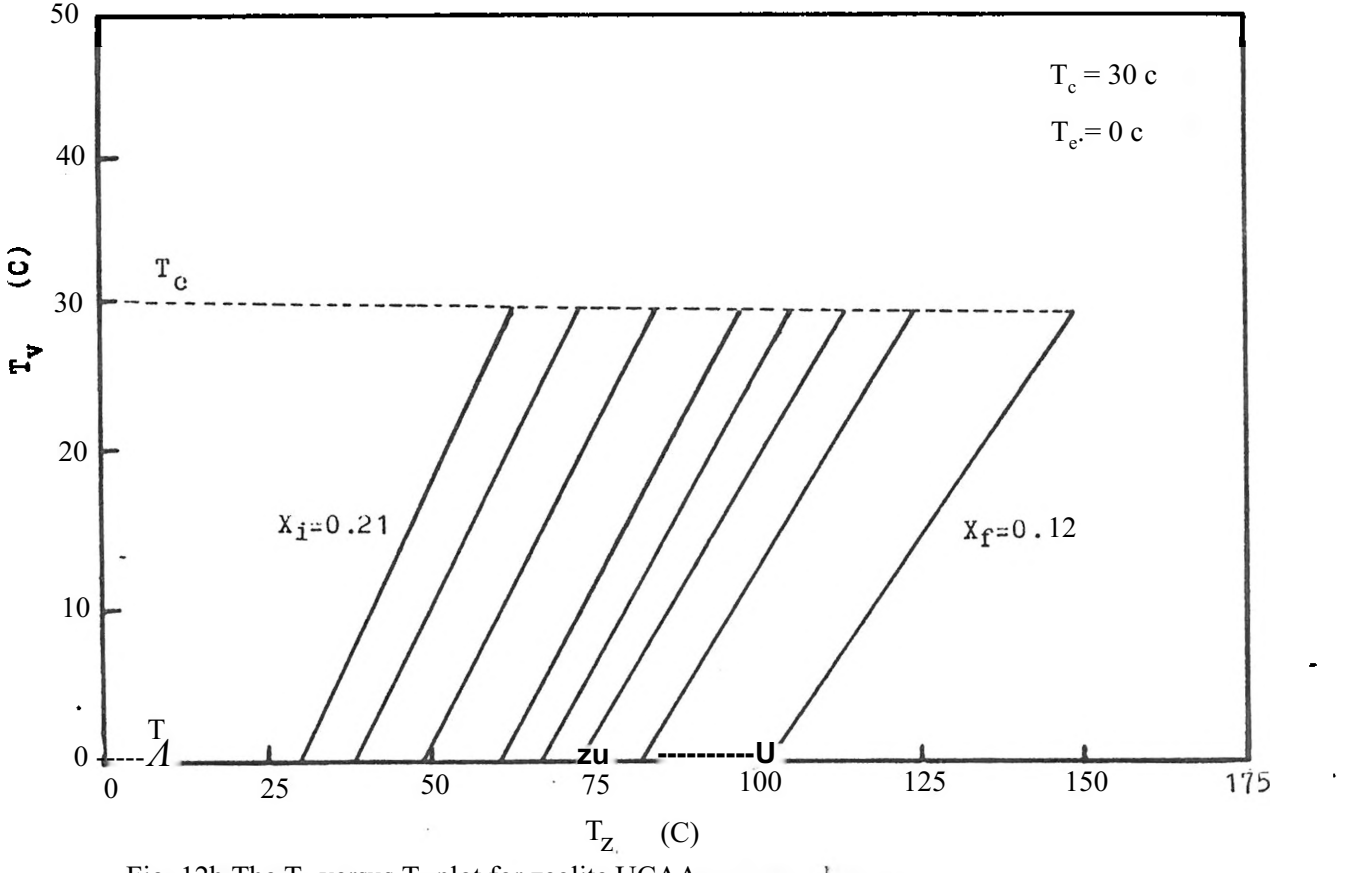

Fig. 12b The T_y versus T_z plot for zeolite UCAA

Cl>
o

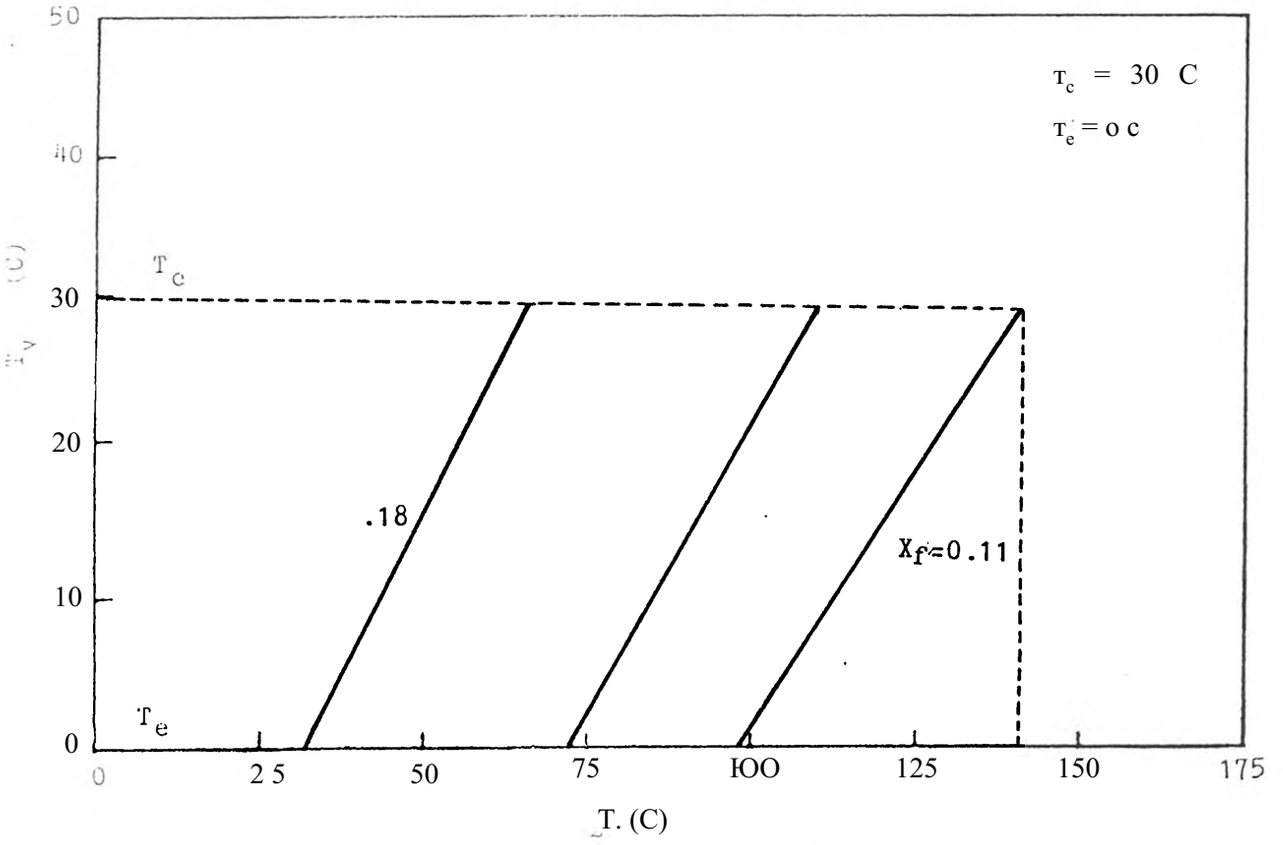

Fig. 12c The T_y versus T_z plot for zeolite UCA.

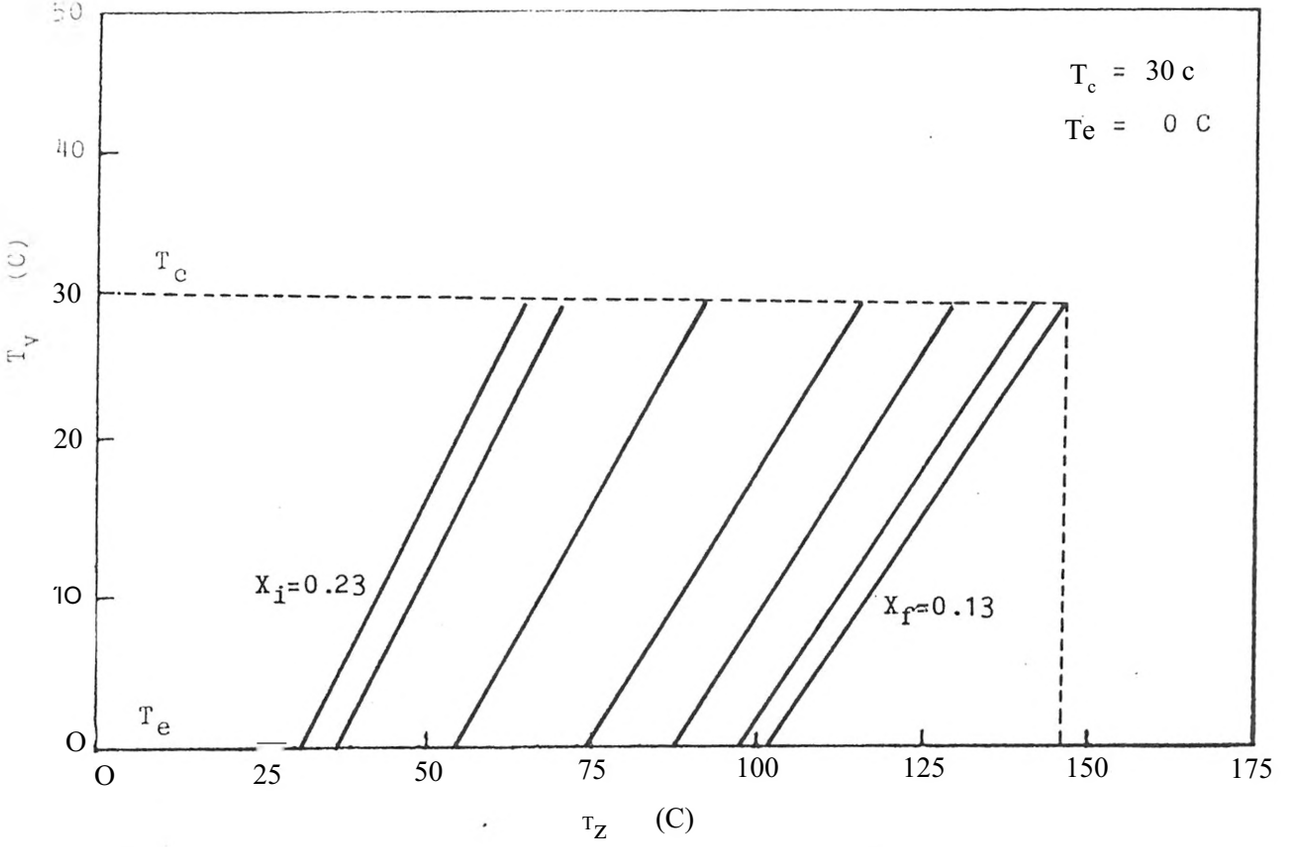

Fig. 12d The T_y versus T_z plot for zeolite UC13

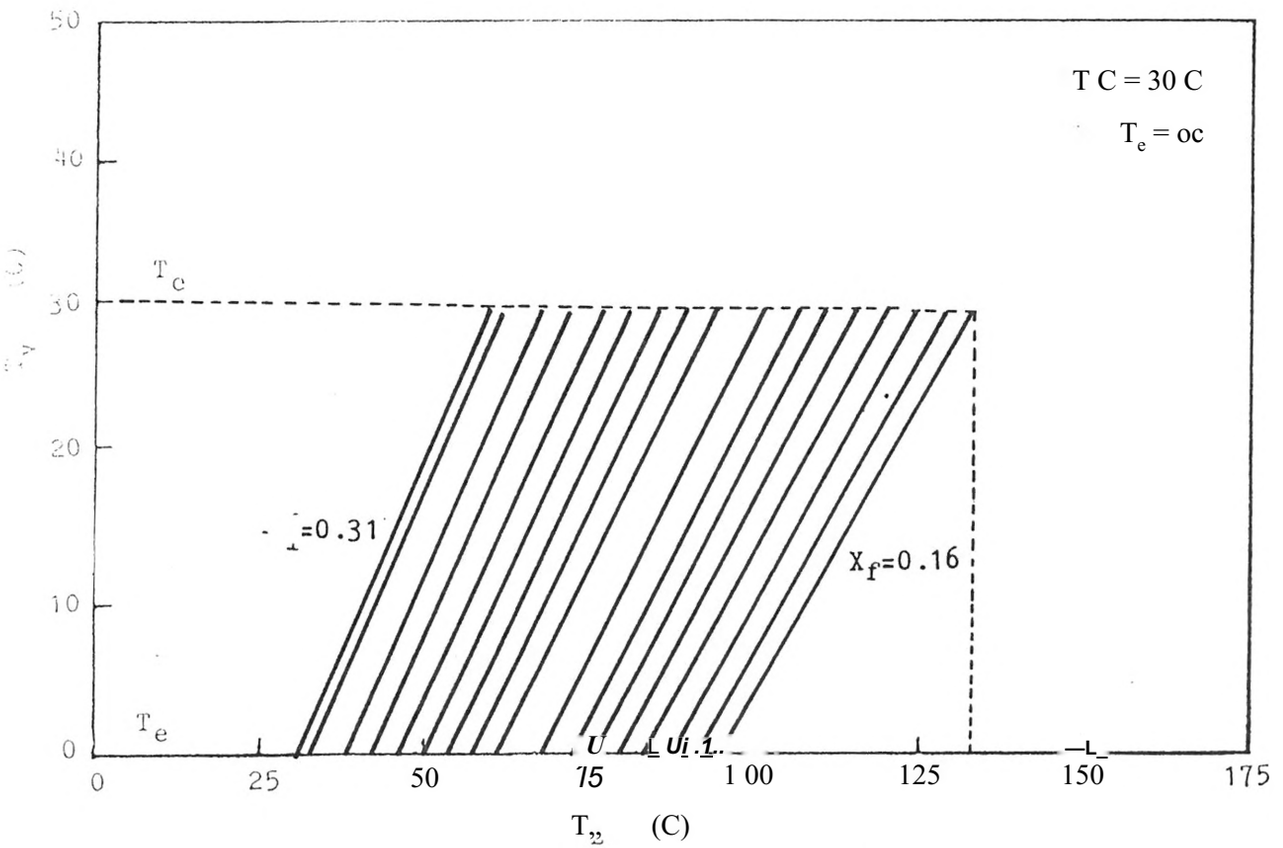

Fig. 12é The T versus T_{2} plot for zeolite NaZ

4 .2 Effect of Absorbent Slope Upon _ Desorjption Temperature

The solar collector efficiency is an important parameter in determining system performance for both the heat pump and refrigeration systems. According to Eq.(31), the zeolite temperature strongly affects the solar collector efficiency. Therefore, the heat pump and refrigeration system performances will be dependent on the zeolite desorption temperature. A low desorption temperature will yield a high solar collector efficiency, thus a high system performance, and a high desorption temperature will likewise yield a lower system performance.

Moreover, a low initiation desorption temperature will result in a high solar collector efficiency for the desorption process. Hence, the system performance will be increased if the initiation desorption temperature can be kept low. The absorption properties equation, Eq. (29), shows the relationship between the desorption temperature and the absorbent slope, m_z. By holding the other parameters in Eq. (29) constant, the zeolite desorption temperature can be treated as a function of the slope of the constant mass concentration lines.

Figure 13 shows the variation of the desorption temperature for different values of m_z. The zeolite temperatur eś, T_z p T_{z2}, and T_{ζ}·^ are based on three different absorbent slopes, m_zp m_Z£, and m_z^, respectively. It is seen that the high slope value yields a lower zeolite desorption initiation temperature. This implies the solar collector

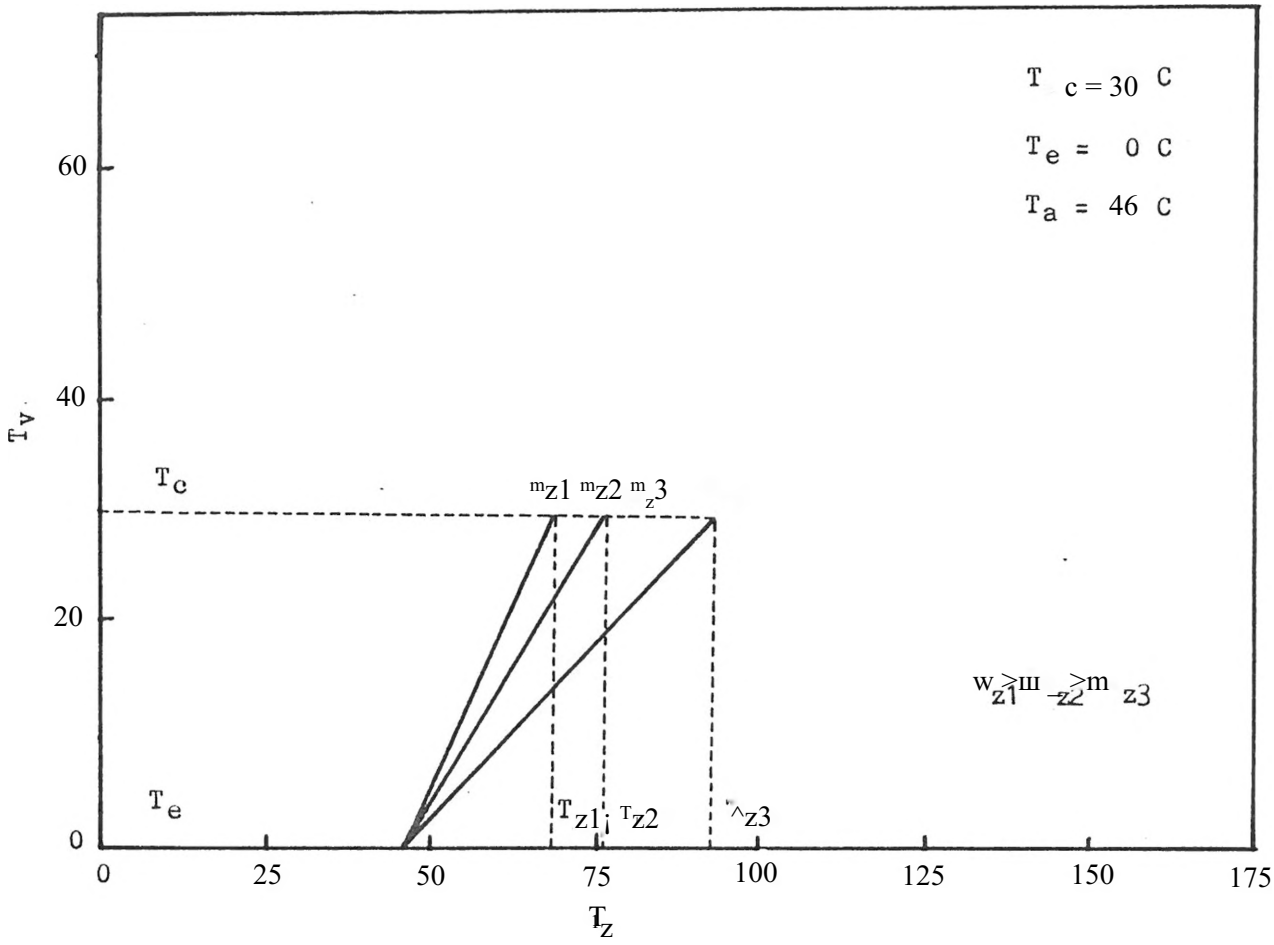

Fig. 13 Effect of tue siope, m_z, on desorption temperature.

efficiency will be improved by a high absorbent slope. However, the system performances for both the heat pimp and refrigerator are also influenced by the heat of absorption, ΔH, as well as by the solar collector efficiency. A high slope(m_z) value also means a high heat of absorption, (as seen in Eq.(18)) and could reduce the system performance (as seen in Eqs.(7) and (49)). The determination of the optimum absorbent slope value is important to maximize system performance for the solar zeolite system. The optimization of m_z with respect to system performance will be illustrated later.

4.3 Heat Pump System Performance and Zeolite Ten per at ure

The dependence of the heat pimp system performance on zeolite temperature for zeolite ZSC is shown in Fig. 14a. Curve A is the Carnot cycle efficiency, Eq. (4); curve B represents the Carnot cycle efficiency based on pairs of absorption and desorption temperatures, Eq. (5); curve C stands for the absorption cycle efficiency, Eq. (14); curve D is the mean system performance for the heat punp neglecting the heat capacity losses in the absorption process, Eq. (34b); curve E represents the mean system performance for the heat pump considering the heat capacity losses in the absorption process, Eq.(35); curve F is the system performance for a solar collector alone. Curve F demonstrates the use of a solar collector with no zeolite heat punp.

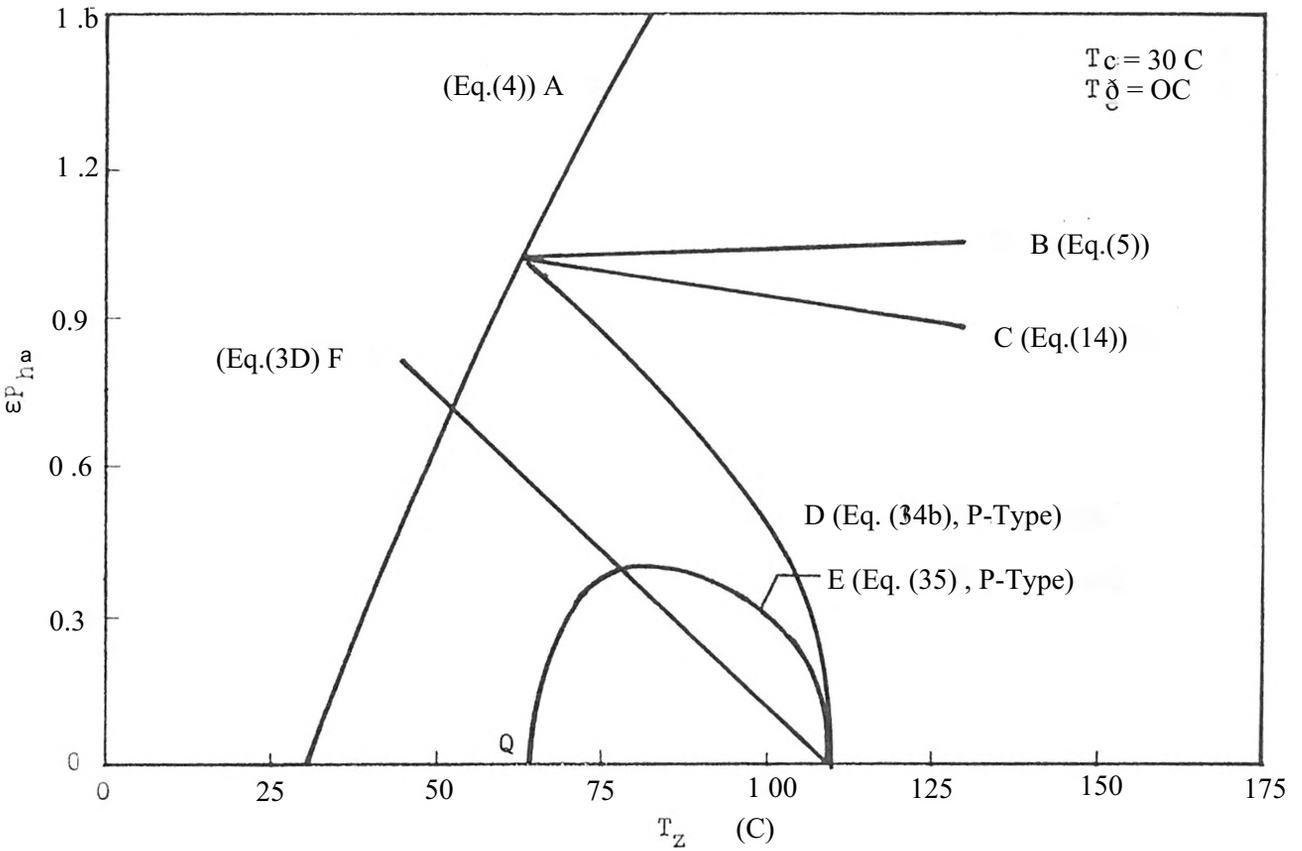

Fig. 14a Dependence of heat pump system perofrmance on zeolite temperature for zeolite ZSC.

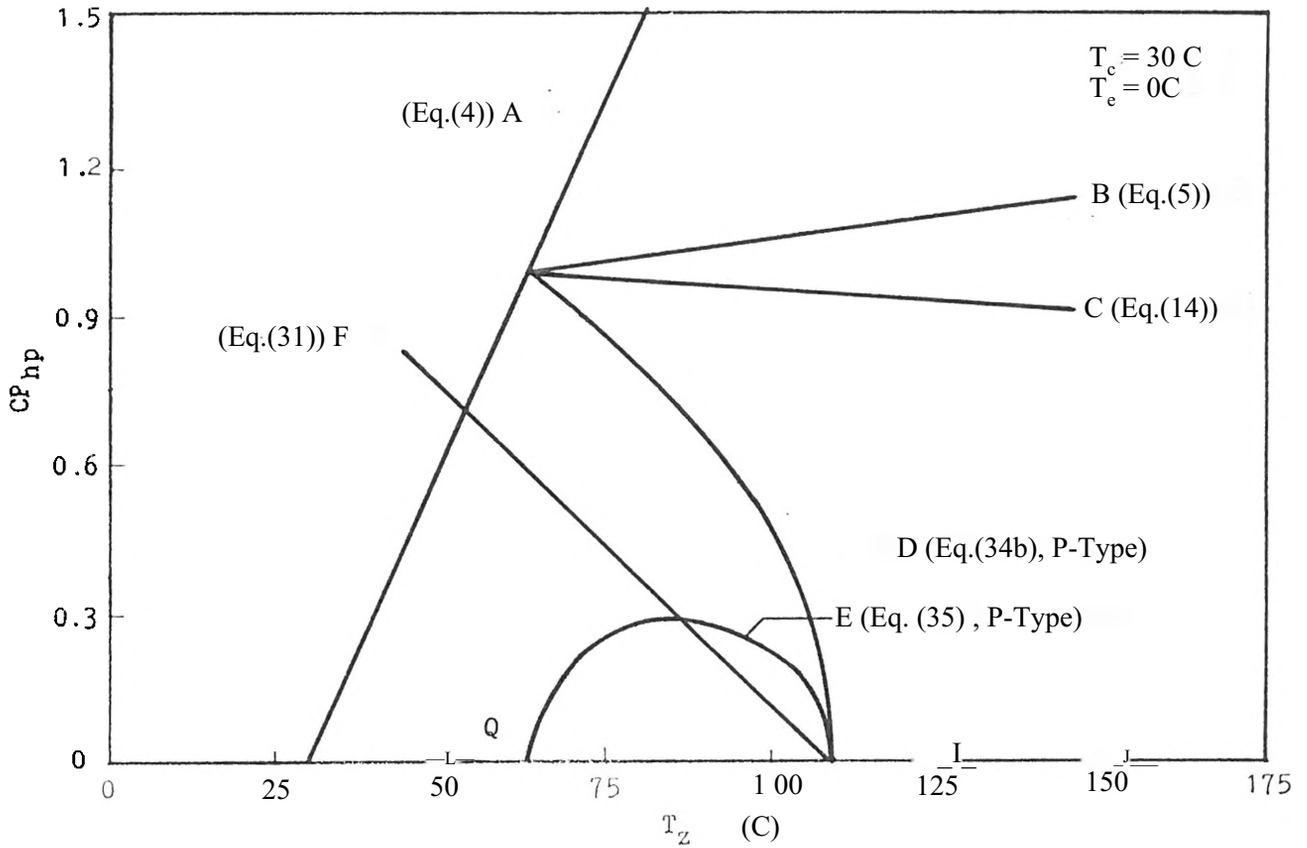

Fig. 14b Dependence of heat pump system perofrmance on zeolite temperature for zeolite UC4A.

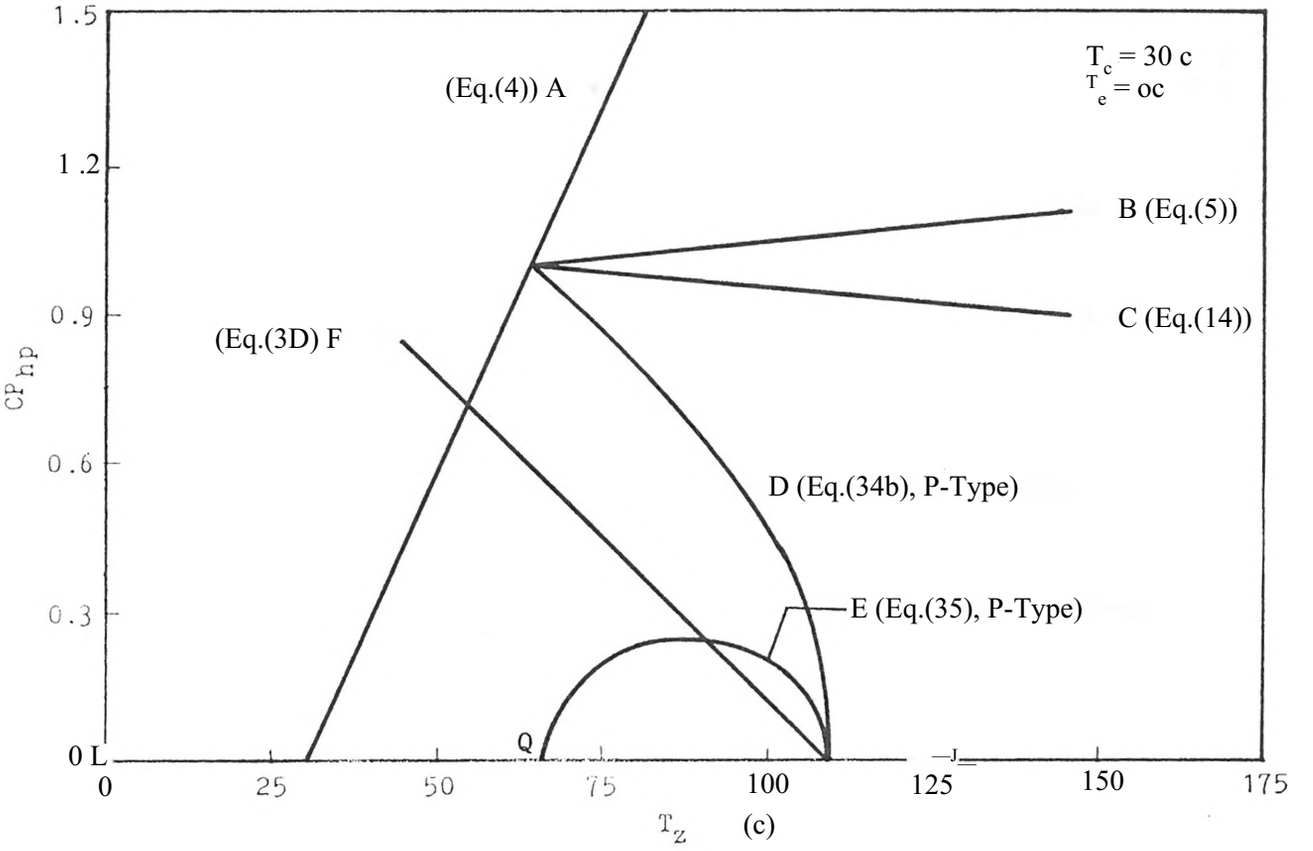

Fig. 14c Dependence of heat pump system per of rmance on zeolite temperature for zeolite UCA.

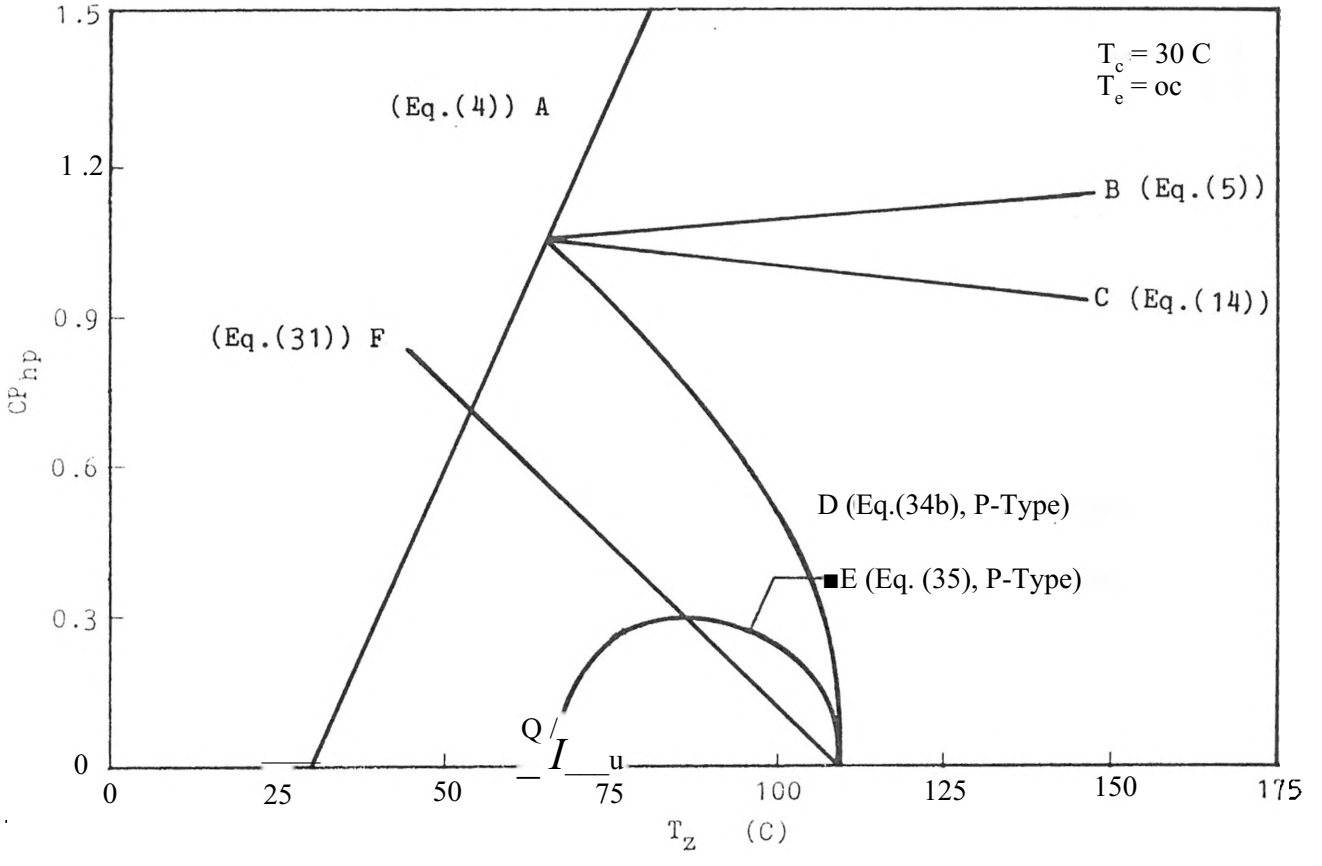

Fig. 1 4d Dependence of heat pump system pertofrmance on zeolite temperature for zeolite UC13.

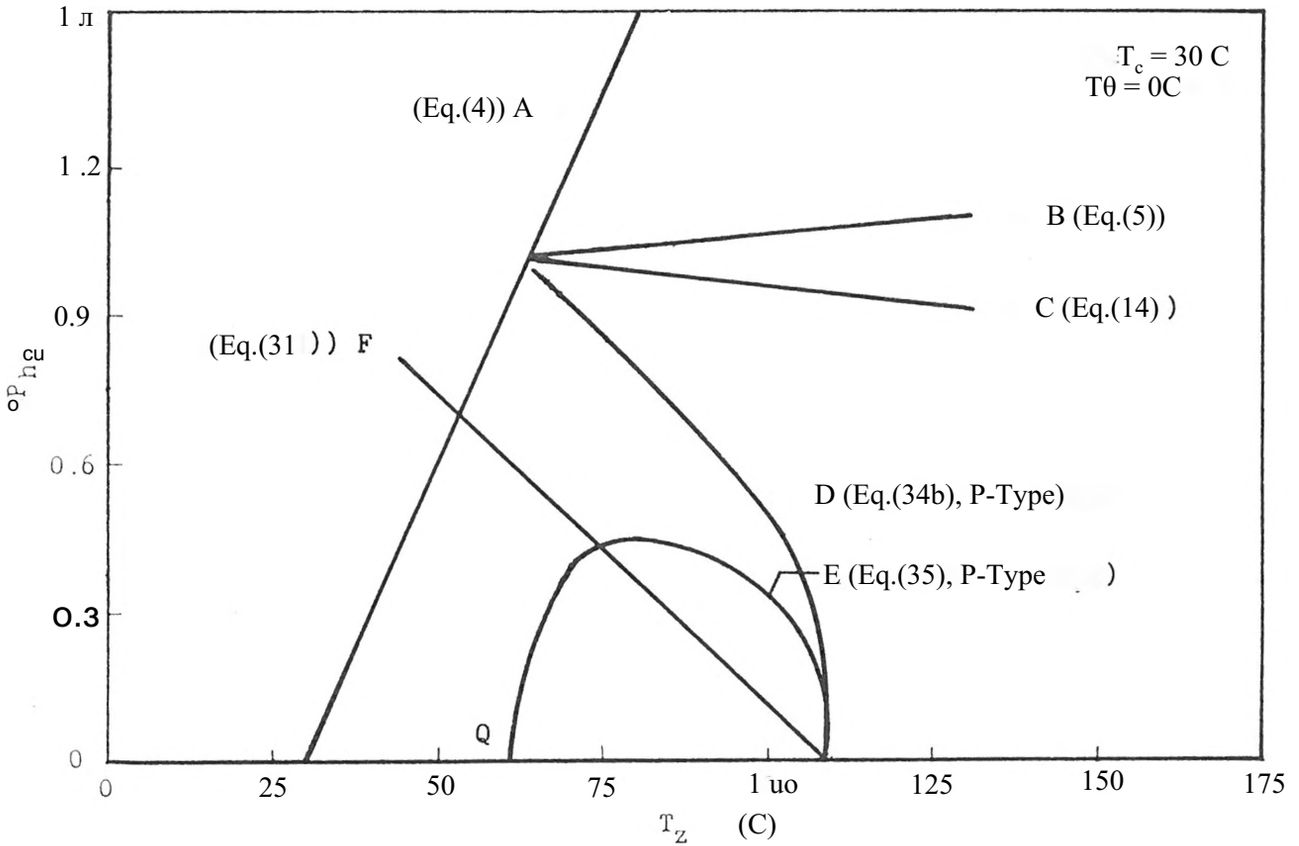

Fig. 14e Dependence of heat pump system perofrmance on zeolite temperature for zeolite NaZ .

In comparison to curve E, curve F has a higher system performance at lower temperatures (under 80 C) . However, with increasing zeolite temperature, the zeolite system performs better than the solar collector alone. Furthermore, the collected solar energy can be stored with a zeolite system, while a solar collector alone can not function as a storage device.

Since there is no refrigerant mass circulating in the heat pump cycle until the zeolite temperature reaches the initiation desorption temperature, it can be seen that the curves for mean system performance, curves D and E, will remain zero until the initiation desorption temperature, point Q in Fig. 14a, is attained. After the zeolite temperature reaches the initiation desorption temperature, the heat pump cycle starts to operate. Curve D jumps abruptly at the initiation desorption temperature because of neglecting the heat capacity losses in the absorption process. With increasing zeolite temperature, curve D tends to decrease in a similar fashion to the solar collector efficiency. The heat capacity losses (curve E) in the absorption process can influence the heat input to and the heat output fram the heat pump absorption system(see Eq.(35)).

Curve E gradually increases with increasing zeolite temperature from point Q in Fig. 14a, as mass is desorbed fram the zeolite. However, the solar collector efficiency influences the actual heat input to the heat pump absorption cycle. The heat pump system performance will

decline at high zeolite temperatures due to the decreasing solar collector efficiency. Similar figures for zeolites UC4A, UC5A, UC13 , and NaZ are shown in Figs. 14b, 14c, 14d and 14e, respectively. Since the P-type solar collector is the most commonly used, the heat pimp system performance for the P-type solar collector can be used to determine the effectiveness of a solar zeolite system. As seen, the heat pimp system performances for zeolites ZSC and NaZ are higher than those for zeolites UC4A, UC5A and UC13.

4.4 Effect of Solar Collector Type Upon Heat Pump System Performance

In addition to the collector temperature, the solar collector type can influence the heat pump system performance. Three solar collector types were selected for this parameter study (see Fig. 9). Also, an industrial waste heat source was simulated by assuming a solar collector efficiency of unity in the governing equations.

Figure 15a illustrates the mean heat pump system performances, Eq. (35), for zeolite ZSC using different solar collector types and the waste heat source. Curve W is the mean system performance for a waste heat source. Due to the high conversion efficiency for waste heat, curve W rises higher than the other curves and increases with zeolite temperature. Curve V represents the mean system performance operating with a V-type solar collector. Since the V-type solar collector has a high efficiency (see Fig. 9), the system performance will be higher

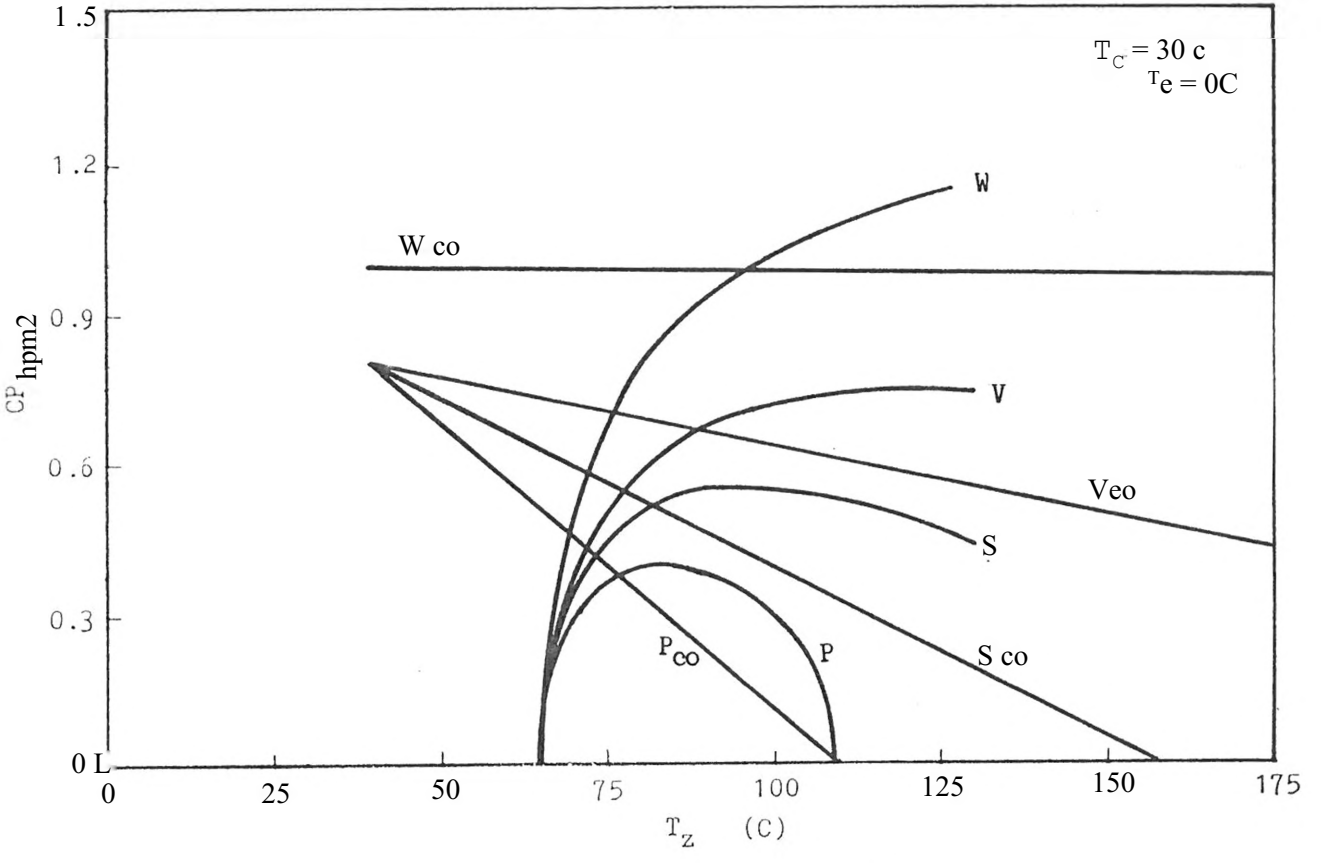

Fig. 15a Effect of solar collector type upon heat pump system performance for zeolite 7 SC.

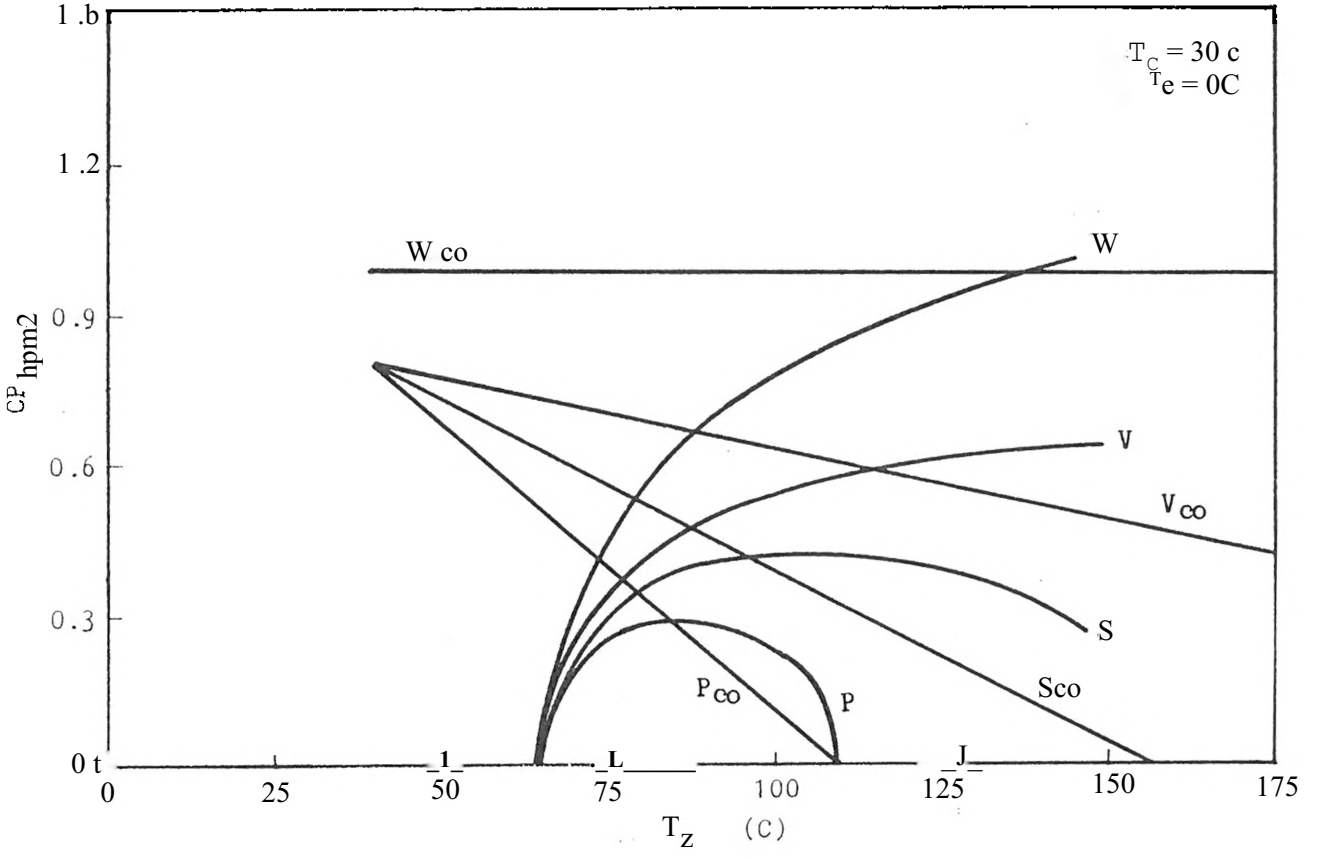

Fig. 15b Effect of solar collector type upon heat pump system performance for zeolite UCA l.

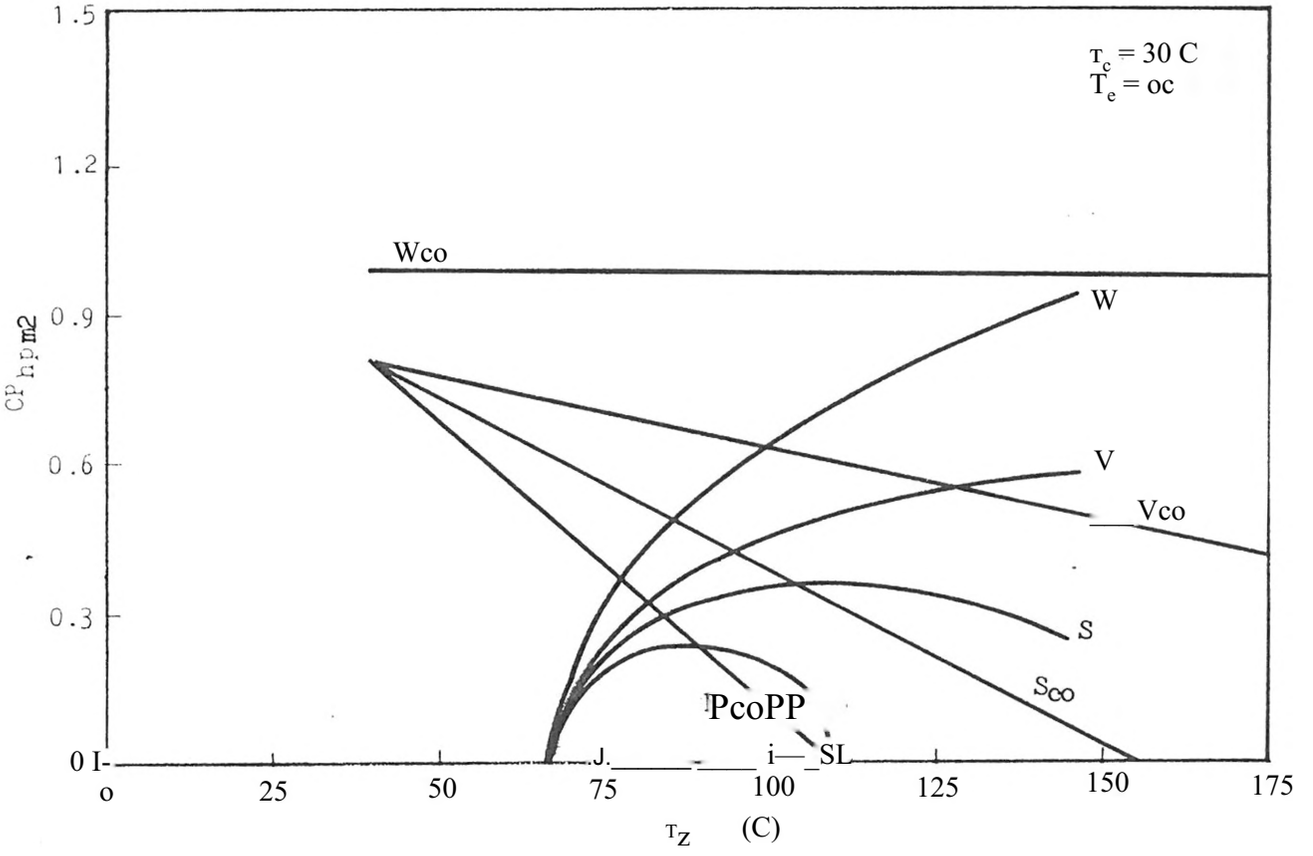

Fig. 15c Effect of solar collector type upon heat pump system performance for zeolite UCSA,

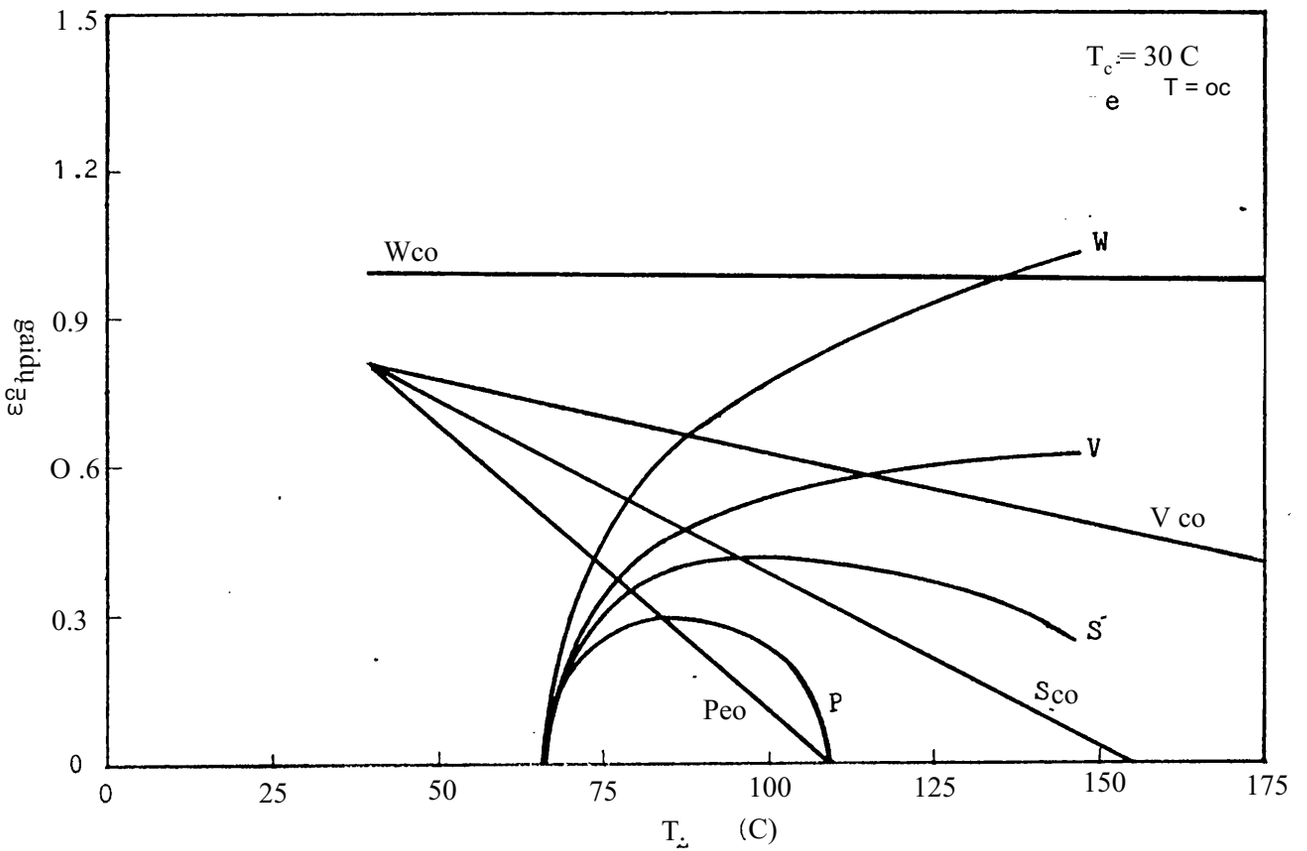

Fig. 15d Effect of solar collector type upon heat pump system performance for zeolite UC13 .

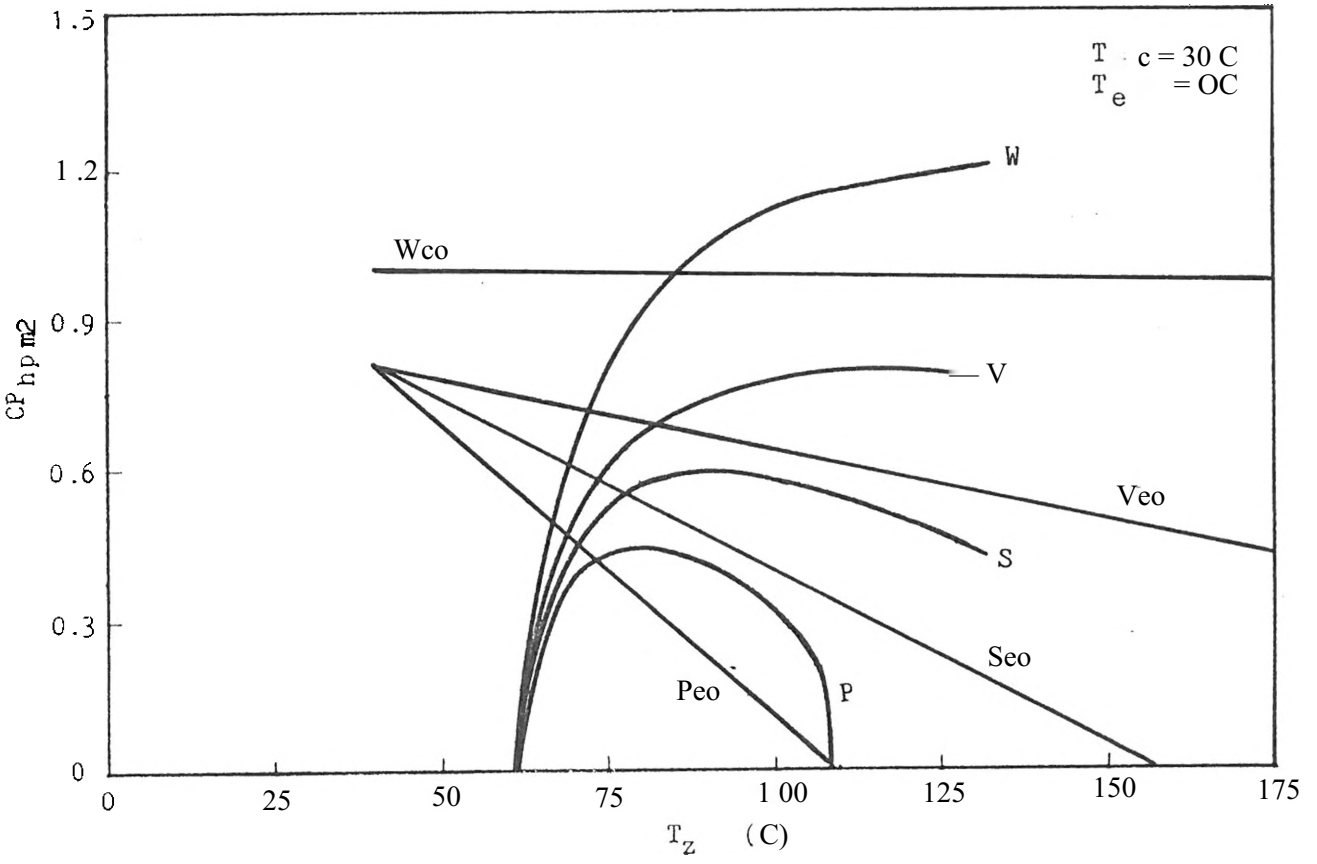

Fig. 15e Effect of solar collector type upon heat pump system performance for zeolite NaZ .

than the other collector types. Curve S decreases at high zeolite temperatures due to the low solar collector efficiency at higher temperatures. Curve P represents the mean system performance using a P-type solar collector. The solar collector efficiency for a P-type solar collector will decrease to zero as the zeolite temperature reaches 112 C. Therefore, the heat pump system performance for a P-type solar collector reaches zero when the zeolite temperature approaches 112 C. Curves P_{co}, Sco, V_{co} and W_{∞} are the heat pump system performance for the P, S, and V-type solar collector and waste heat source alone. As seen, the zeolite heat pump can obtain a higher performance than the solar collectors at higher temperatures. In addition, because of the advantage of energy storage, the zeolite system still can operate when the solar energy is not available.

The effect of solar collector type upon heat pump system performance for the various types of zeolites, UC4A, UC5A, UC13 and NaZ, are shown in Figs. 15b, 15c, 1 5d and 15e, respectively. It is seen that the zeolites USC and NaZ still have higher performances than other zeolites.

4.5 Effect of Ambient Temperature Upon Heat Pump System Performance

The ambient indoor and outdoor temperatures determine the condenser and evaporator temperatures, respectively, in the heat pimp cycle. Figure 16a shows the heat pump performance curves corresponding to various condenser temperatures for zeolite ZSC. Curves A, B, C, D, and E

are the heat pump system performances based on condenser temperatures of 30, 35, 40, 45, and 50 C, respectively. As seen, the variation of condenser temperature changes the initiation desorption temperature of the zeolite system. A higher condenser temperature yields a higher initiation desorption temperature. A high initiation desorption temperature, inturn, yields a low solar collector efficiency. The system performance, thus, will be reduced by increasing condenser temperature. Also, the effect of condenser temperature on the heat pump system performance using other zeolite types is illustrated in Figs. 16b, 16c, 16d and 16e for zeolites UC4A, UCA, UC13, and ZNa, respectively. Similarly, the heat pump system performance for zeolites UCA A, UCA, UC13 and NaZ decrease with increasing condenser temperature. ZSC and NaZ still have higher performances than the other zeolites.

The effect of evaporator temperature on the heat pump system performance is shown in Fig. 17a. Curves A, B, C and D represent the ZSC heat pump system performance based on evaporator temperatures of 0, 5, 10, 15 C, respectively. According to the Eq. (29), the zeolite desorption temperature will not be influenced by the evaporator temperature. This implies the solar collector efficiency will be independent of the evaporator temperature. However, the heat capacity losses will be reduced by increasing the evaporator temperature (as seen in Eq.(39a)). Hence, the mean heat pimp system performance will be weakly influenced by the evaporator temperature. Figure 17a demonstrates that a high evaporator temperature will yield a high mean heat pump system

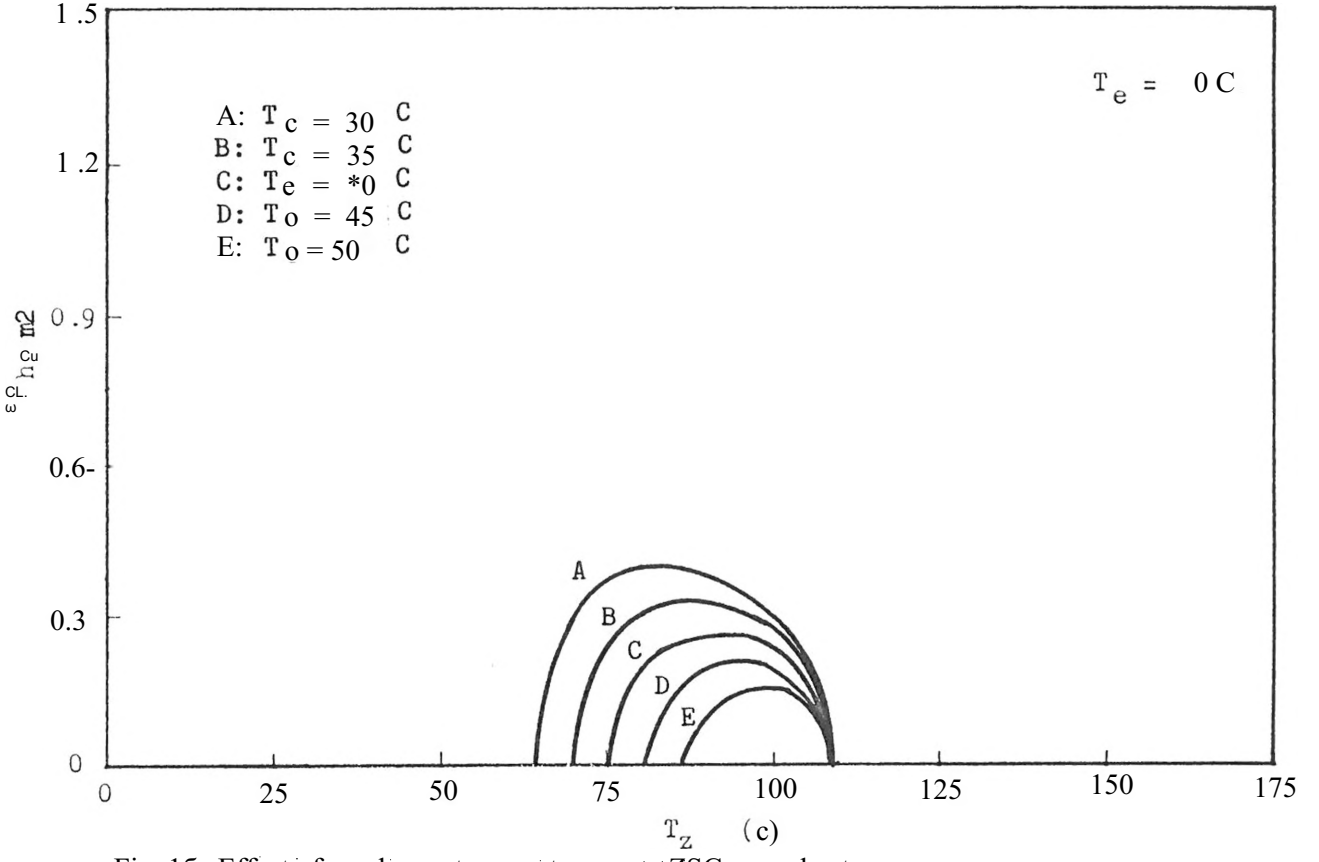

Fig. 16a Effect of condenser temperature upon ZSC mean heat pump system performance with a P-type solar collector.

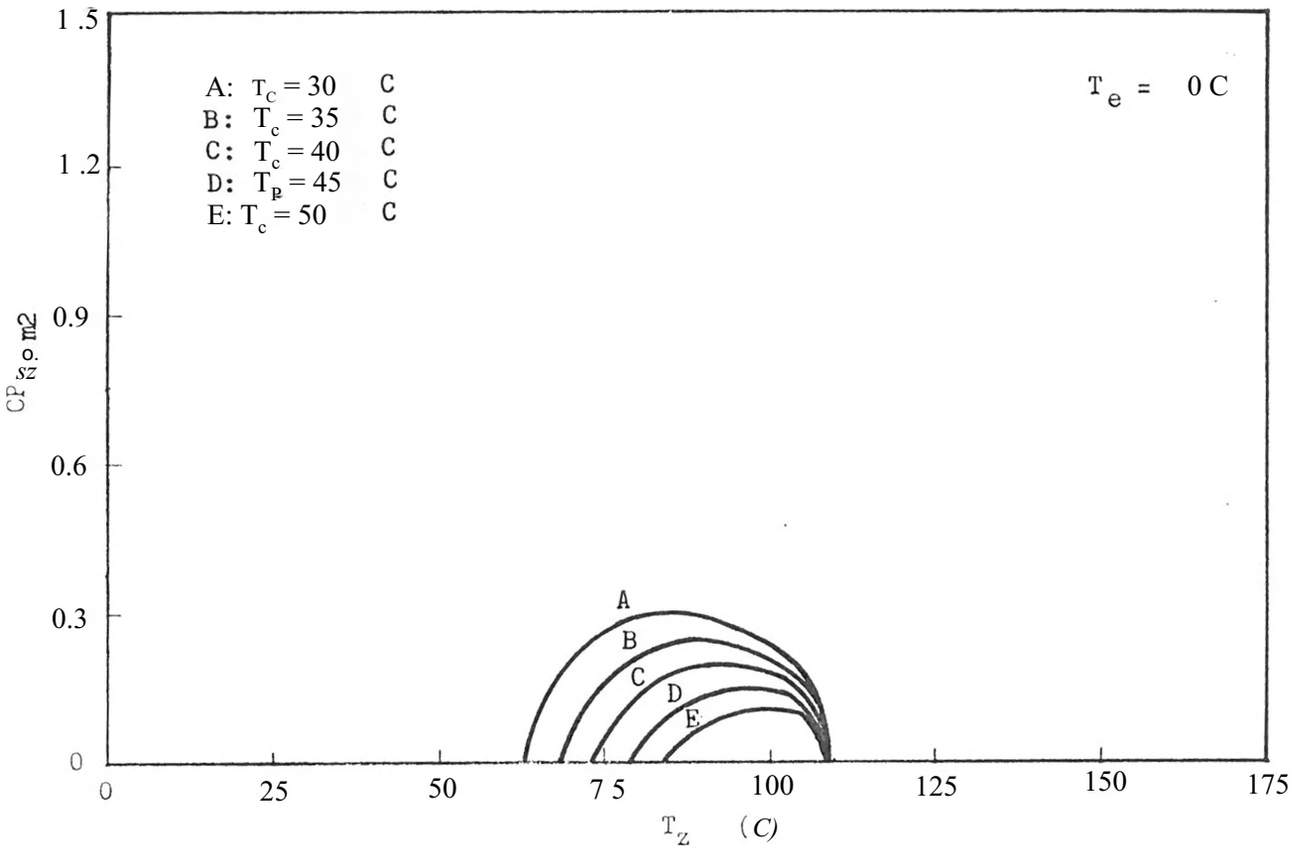

Fig. I6b Effect of condenser temperature upon UCAA mean heat pump system performance with a P-type solar collector.

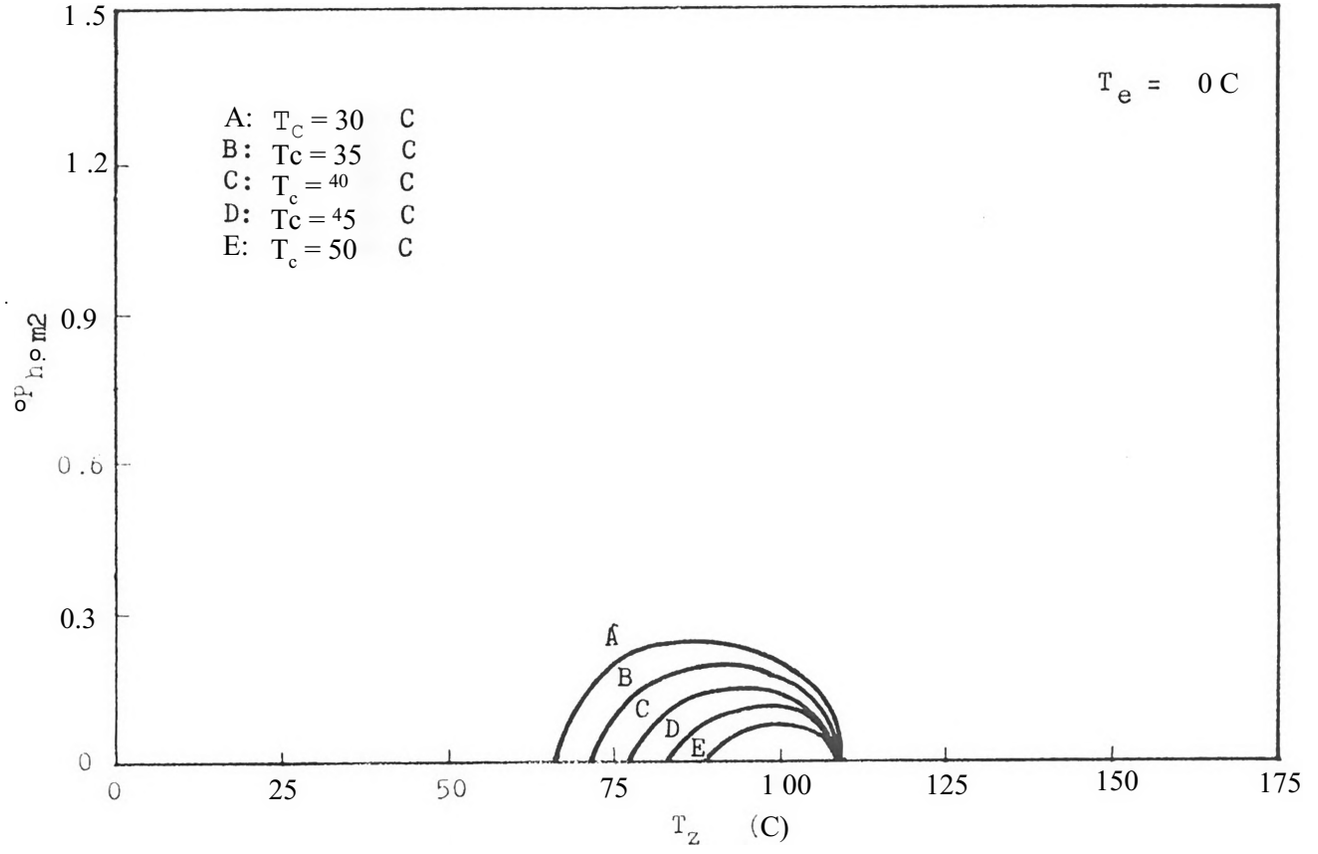

Fig. 16c Effect of condenser temperature upon UC5A mean heat pump system performance with a P-type solar collector.

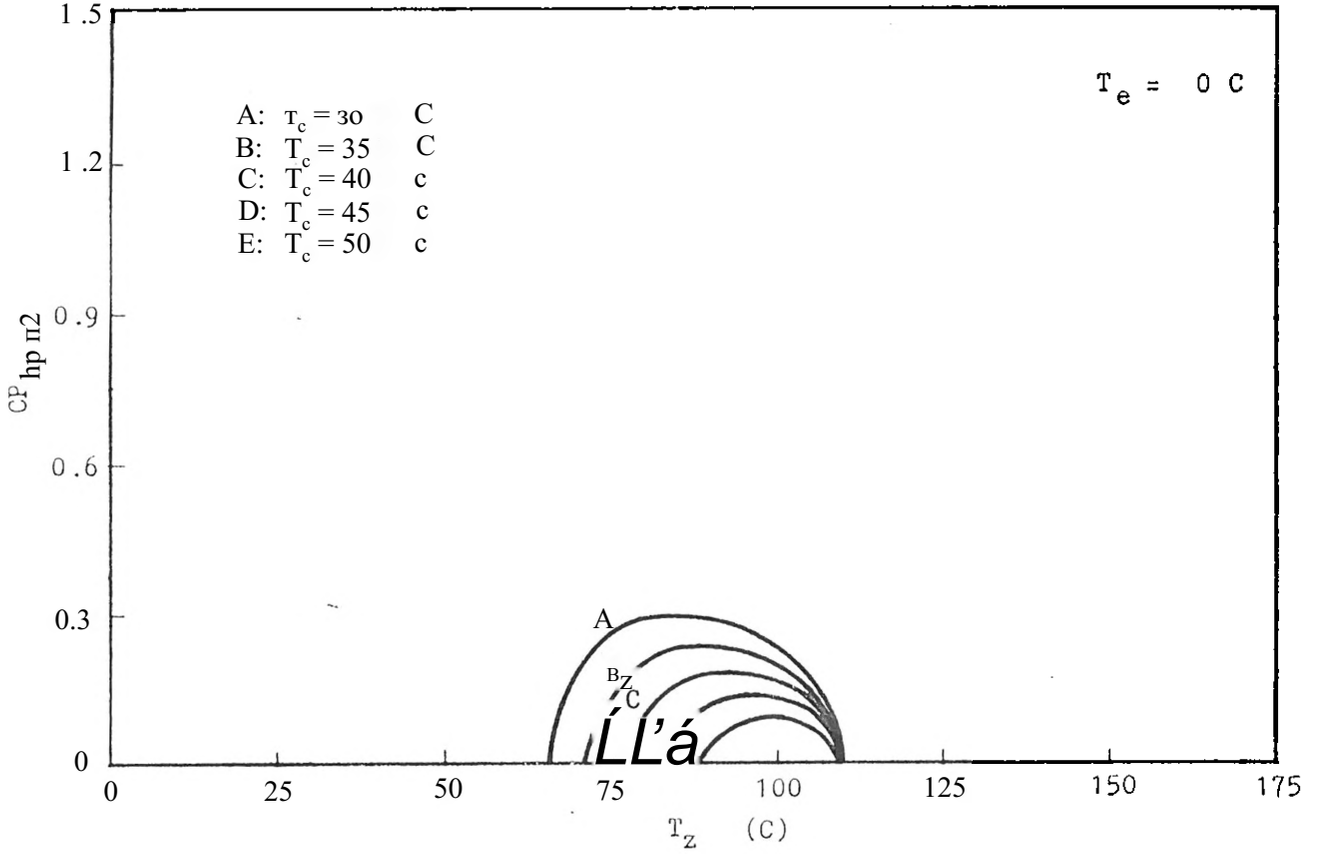

Fig. 16d Effect of condenser temperature upon UC13 mean heat pump system performance with a P-type solar collector.

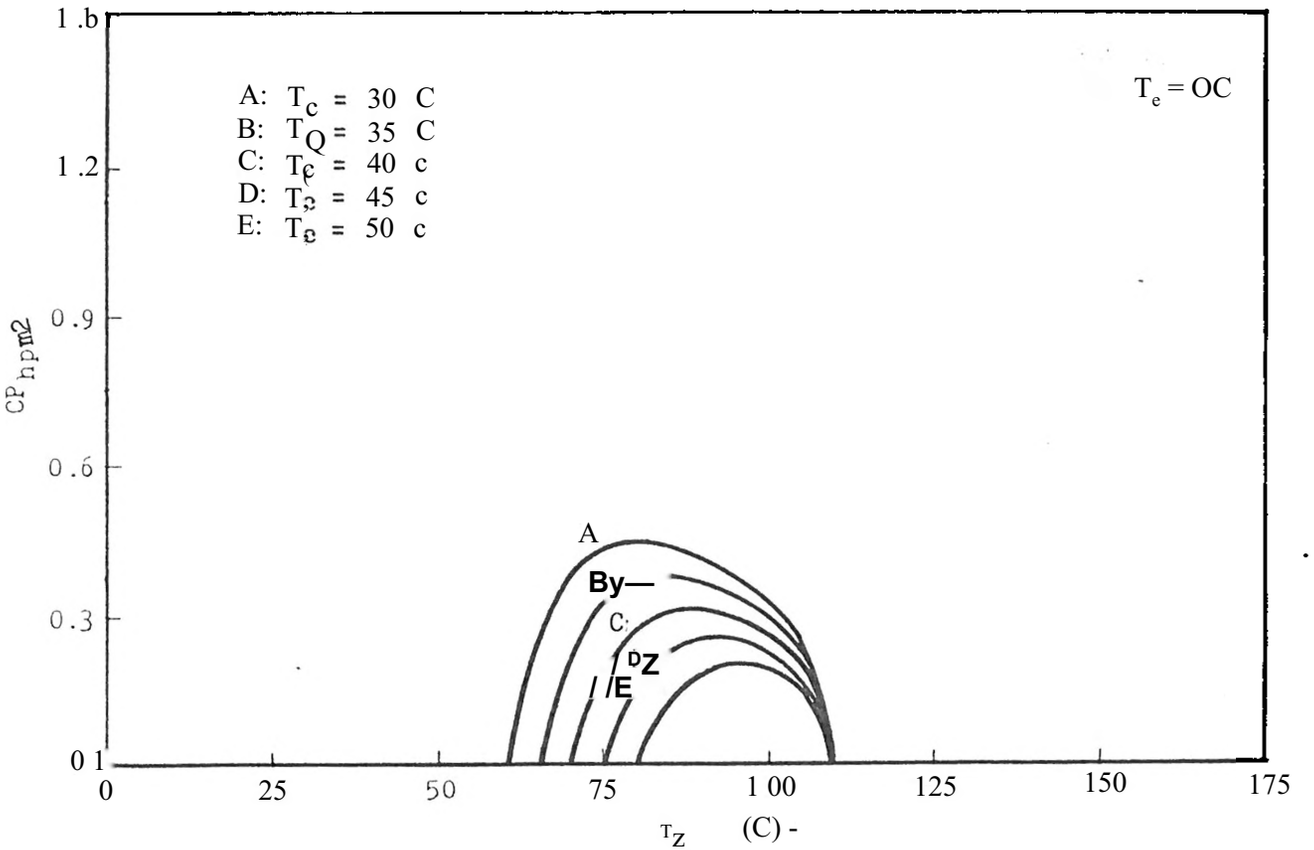

Fig. 16e Effect of condenser temperature upon NaZ mean heat pump system performance with a P-type solar collector.

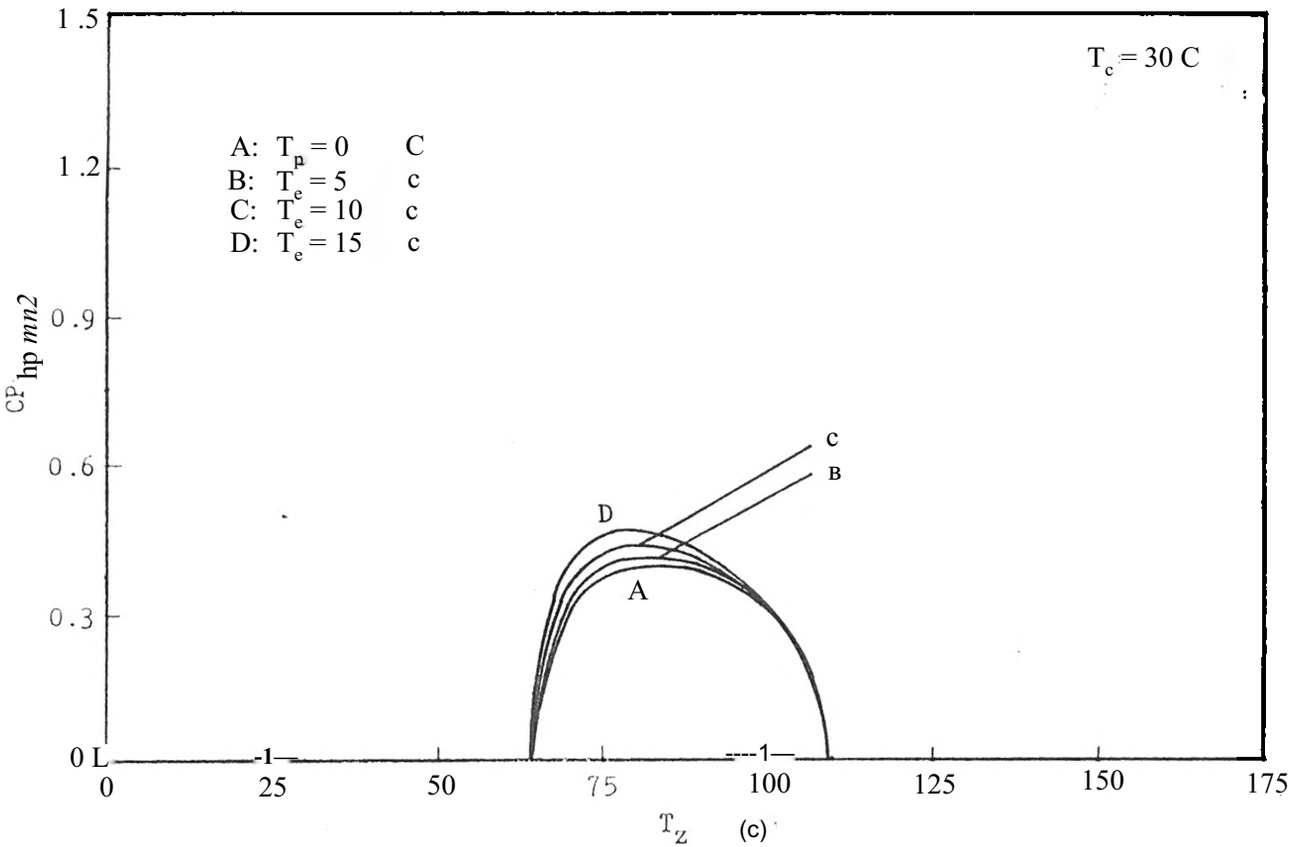

Fig. 17a Effect of evaporator temperature upon ZSC mean heat pump system performance with a P-type solar collector

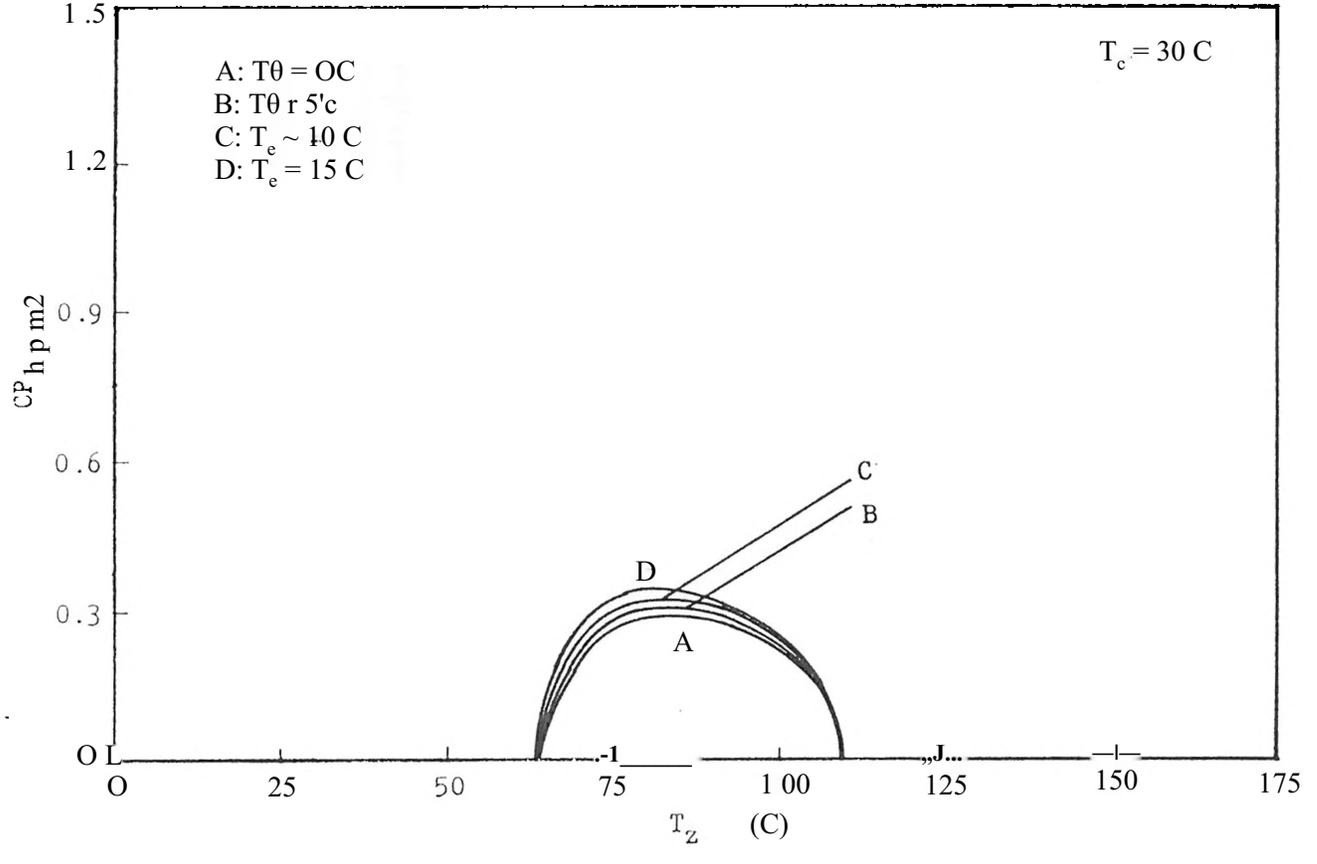

Fig. 17b Effect of evaporator temperature upon UC4A mean heat pump system performance with a P-type solar collector.

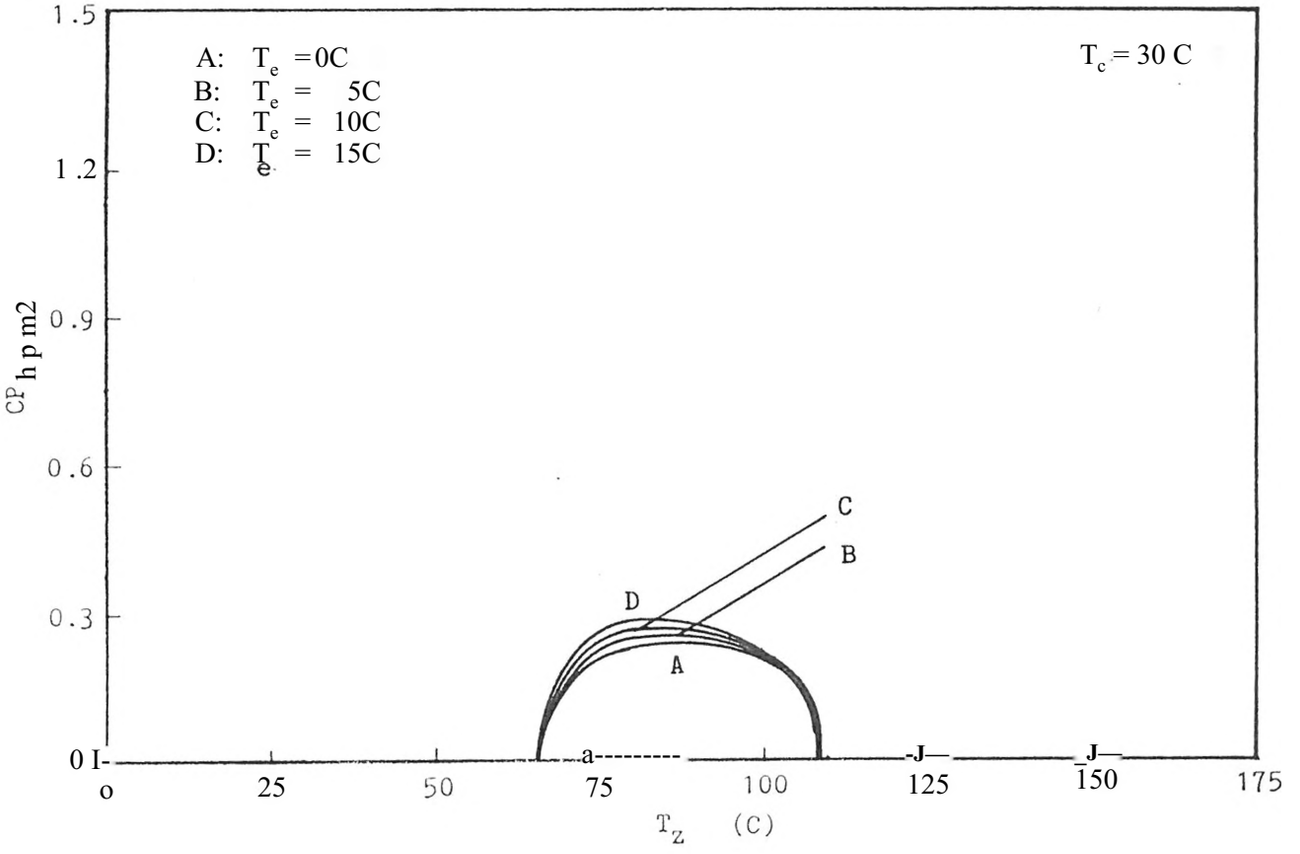

Fig. 17c Effect of evaporator temperature upon UCA mean heat pump system performance with a P-type solar collector

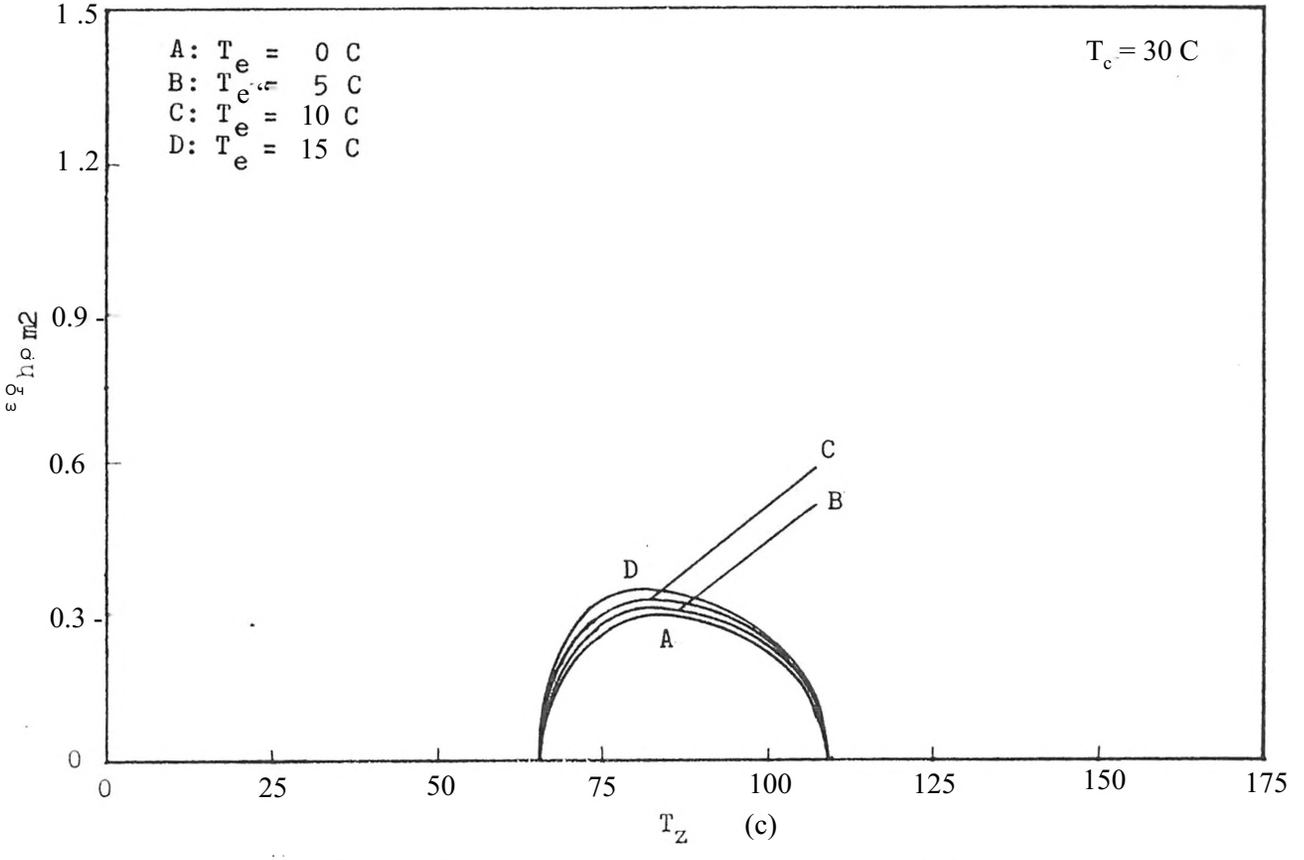

Fig. 17d Effect of evaporator temperature upon UC13 mean heat pump system performance with a P-type solar collector.

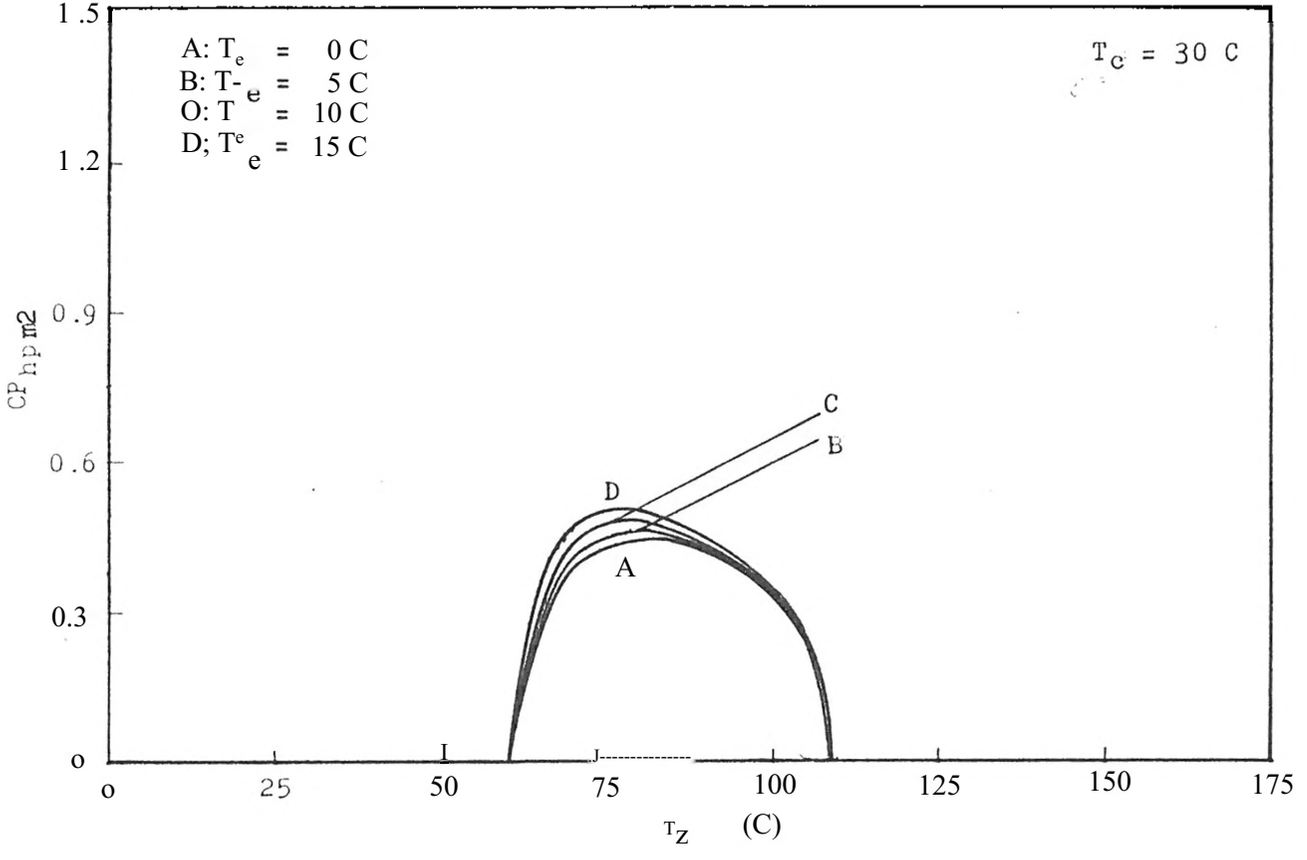

Fig. 17θ Effect of evaporator temperature upon NaZ mean heat pump system performance with a P-type solar collector.

performance. The influences of evaporator temperature on heat pump system performance for zeolites UC4A, UC5A, UC13 and NaZ are shown in Figs. 17b, 17c, 17d and 17d, respectively.

4.6 Uniform Optimum Slope for Heat Pump System Performance

The absorbent slope can influence the heat of absorption and the solar collector efficiency, which are two important factors in determining the zeolite heat pump system performance. From Fig. 2, it was seen that the slope of the constant mass concentration lines, m_z, slightly decreases with increasing mass concentration, X_z. To simplify the optimization problem and since the slopes only change slightly, the absorbent slope was assumed to be a constant. This means the absorbent slope is independent of the mass concentration, X_z, and the mass concentration lines on the log P_v versus $1/T_Z$ graph are parallel to one other.

As seen from Sec. 4.2, the absorbent slope value can influence the desorption temperature (see Fig. 13). Therefore, the system performance is dependent of the m_z value. Here, an instantaneous heat pump system performance can be obtained by varying the absorbent slope at fixed absorption temperatures (see Eq. (40b)), Figure 18 shows the instantaneous heat pump system performance versus the absorbent slope at a fixed absorption temperature. Curves F, S, V and W are the heat pump system performance values for the F, S, and V-type solar collectors and the

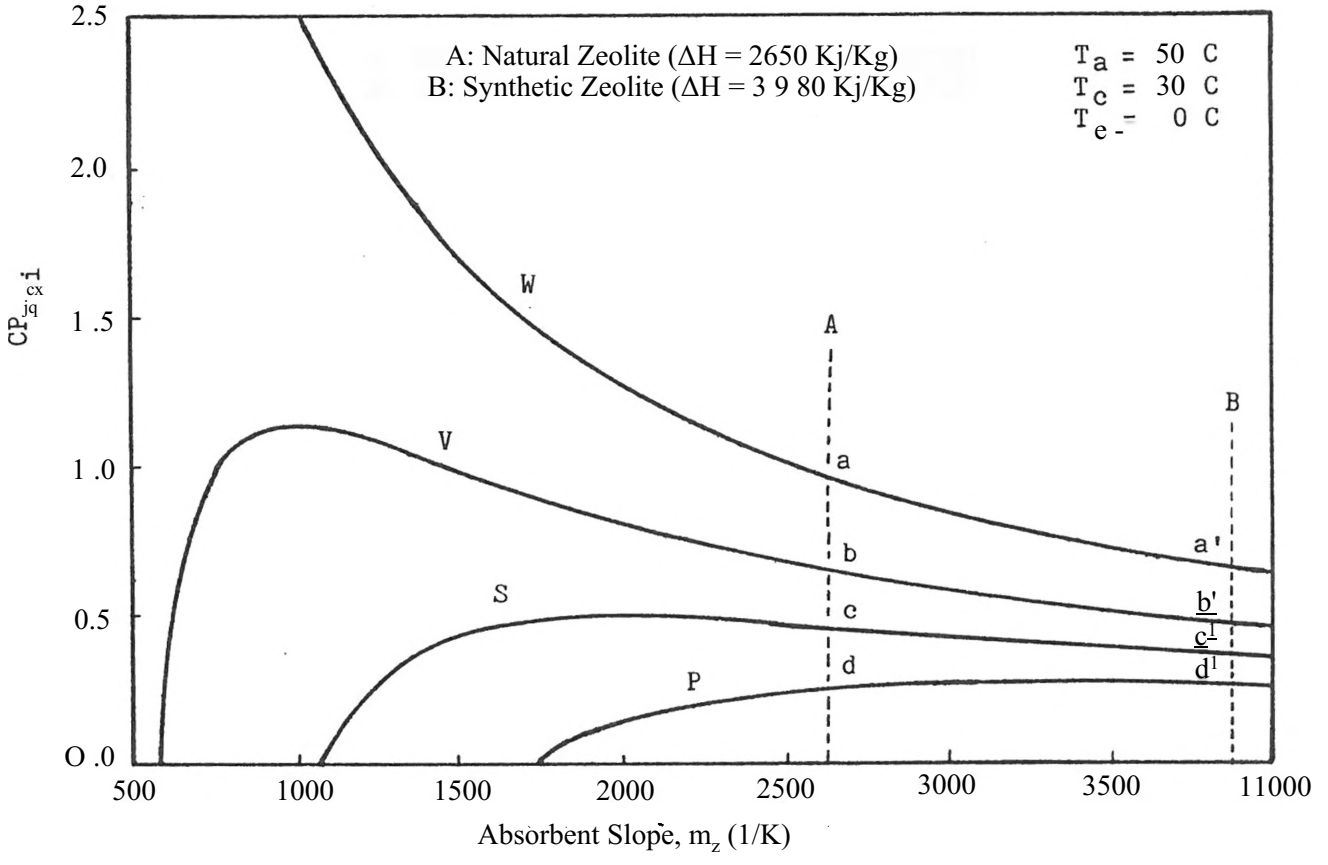

Fig. 18 Instantaneous heat pump system performance versus absorbent slope.

industrial waste heat source, respectively. Points a, b, c and d are the instantaneous heat pimp system performances corresponding to a natural zeolite. The instantaneous synthetic zeolite heat pump system performances are located at points a', b', C , and d'. It was found that the natural zeolite has a higher "instantaneous" system performance than the synthetic zeolite for any given solar collector type and a waste heat source.

Point s is the maximum instantaneous heat pump system performance for the S-type solar collector. The absorbent slope which yields the instantaneous maximum heat pump system performance is defined as the instantaneous optimum slope for the heat pimp. According to Eq.(43), the instantaneous optimum slope for the heat pump can be treated as a function of the absorption temperature, T_a. The relationship between the instantaneous optimum slope and the adsorption temperature is illustrated in Fig. 19. Curves P, S, V and W represent the instantaneous optimum slope for the P, S and V-type solar collector and the waste heat source, respectively. Point s' in Fig. 19 corresponds to point s Fig. 18, which is the instantaneous optimum slope for the S-type solar collector. Similarly, the instantaneous optimum slopes for the S and V-type solar collectors and the waste heat source can be found at points s', v' and w'. The instantaneous optimum slope for the V-type solar collector and waste heat source are seen to be weak functions of the adsorption temperature, while the instantaneous optimum slope for P-type

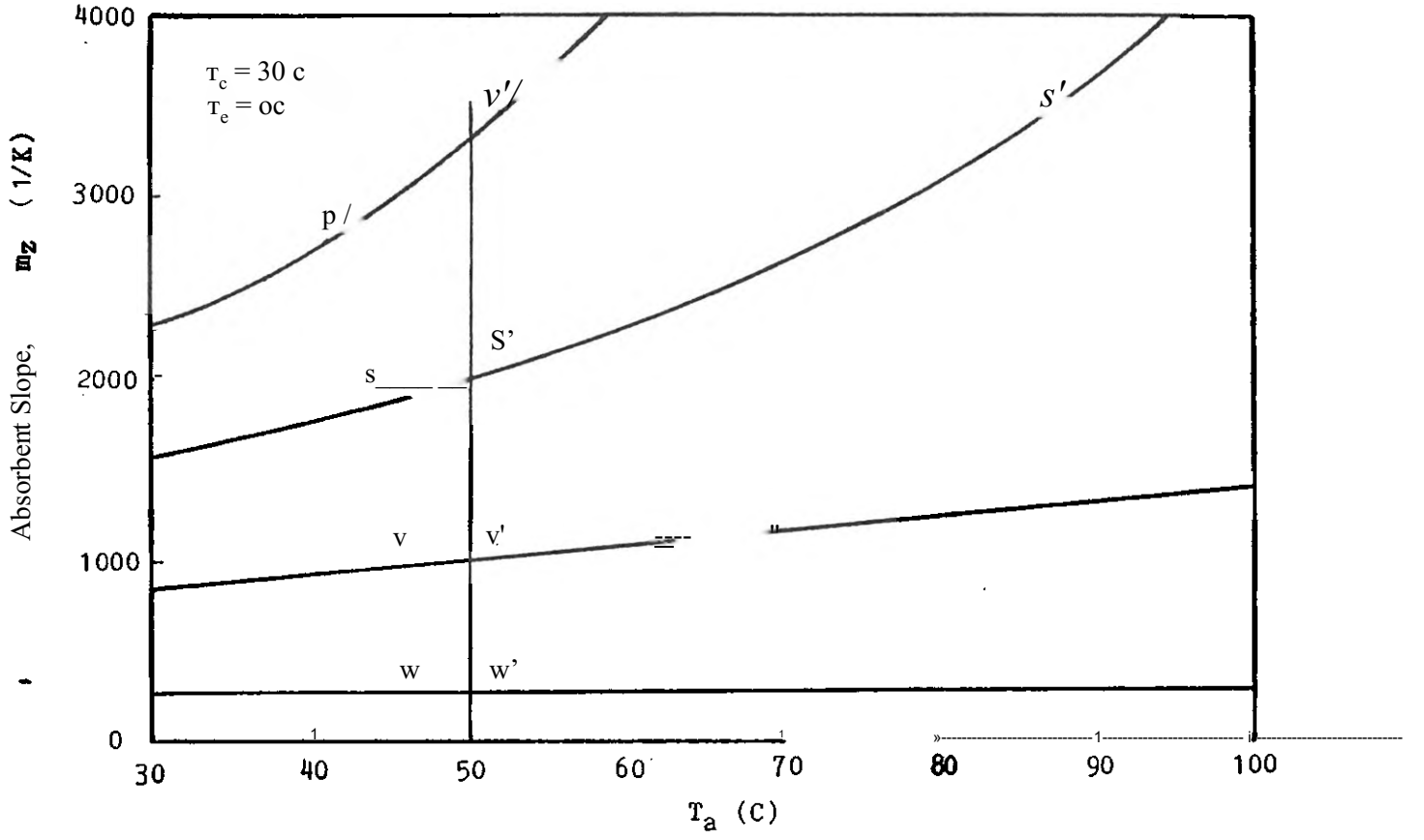

Fig. 19 Dependence of optimum instantaneous system perofrmance on adsorption temperature.

solar collector sharply increases with the increasing adsorption temperature.

From a practical point of view, the mean system performance is more useful than the instantaneous system performance to estimate the effectiveness of the solar zeolite heat pimp system. Figure 20 demonstrates the relationship between the maximum mean heat pump system performance, Eq. (35), and the absorbent slope. Curves P, S, V and W represent the maximum mean heat pump system performance for the P, S and V-type solar collectors and the waste heat source. Points 1, 2, 3 and 4 are the maximum mean heat pump system performances for the natural zeolite, while the maximum system performance for the synthetic zeolite are represented by points 1', 2', 3' and 4'.

Point w in Fig. 20 is the optimum system performance for a waste heat source for the zeolite heat pump system. The absorbent slope yielding the optimum mean heat pump system performance is defined as the ideal slope for the heat pump. As seen, the synthetic zeolite has a higher mean system performance compared to the natural zeolite when using the solar collector as a heat source, while the natural zeolite obtains higher system performance when using a waste heat source. Hence the determination of the ideal slope for optimum heat pump system performance depends on the solar collector type or if waste heat is used. Also, the maximum mean heat pump system performance is seen to be a strong function of the absorbent slope, m_2, at low values of absorbent

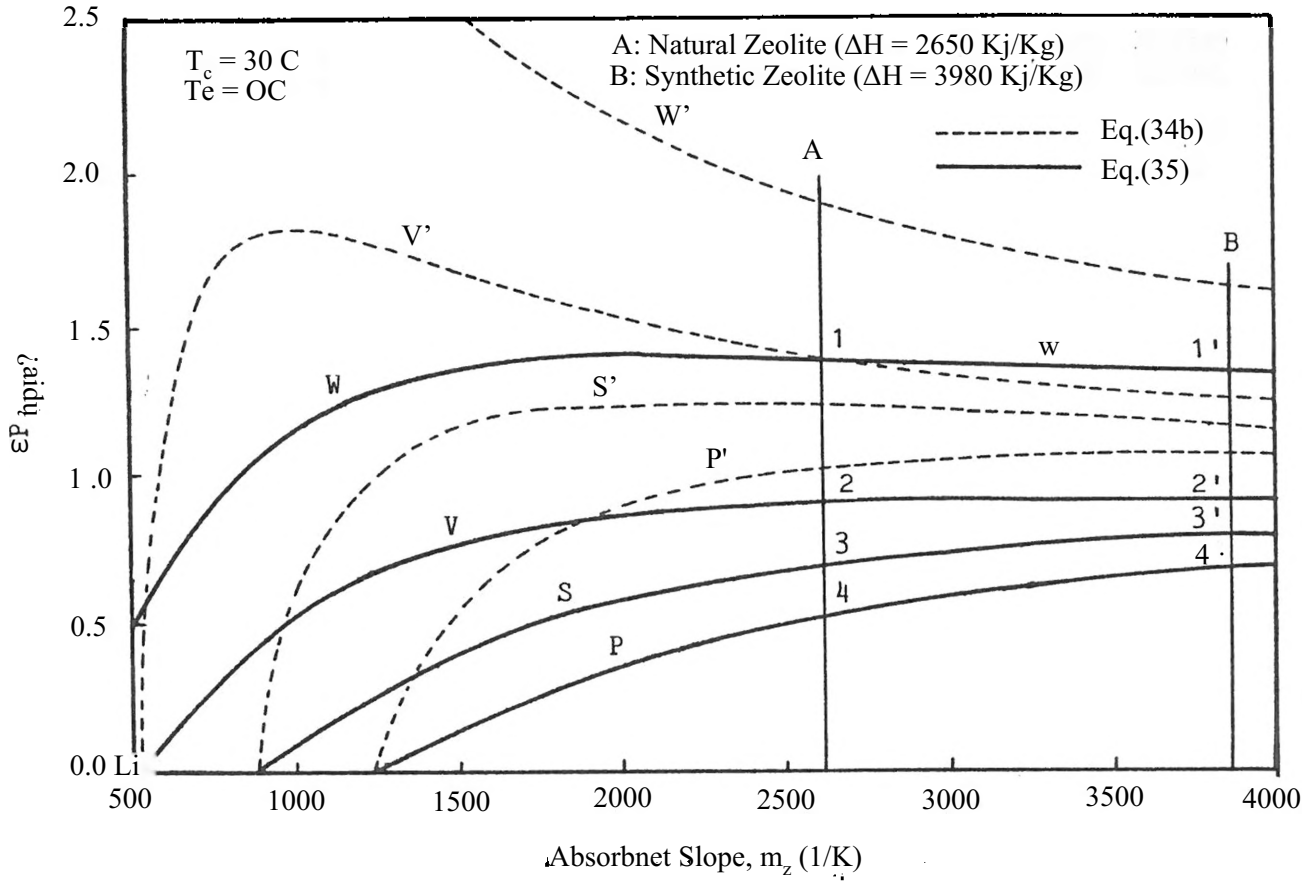

Fig. 20 Relationship between the maximum mean heat pump system performance and absorbent slope.

slope. Dashed curves W', P' , S' and V' represent the maximum mean system performance neglecting the heat capacity losses.

4 .7 Comparison of the LiBr-Water and Z eoi ite-Water Heat Pump Systems

Figure 21a demonstrates the comparison between the LiBr-water and the z eoi ite-water heat pump systems for the P-type solar collector. Curve A is the LiBr-water heat pump system performance; curves E, C, D, E and F represent the heat pump system performances for zeolites ZSC, UCAA, UC5A, UC13 and NaZ, respectively. The LiBr m_2 values , which are around 2400 (1/K) , are lower than those of most zeolites. With a lower heat of absorption, the LiBr-water system could yield a higher system performance. However the initiation desorption temperature for LiBr is high (about 79 C or 174 F). The low solar collector efficiency at high temperatures decreases the LiBr-water heat pump system performance. Also, the crystallization limitation of the LiBr-water system restricts the temperature range for heat rejection, while the zeol ite-water system has a wider heat rejection temperature range (30 C to 80 C). The comparison between the LiBr-water and the zeolite-water heat pump systems for the S- and V-type solar collector types and the waste heat source are shown in Figs. 21b, 21c and 21d, respectively. Here, the LiBr-water system is seen to become slightly better than the zeolite-water system; however, the narrow heat-rej ection temperature range can reduce the heat pump system performance.

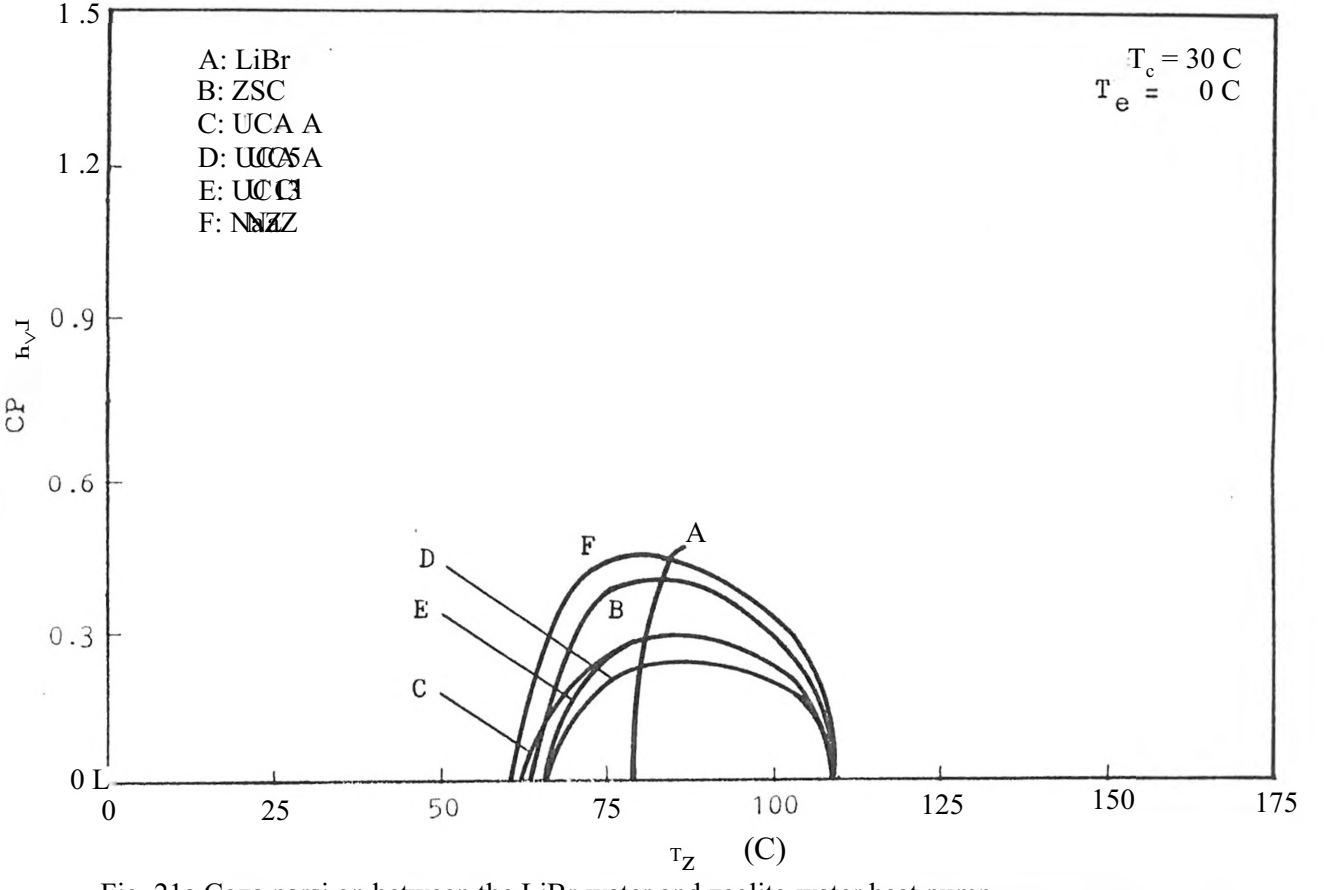

Fig. 21a Седа parsi on between the LiBr-water and zeolite-water heat pump systems for a P-type solar collector.

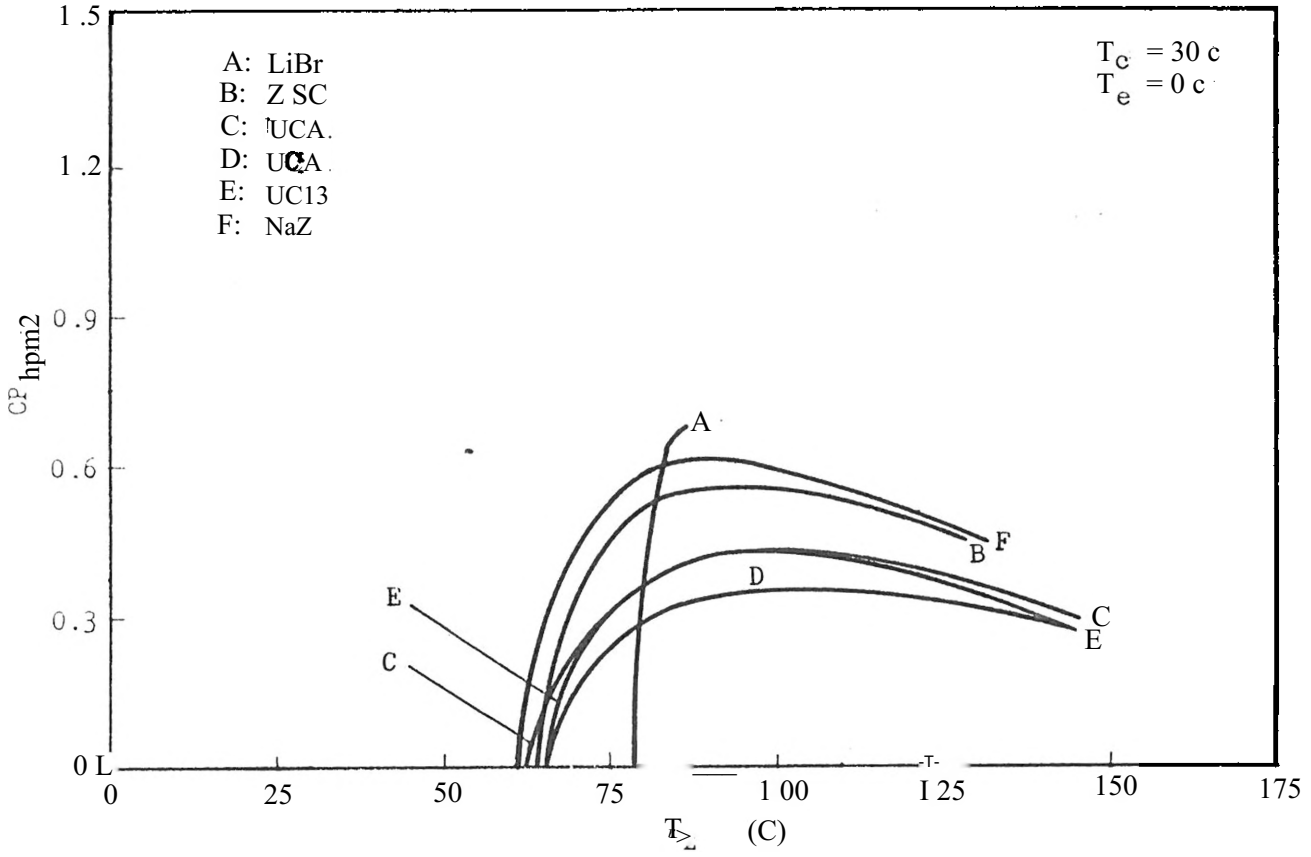

Fig. 21b Comparsion between the LiBr-water and zeolite-water heat pump systems for a S-type solar collector.

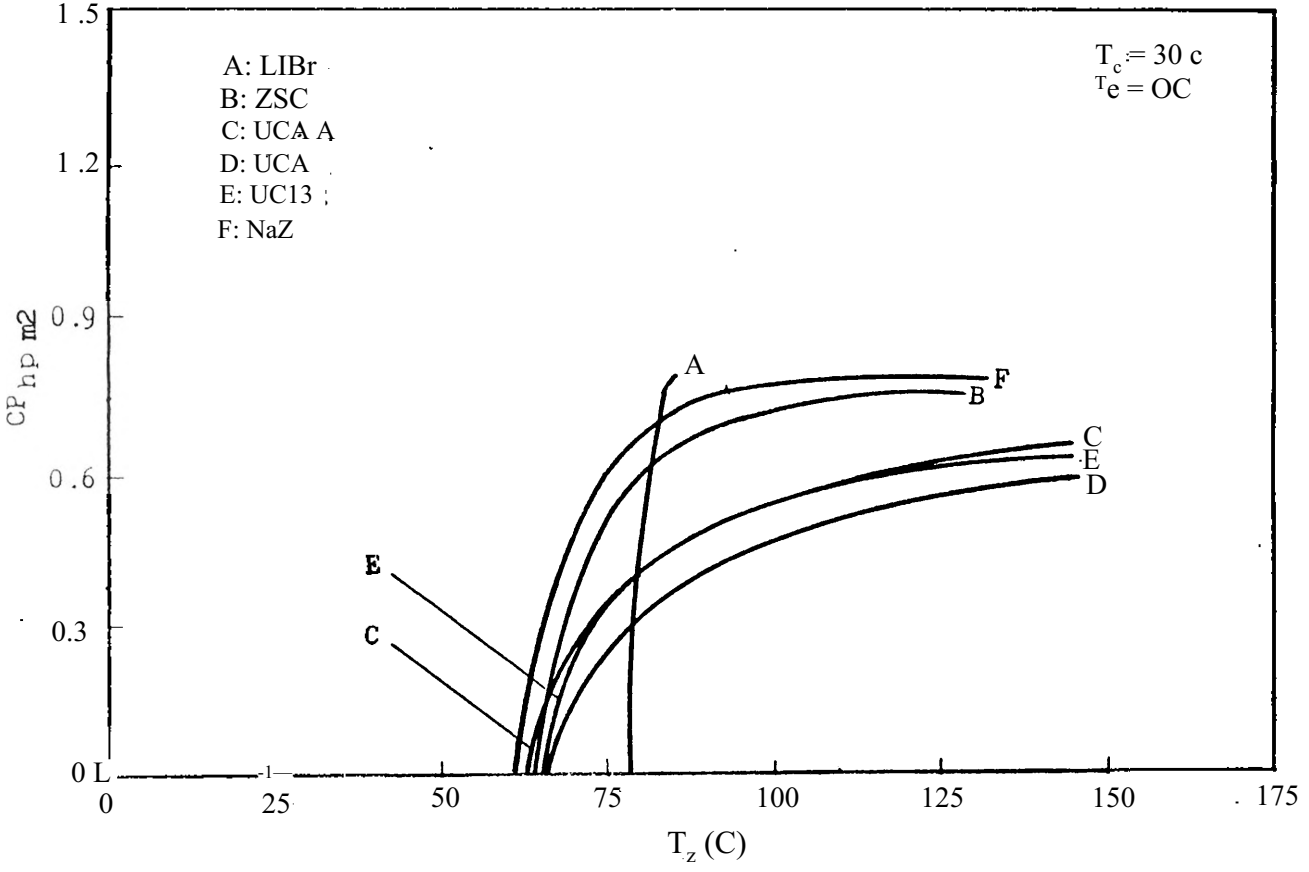

Fig. 21c Comparsion between the LiBr-water and zeolite-water heat pump systems for a V-type solar collector.

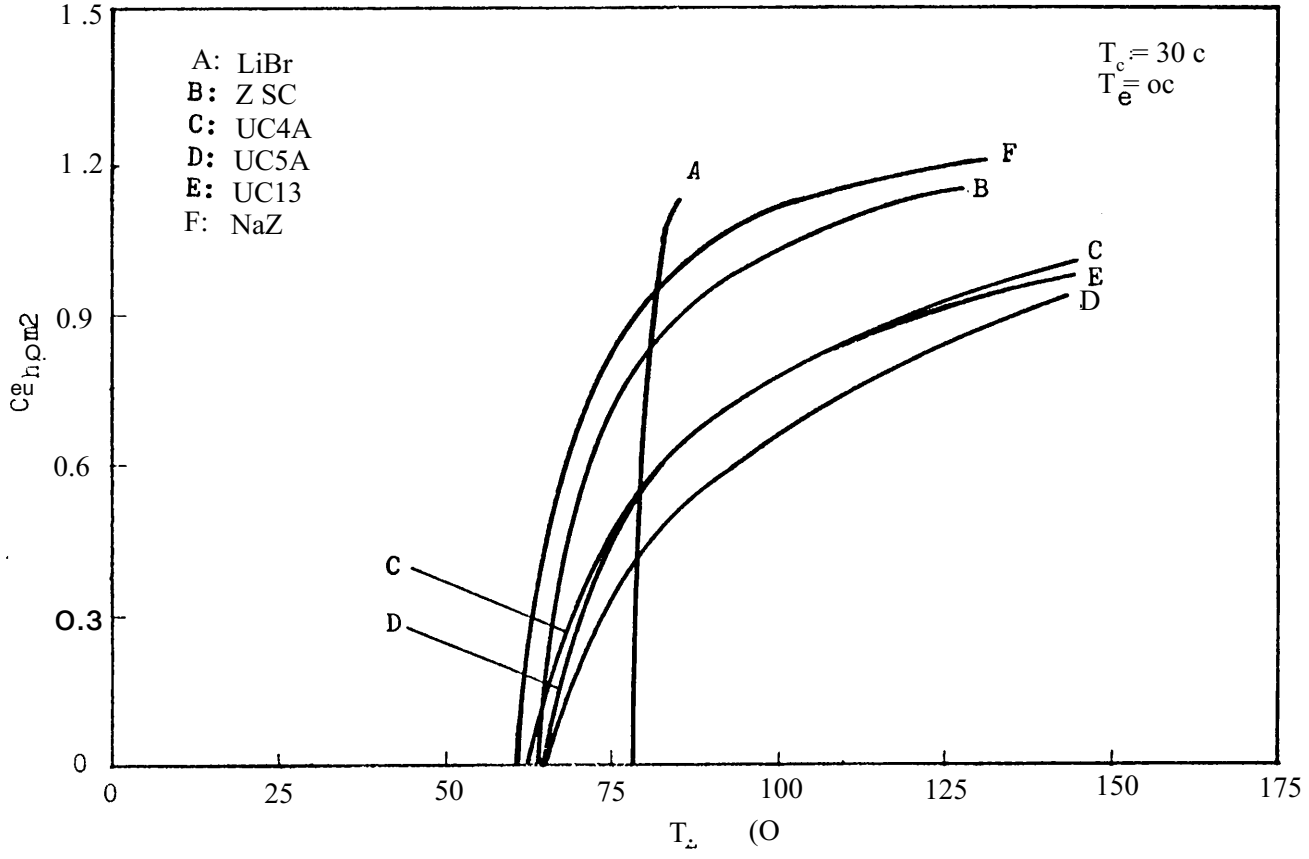

Fig. 21d Cemparsion between the LiBr-water and zeolite-water heat pump systems for a waste heat source.

4.8 -0 Zeolite Refrideration System .

Results for the zeolite refrigeration system will be demonstrated in the following sections. Also, optimum absorbent slope, m_z, for the refrigeration system will be discussed.

4.8 Refrigeration System Performance and Zeolite Tгп per ature

The relationship between refrigeration system performance and the zeolite temperature for zeolite ZSC is illustrated in Fig. 22a. Curve A is the Carnot cycle efficiency for the refrigeration system, Eq. (45); curve B stands for the Carnot cycle efficiency based on pairs of absorption and desorption temperatures for the refrigeration system, Eq. (46); curve C is the absorption refrigeration system performance, Eq. (50); curve D is the mean system performance neglecting the heat capacity losses, Eq.(54); curve E represents the mean system performance which does account for the heat capacity losses in the desorption process, Eq.(55) .

As mentioned earlier, the mean system performance will remain zero until the initiation desorption temperature is reached (point Q) . Curve D jumps abruptly due to neglecting the heat capacity losses, while curve E increases gradually. The low solar collector efficiency yields a lew mean refrigeration system performance at high zeolite temperatures. The dependence of the refrigeration system performance on zeolite temper-

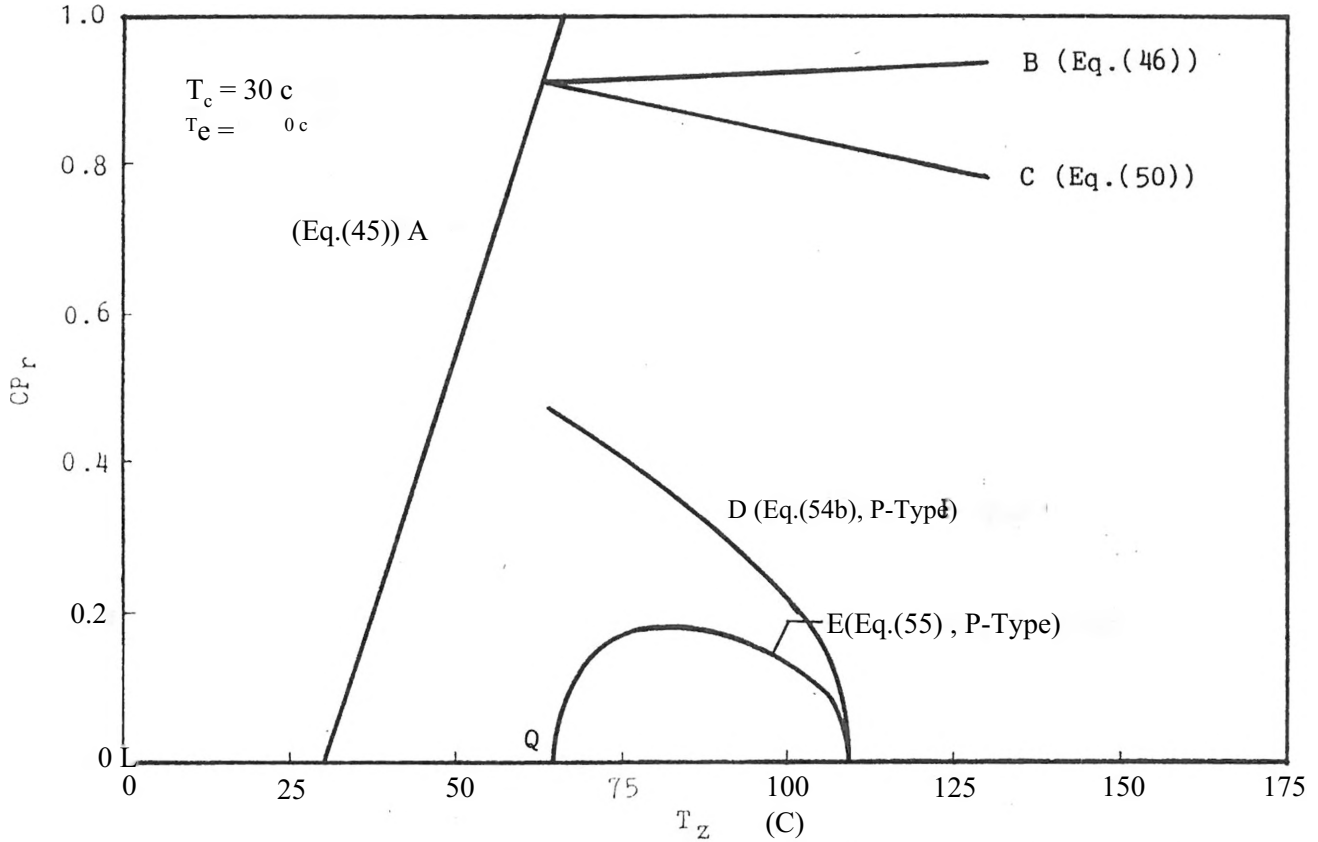

Fig. 22a Dependence of refrigeration system perofrmance on zeolite temperature for zeolite ZSC.

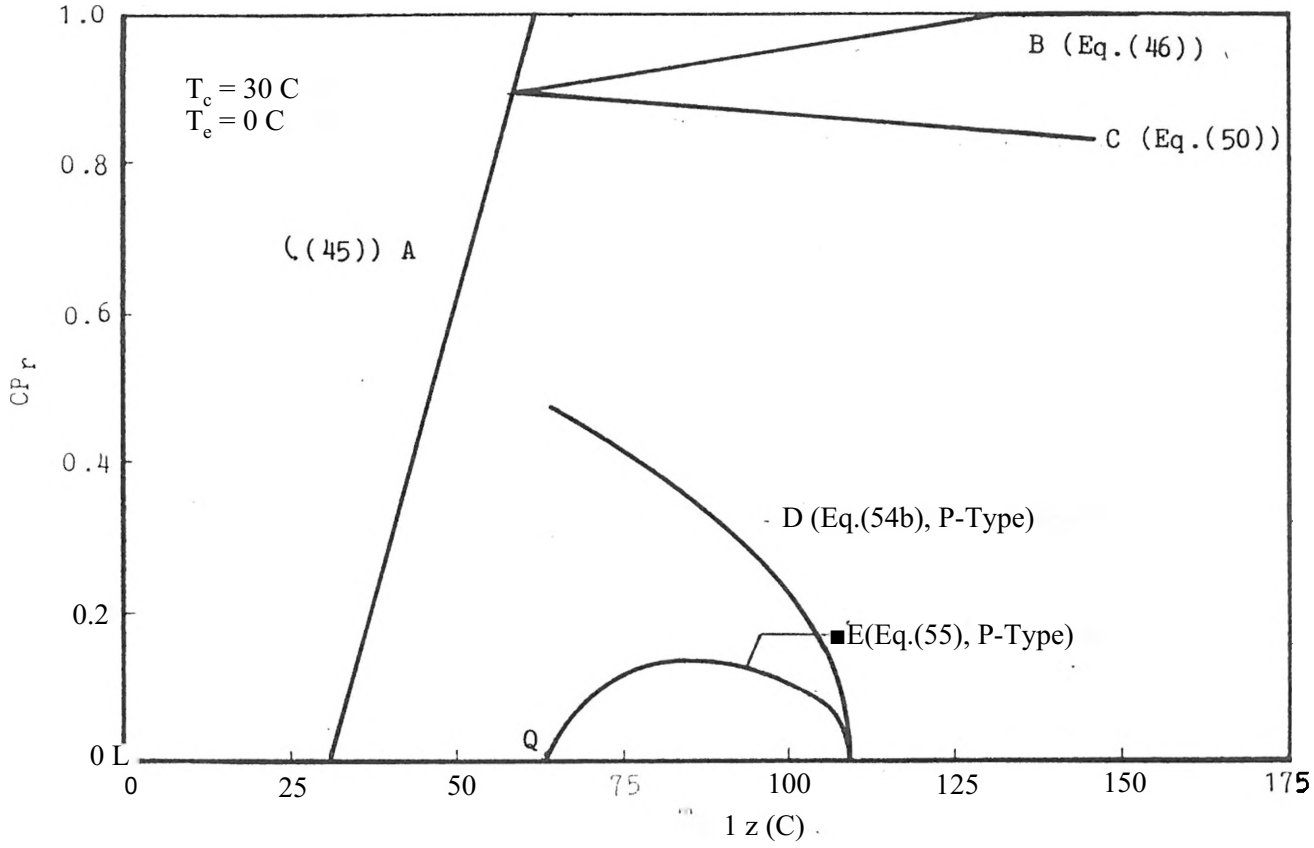

Fig. 22b Dependence of refrigeration system perofrmance on zeolite temperature for zeolite UCAA.

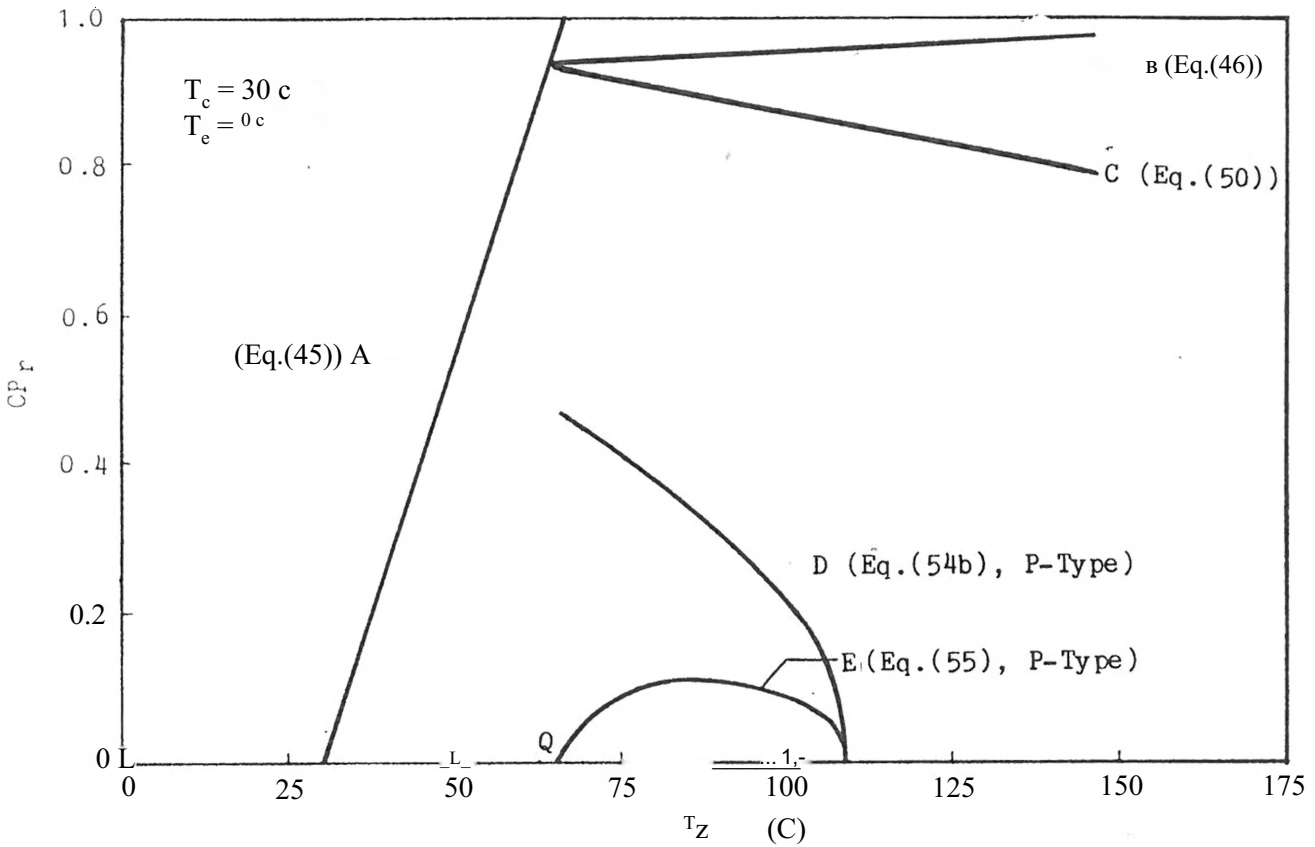

Fig. 22c Dependence of refrigeration system perofrmance on zeolite temperature for zeolite UC5A.

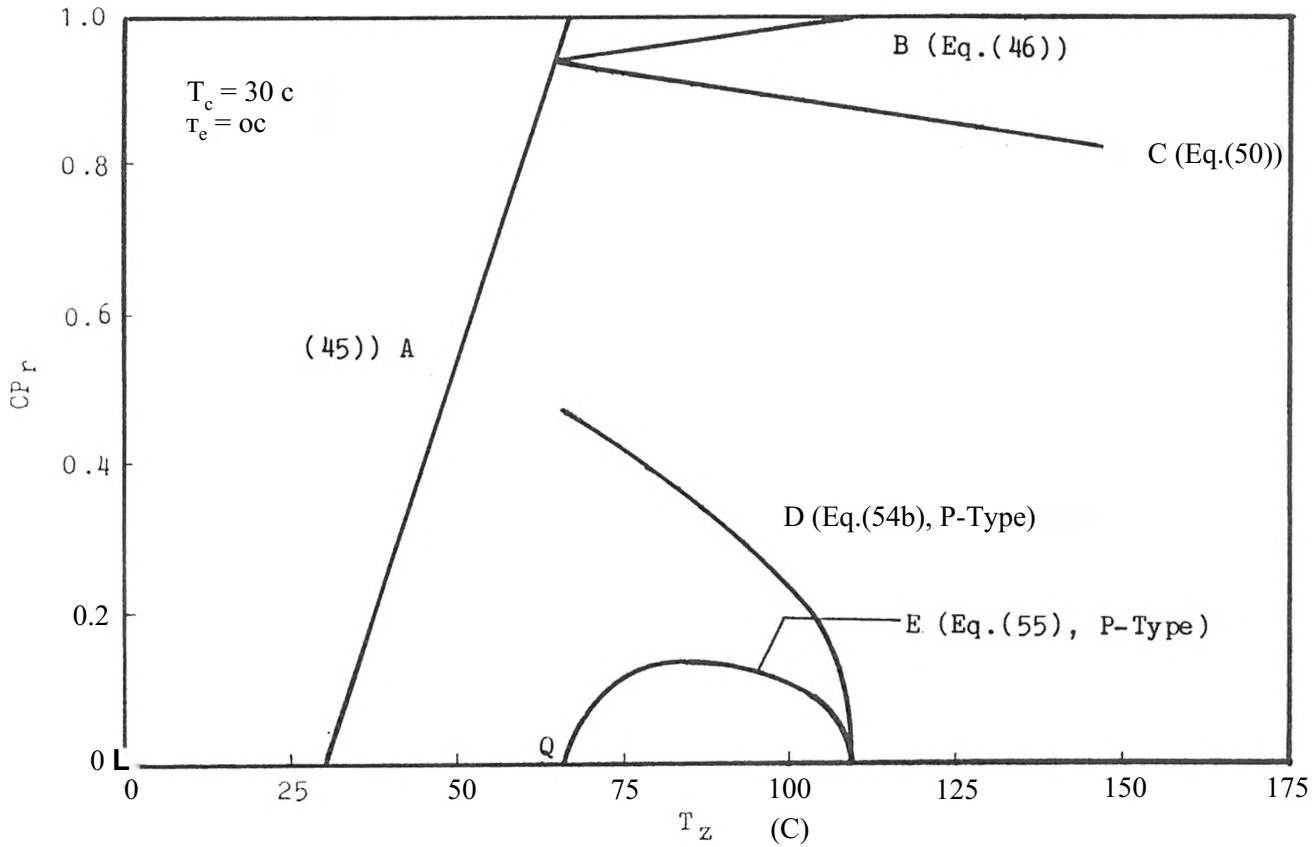

Fig. 22d Dependence of refrigeration system perofrmance on zeolite temperature for zeolite UC13.

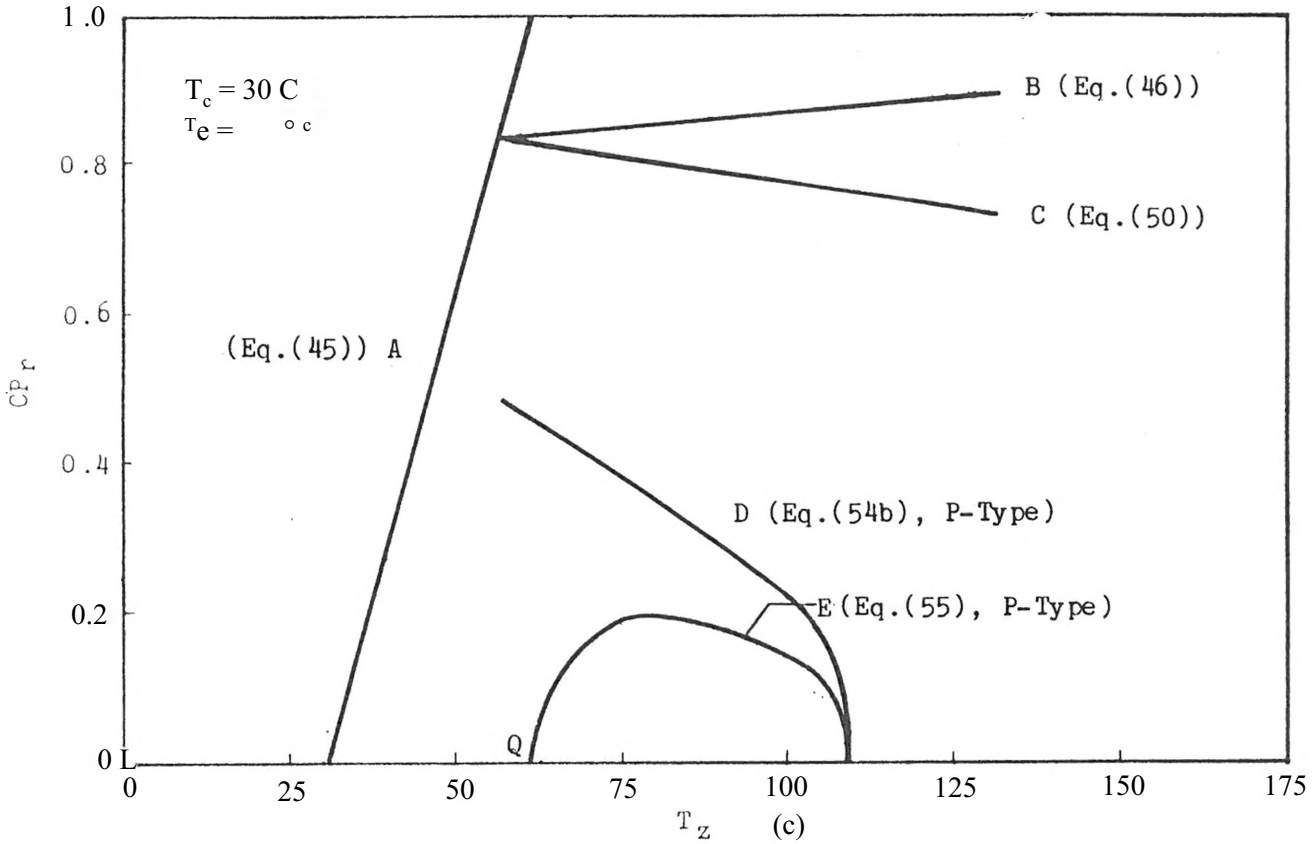

Fig. 22e Dependence of refrigeration system perofrmance on zeolite temperature for zeolite Naz.

ature for the different types of zeolites, UC4A, UCA, UC13 and NaZ, are shown in Fig. 22b to 22e.

4.9 Influence of Solar Collector Type Upon Refrigeration System Performance

Figure 23a demonstrates the mean refrigeration system performance for different solar collector types and a waste heat source. Curves P, S, V and W are the mean refrigeration system performances for the P, S and V-type solar collectors and a waste heat source, respectively. As seen, curve W increases with zeolite temperature due to the constant high conversion efficiency for a waste heat source. Also, the mean refrigeration system performance using a solar collector as the heat source will produce a lew system performance at high zeolite temperatures. The influence of the solar collector type upon mean refrigeration system performance for various zeolite types are shewn in Figs. 23b to 23e.

4.10 Influence of Condenser and Evaporator Temperatures Upon Refrigeration System Performance

The mean refrigeration system performance, Eq.(55), is dependent on the condenser and the evaporator temperatures. Figure 24a shows the mean refrigeration system performances for different condenser temperatures. Curves A, B, C, D and E represent the mean refrigeration system

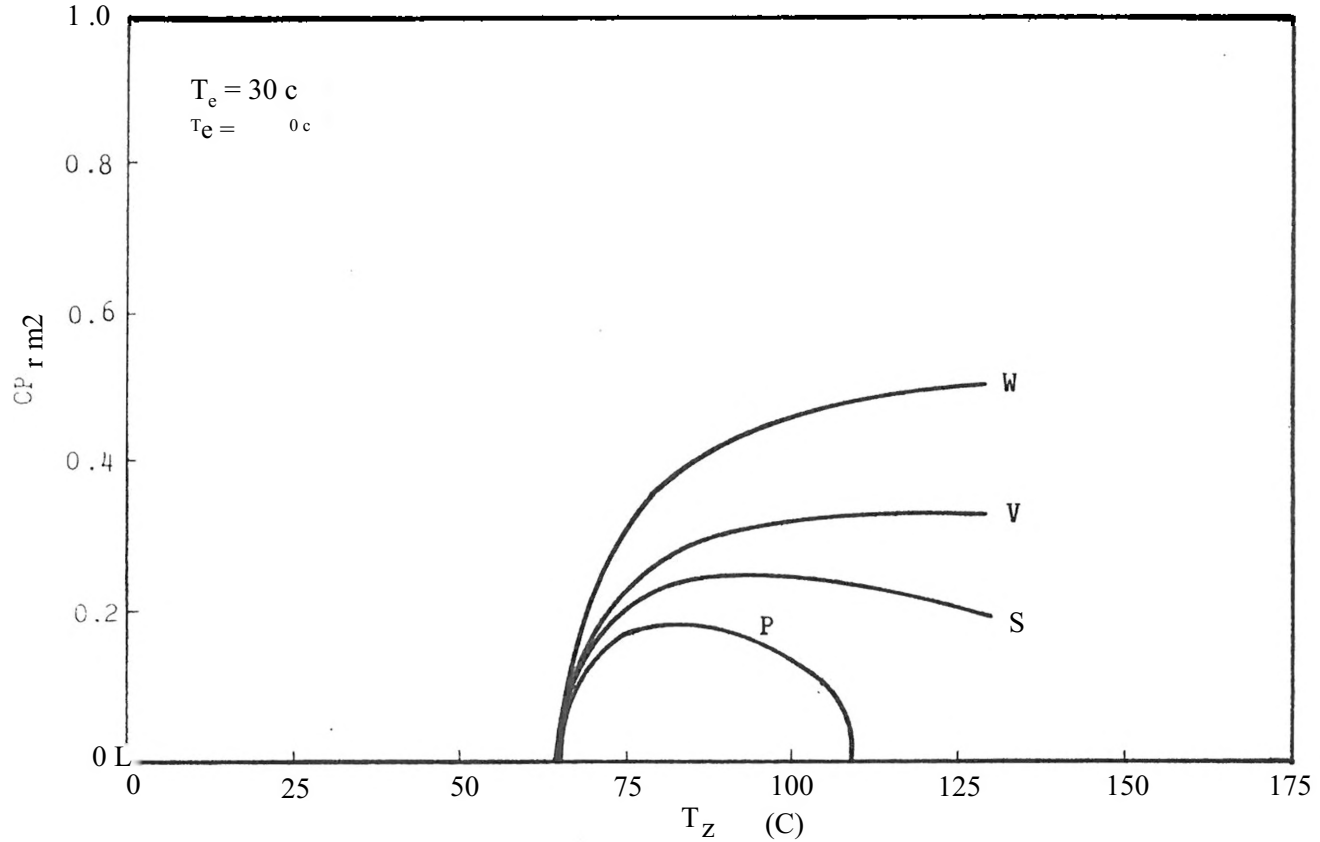

Fig. 23a Effect of solar collector type upon refrigeration system performance for zeolite ZSC.

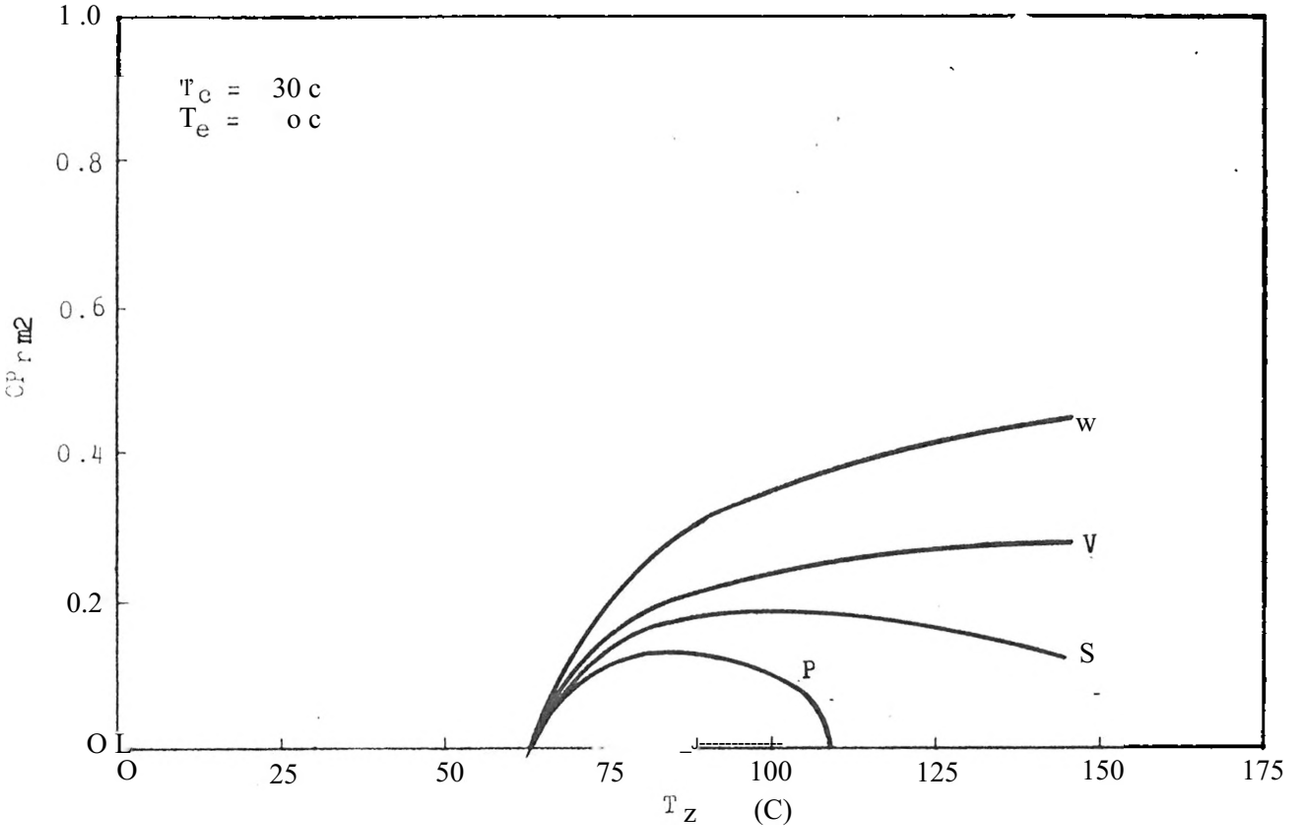

Fig. 23b Effect of solar collector type upon refrigeration system performance for zeolite UC4A$_V$

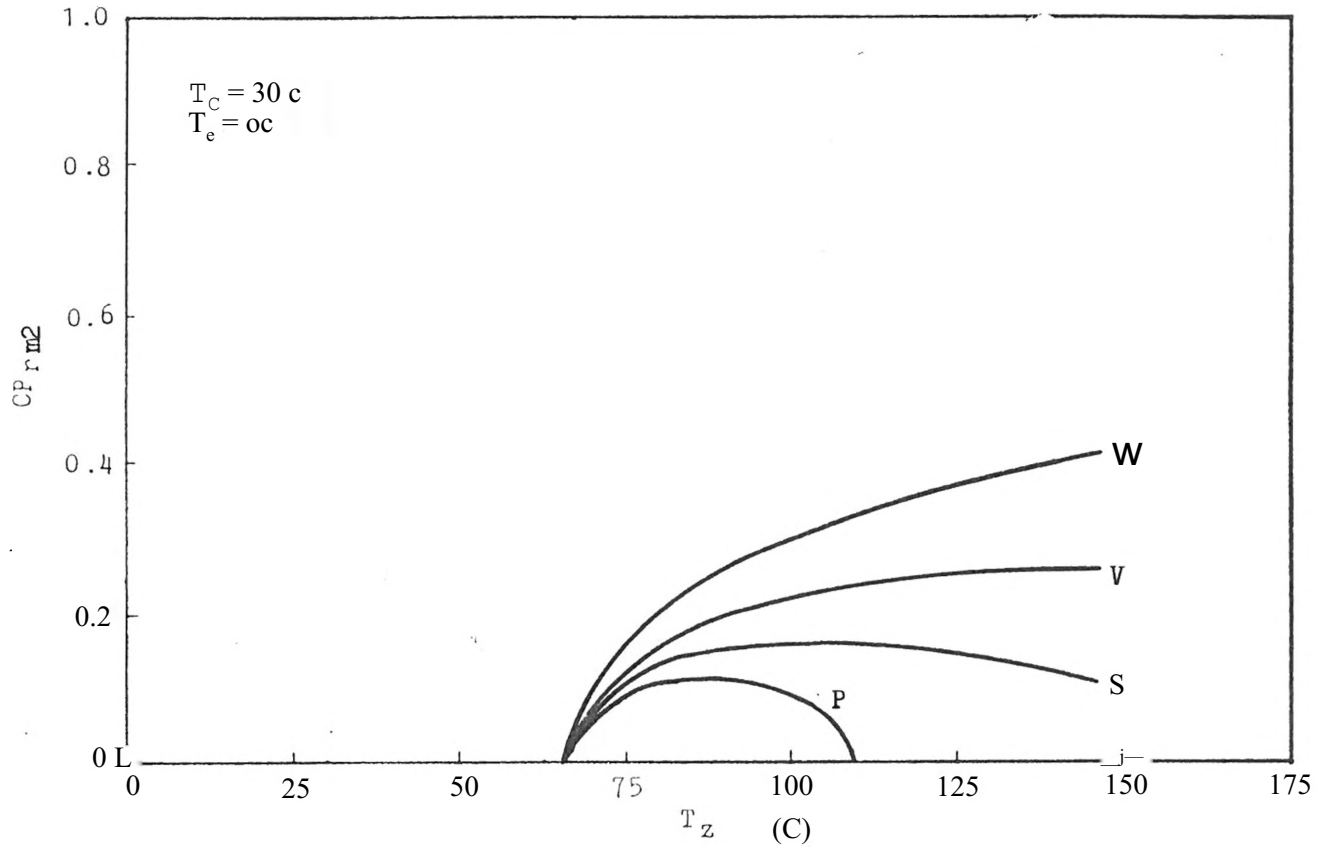

Fig. 23c Effect of solar collector type upon refrigeration system performance for zeolite UCA1

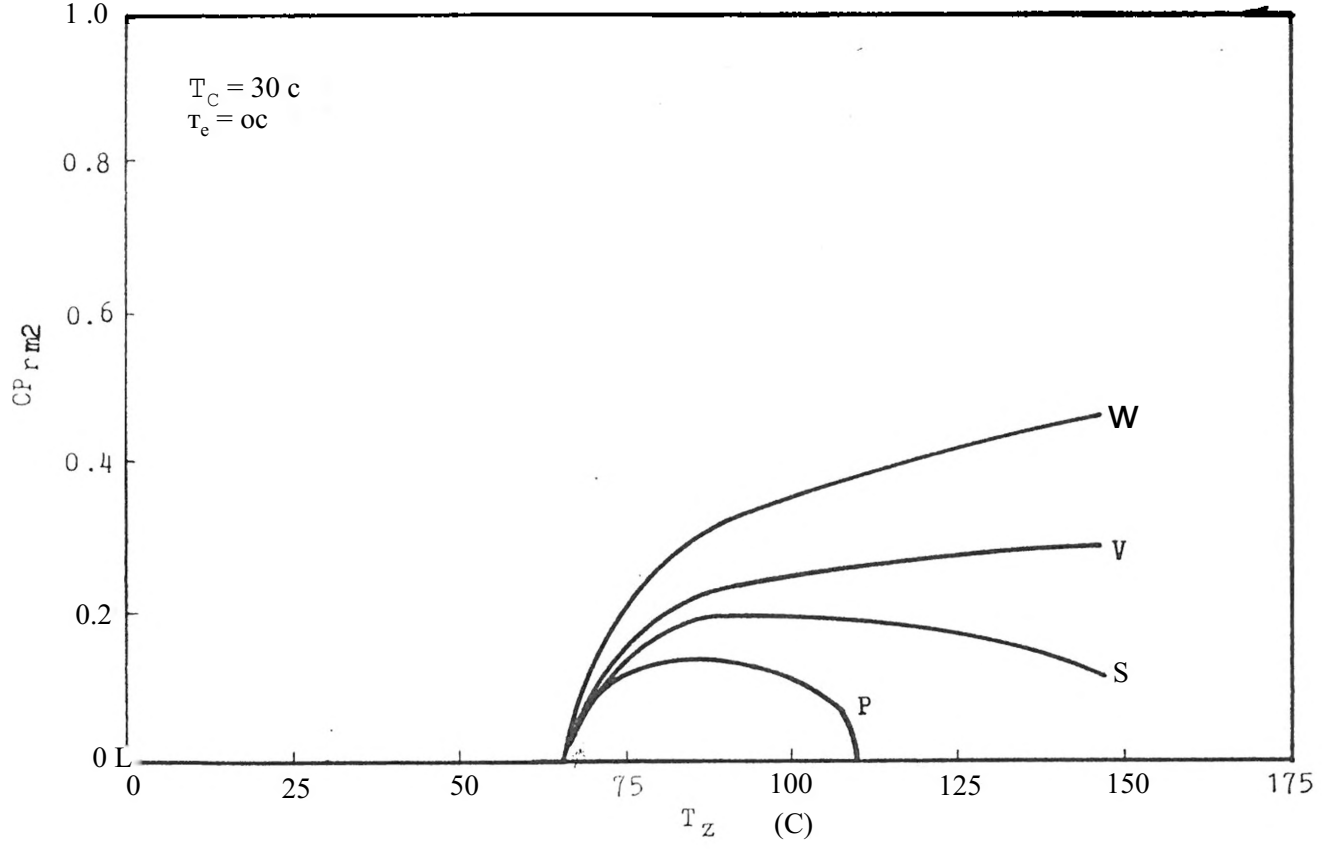

Fig. 23d Effect of solar collector type upon refrigeration system performance for zeolite UC13 .

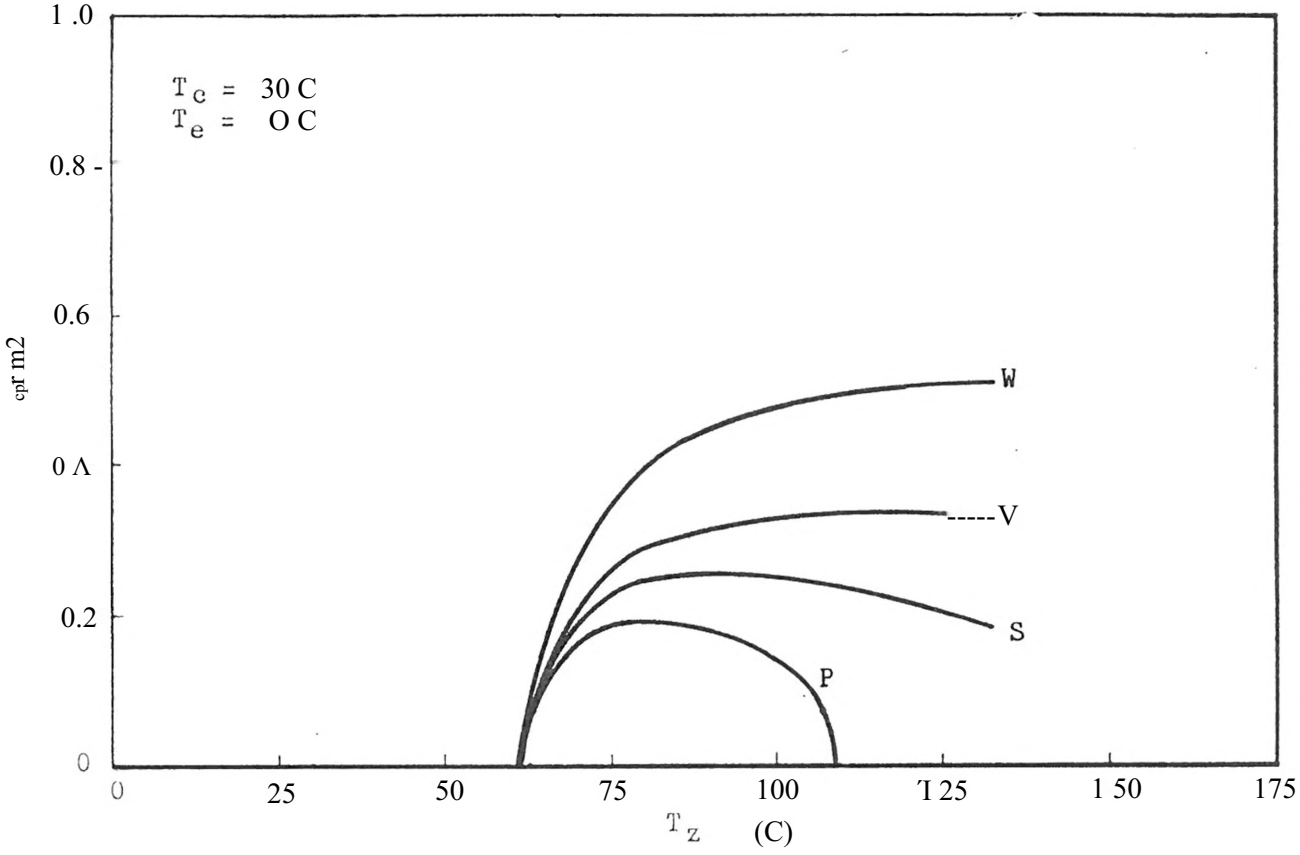

big. 23e Effect of solar collector type upon refrigeration system performance for zeolite NaZ.

performance for condenser temperatures of 30, 35, 40, 45 and 50 C, respectively. Since the initiation desorption temperature increases as the condenser temperaure increases, the mean refrigeration system performance decreases at high condenser temperatures. The effect of the condenser temperature upon the refrigeration system performance for zeolites Z4A, Z5A, Z13P and NaZ are shewn in Figs. 24b, 24c, 24d and 24e, respectively.

Figure 25a illustrates the variation of the mean ZSC refrigeration system performance for different evaporator temperatures. Curves A, B, C and D correspond to the mean refrigeration system performance for evaporator temperatures of 0 , 5, 10 and 15 C, respectively. The initiation desorption temperature will not be changed by varying the evaporator temperature. However, the evaporator temperature can slightly influence the refrigeration system performance by affecting the heat capacity losses in the desorption process. As seen, the mean refrigeration system performance increases as the evaporator temperature increases. Figures 25b to 25e show the influence of evaporator temperature on the mean refrigeration system performance for various zeolite types.

4.11 Uniform Optimum Slope for Refrigeration System Perfromance

For the solar zeolite refrigeration system, the heat of absorption and the solar collector efficiency are affected by the absorbent slope,

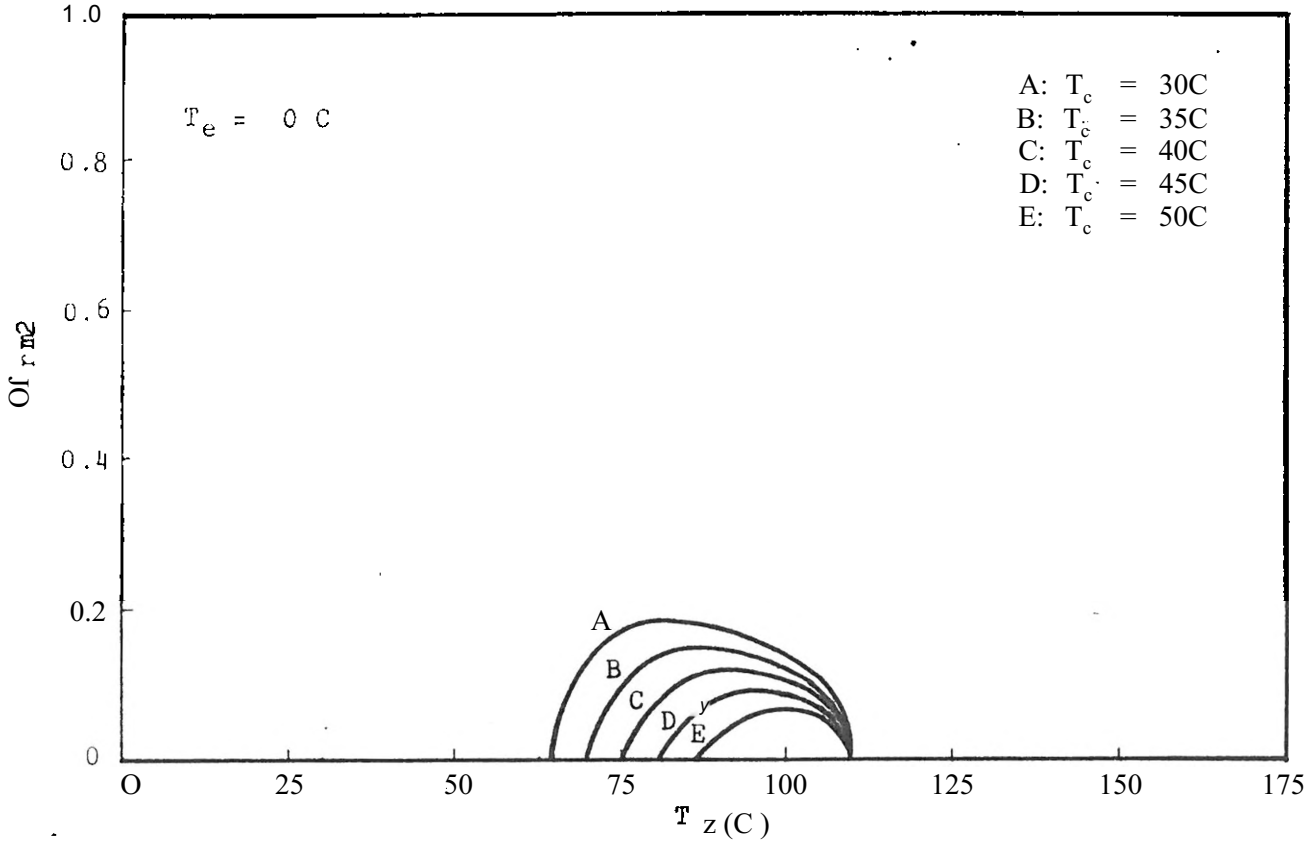

Fig. 24a Effect of condenser temperature upon ZSC mean refrigeration system performance with a P-type solar collector.

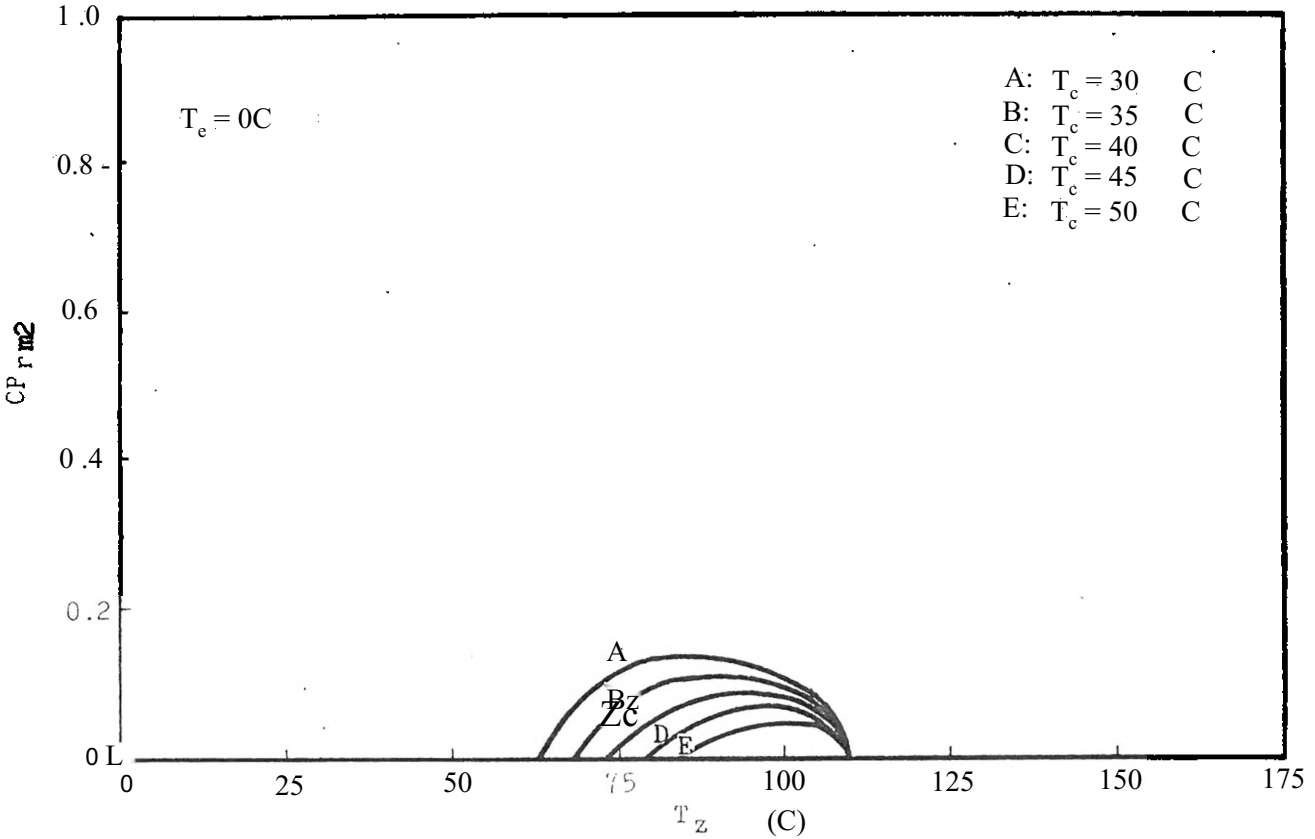

Fig. 24b Effect of condenser temperature upon UC4A mean refrigeration system performance with a P-type solar collector.

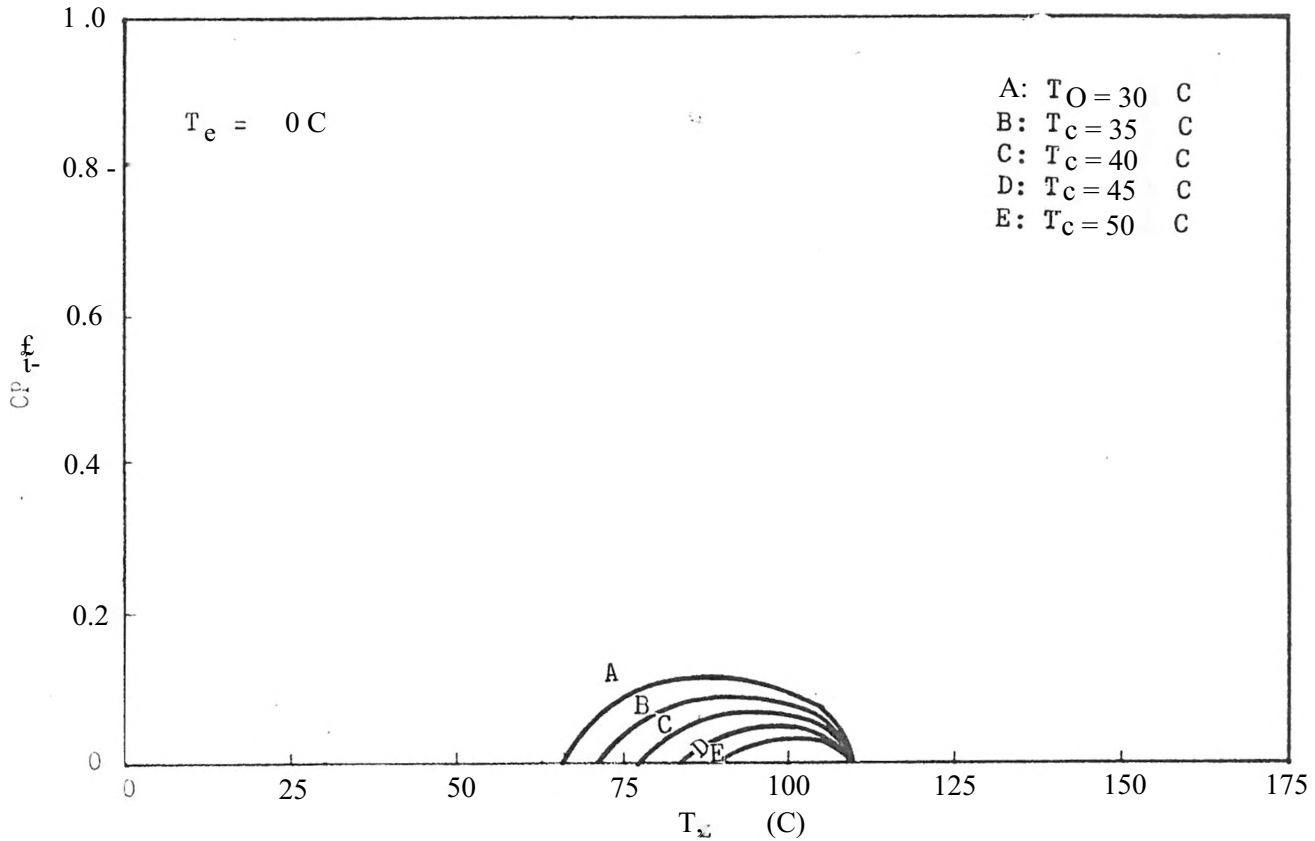

Fig. 24c Effect of condenser temperature upon UCA mean refrigeration system performance with a P-type solar collector

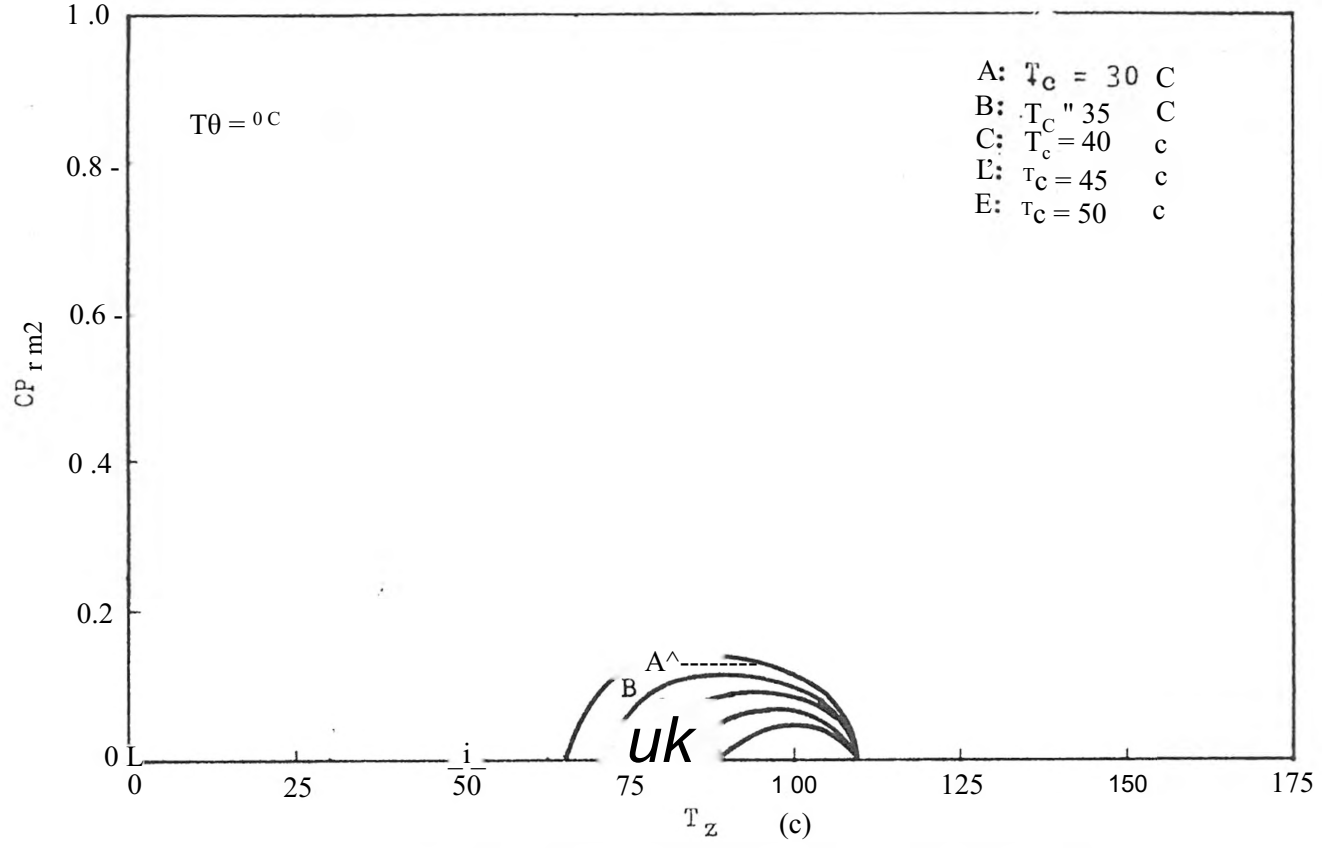

Fig. 24d Effect of condenser temperature upon UC13 mean refrigeration syst em performance with a P-type solar collector.

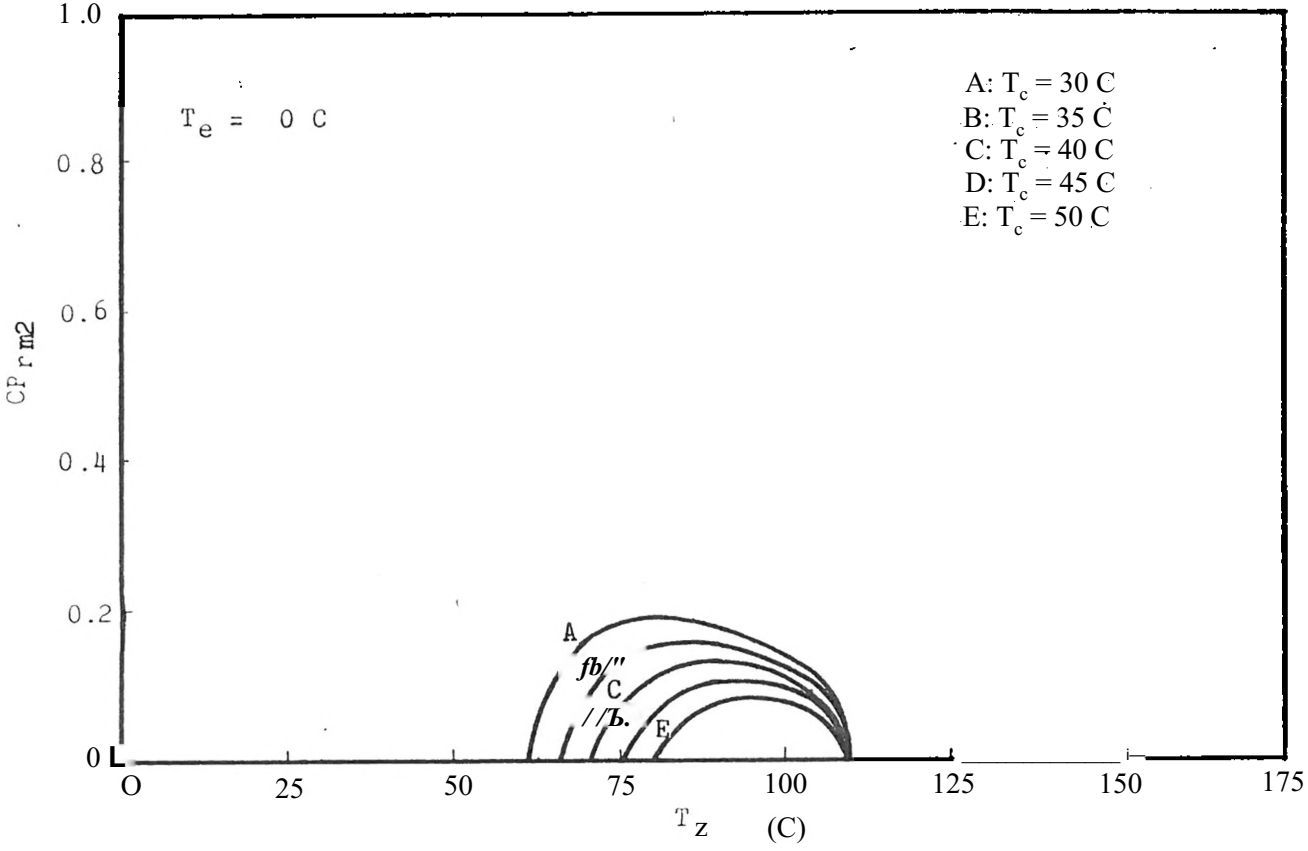

Fig. 24e Effect System of condenser temperature upon NaZ mean refrigeration performance with a P-type solar collector.

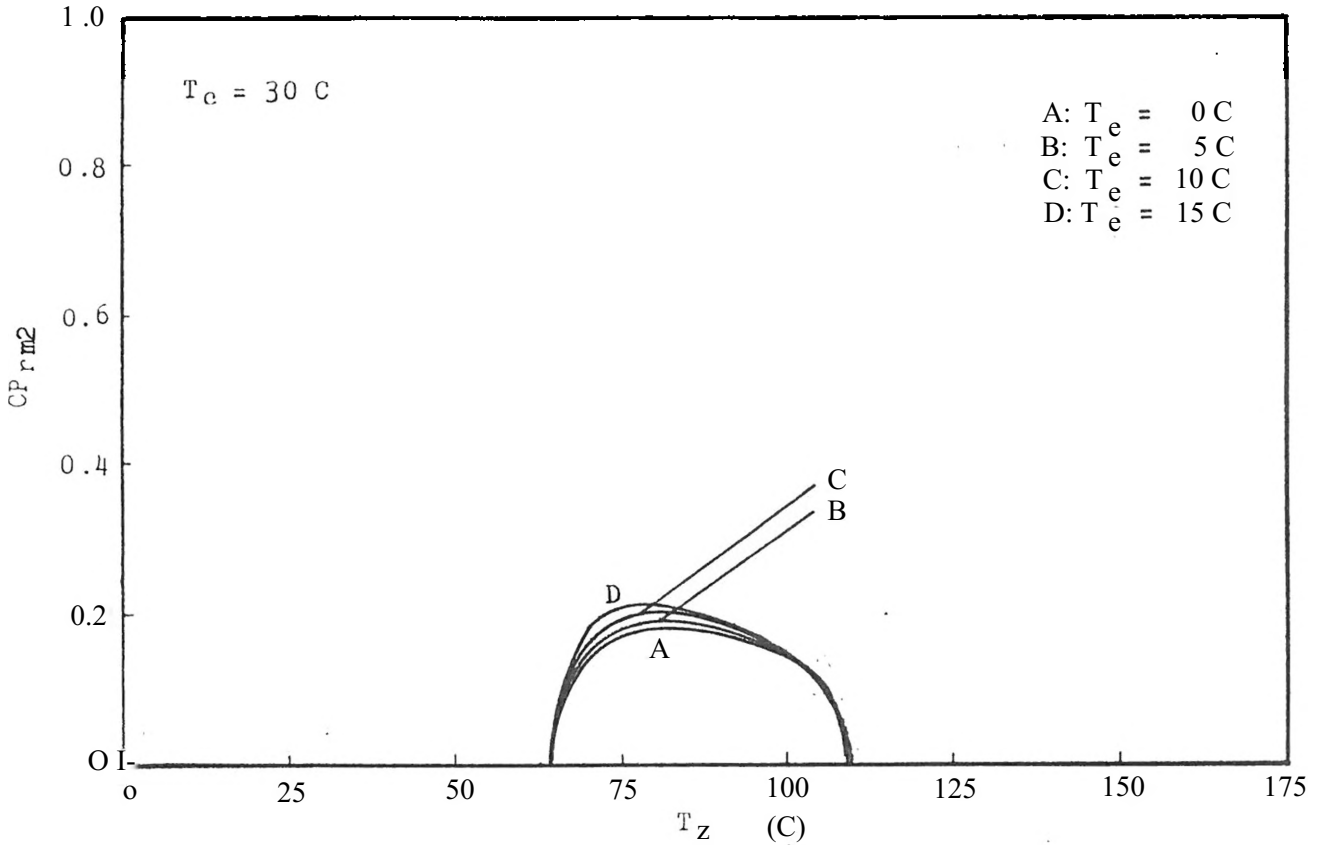

Fig. 25a Effect of evaporator temperature upon ZSC mean refrigeration system performance with a P-type solar collector.

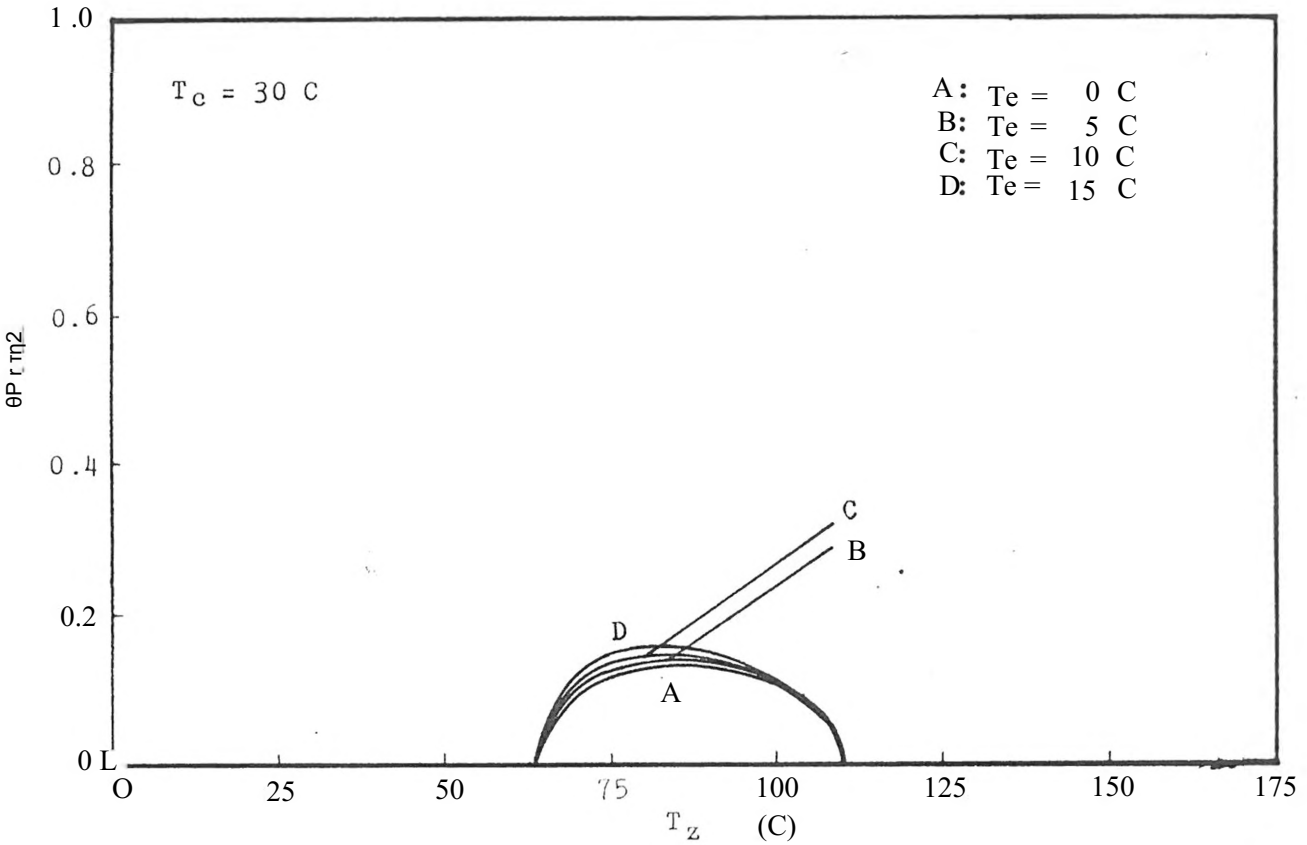

Fig. 25b Effect of evaporator temperature upon UCAA mean refrigeration sy stem performance with a P-type solar collector.

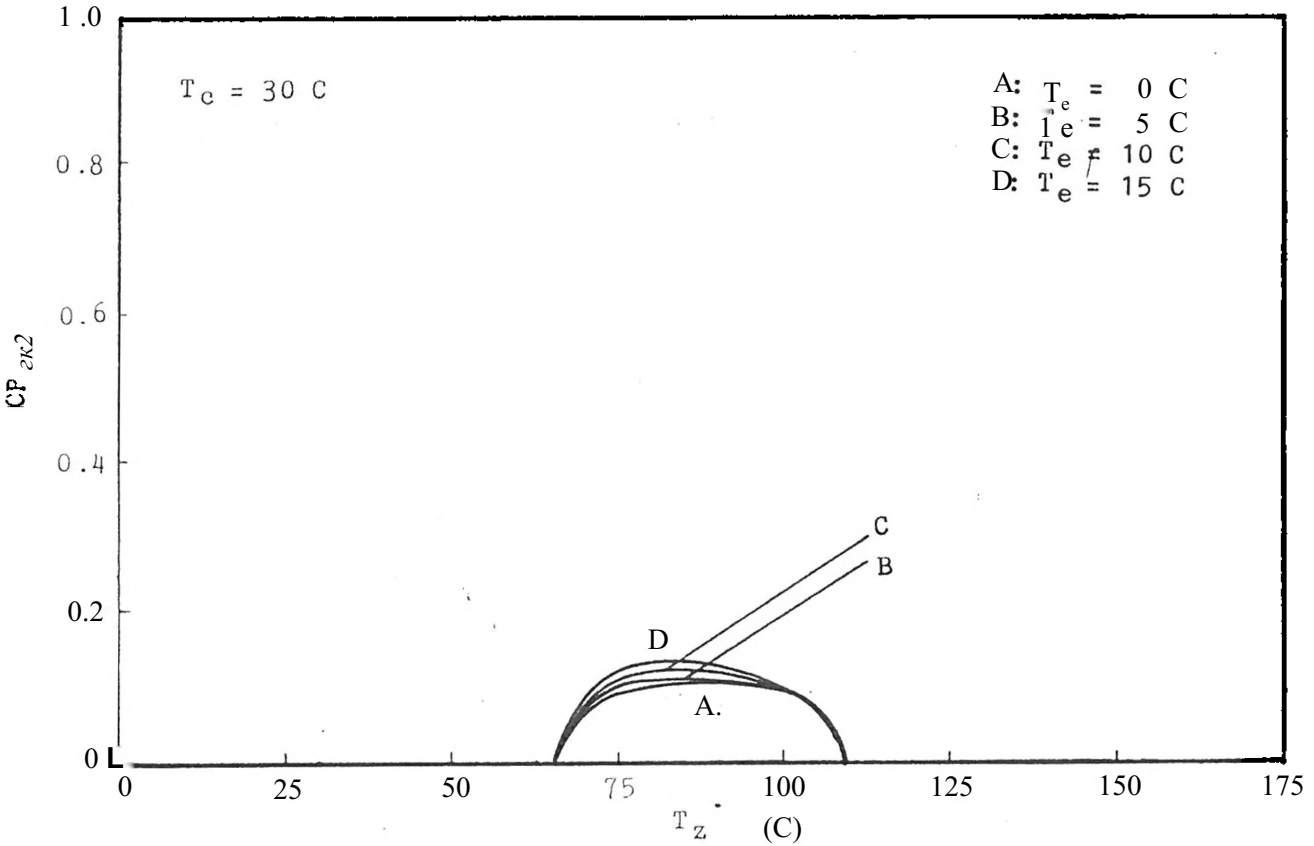

Fig. 25c Effect of evaporator temperature upon UCA mean refrigeration sy stem performance with a P-type solar collector.

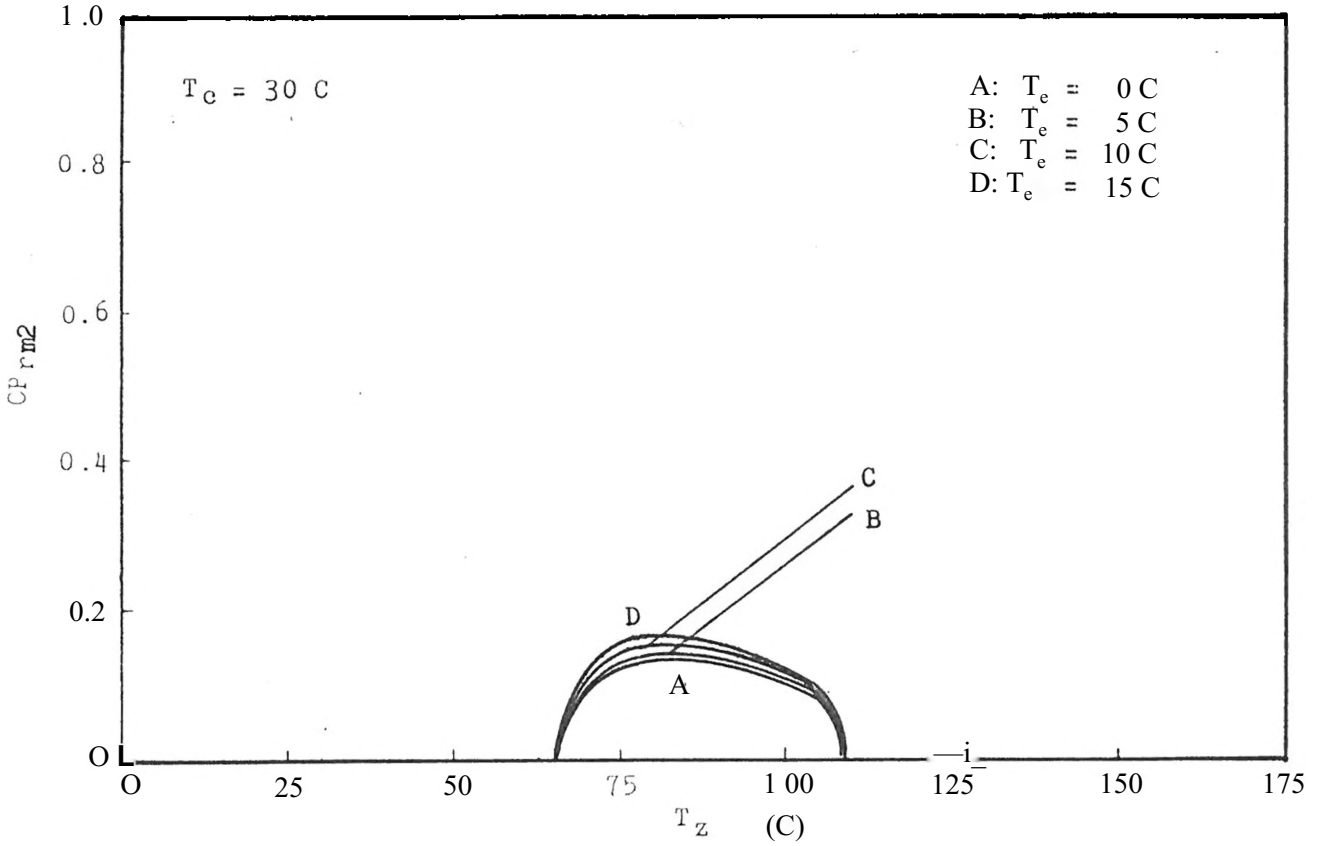

Fig. 25d Effect of evaporator temperature upon UC13 mean refrigeration system performance with a P-type solar collector.

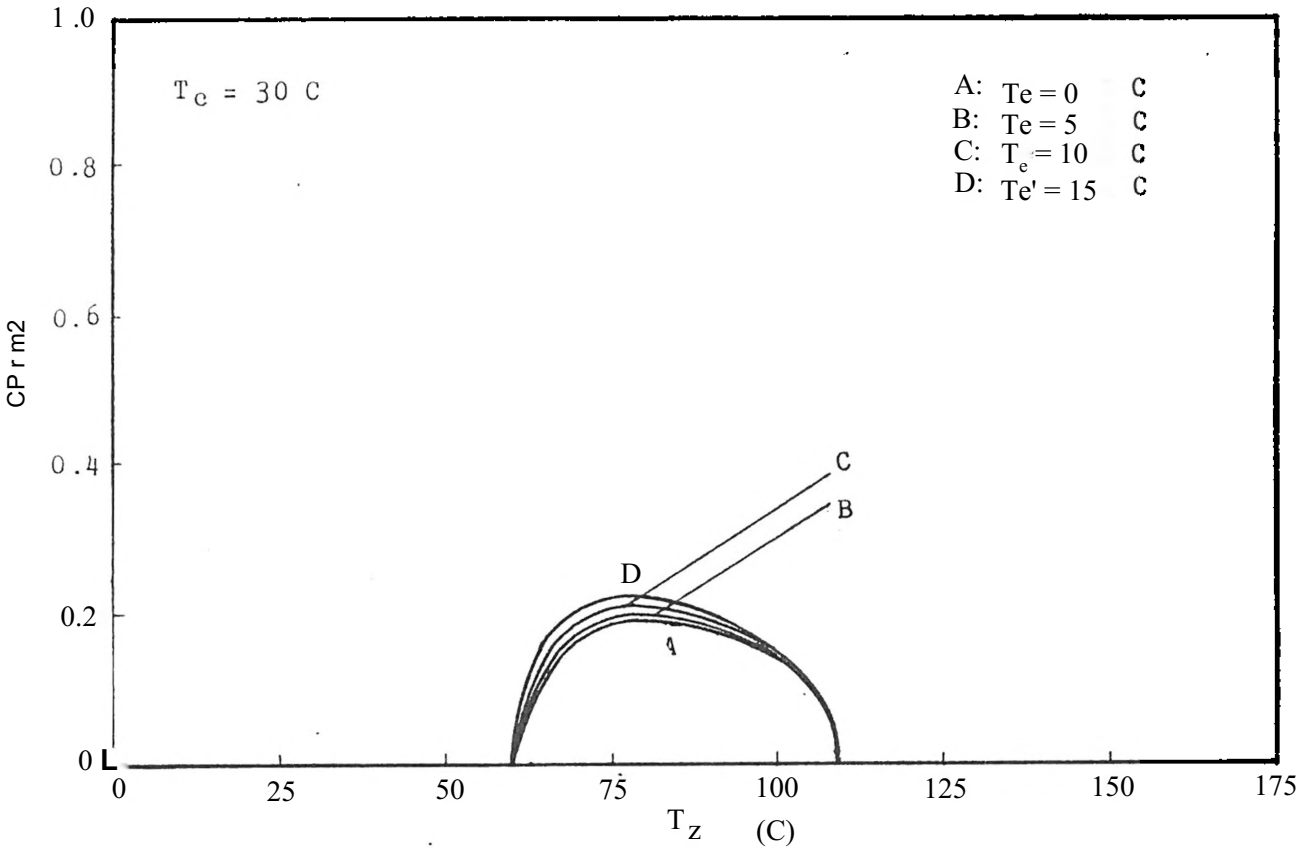

Fig. 250 Effect of evaporator temperature upon NaZ mean refrigeration system performance with a P-type solar collector.

m_z. To obtain an optimum absorbent slope for maximum refrigeration system performance, again the slope of the constant mass concentration lines on a log P_v versus $1/T_Z$ graph was assumed to be constant. By this assumption, an instantaneous refrigeration system performance can be acquired by varying the absorbent slope at a fixed absorption temperature (see Eq.(56)). Figure 26 demonstrates the variation of the . instantaneous refrigeration system performance with respect to different values of absorent slope at a fixed absorption temperature. Curves P, S, V and W correspond to the instantaneous refrigeration system performance for the P, S and V-type solar collectors and a waste heat source, respectively. Points a, b, c and d are the instantaneous refrigeration system performances for a natural zeolite and points a', b‘, c' and d’ are the system performances for a synthetic zeolite. As seen, the natural zeolite has a higher instantaneous refrigeration system performance than the synthetic zeolite. Moreover, the instantaneous refrigeration system performance decreases as the absorbent slope increases. Since Eq.(59) is the same as Eq. (43), the relationship between the optimum absorbent slope and the adsorption temperative is the same as in Fig. 19.

A maximum mean refrigeration system performance can be obtained with respect to absorbent slope. Figure 27 shows the dependence of the maximum mean refrigeration system performance on absorbent slope. Curves P, S, V and W are the maximum system performances for P, S and V-type solar collectors and a waste heat source, respectively. Points 1,2,3 and 4

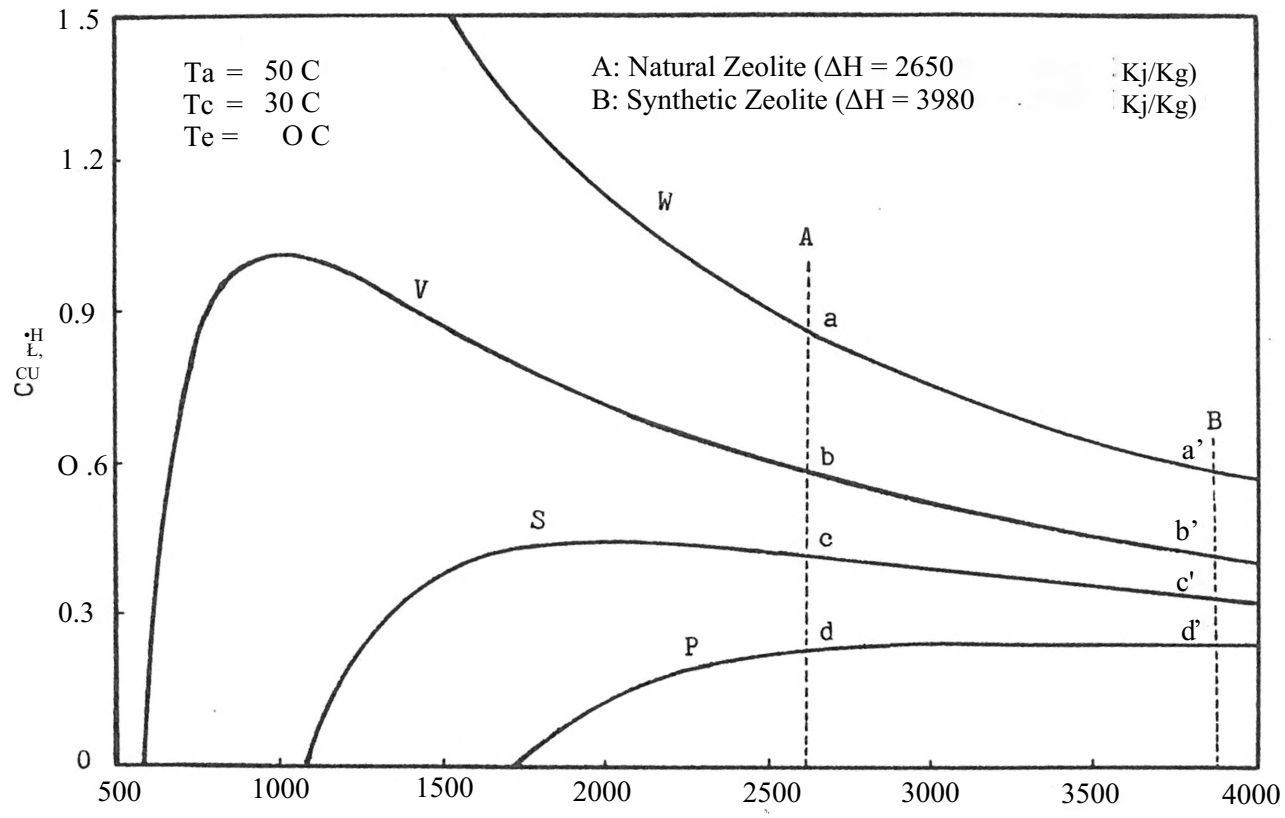

Fig. 26 Instantaneous refrigeration system performance versus absorbent solpe.

represent the maximum mean refrigeration system performances for natural zeolites, while the system performances for synthetic zeolites are presented by points 1', 2', 3' and 4'. As seen, the natural zeolite has a higher mean refirgeration system performance when using the V-type solar collector and the waste heat source. Moreover, the maximum refrigeration system performance is seen to decrease as the absorbent slope, mz, increases. This is in agreement with the experimental finding of Tchernev[l4] who found that natural zeolites perform superior to synthetic zeolites for a P-type solar collector.

An optimum mean refrigeration system performance with respect to absorbent slope can be found at the peak for each curve. The absorbent slope yielding the optimum refrigeration system performance, points w in Fig. 27, is defined as the ideal slope for refrigeration. Similarly, the optimum system performance for the S and V-type solar collector and the waste heat is shown by points s, v, w. Dashed curve P' , S' , V' and W' stand for the maximum mean refrigeration system performances which neglect the heat capacity losses.

4.12 Comparison Between the LiBr-Water and Z eoi ite-Water Refrigeration System

Figure 28a shows the comparison between the LiBr-water and the z eoi it e-wat er refrigeration systems for the P-type solar collector. Curve A is the LiBr-water refrigeration system performance; curves B, C,

D, E and F are the refrigeration system performances for zeolites ZSC, UC4A, UC5A, UC13 and NaZ, respectively. As mentioned earlier, the LiBr-water system has a narrev temperatore range for heat rejection due to the crystallization limitation. This causes heat rejection difficulties on hot simmer days. A water cooler is necessiated by a LiBr-water refrigeration system. In contrast, the zeoi ite-water refrigeration system has a wider temperature and a longer time period (a whole night) for heat rejection. The comparison between the LiBr-water and the zeolite-water refrigeration systems for the S and V-type solar collector types and the waste heat are shewn in Figs. 28b, 28c and 28d, respectiv ely.

The results for the investigation of the zeolite heat pump and refrigeration systems performances have been shown. Also, the system performances for zeolite-water and LiBr-water were compared. Several conclusions will be made in the next chapter for the use of the solar zeolite system.

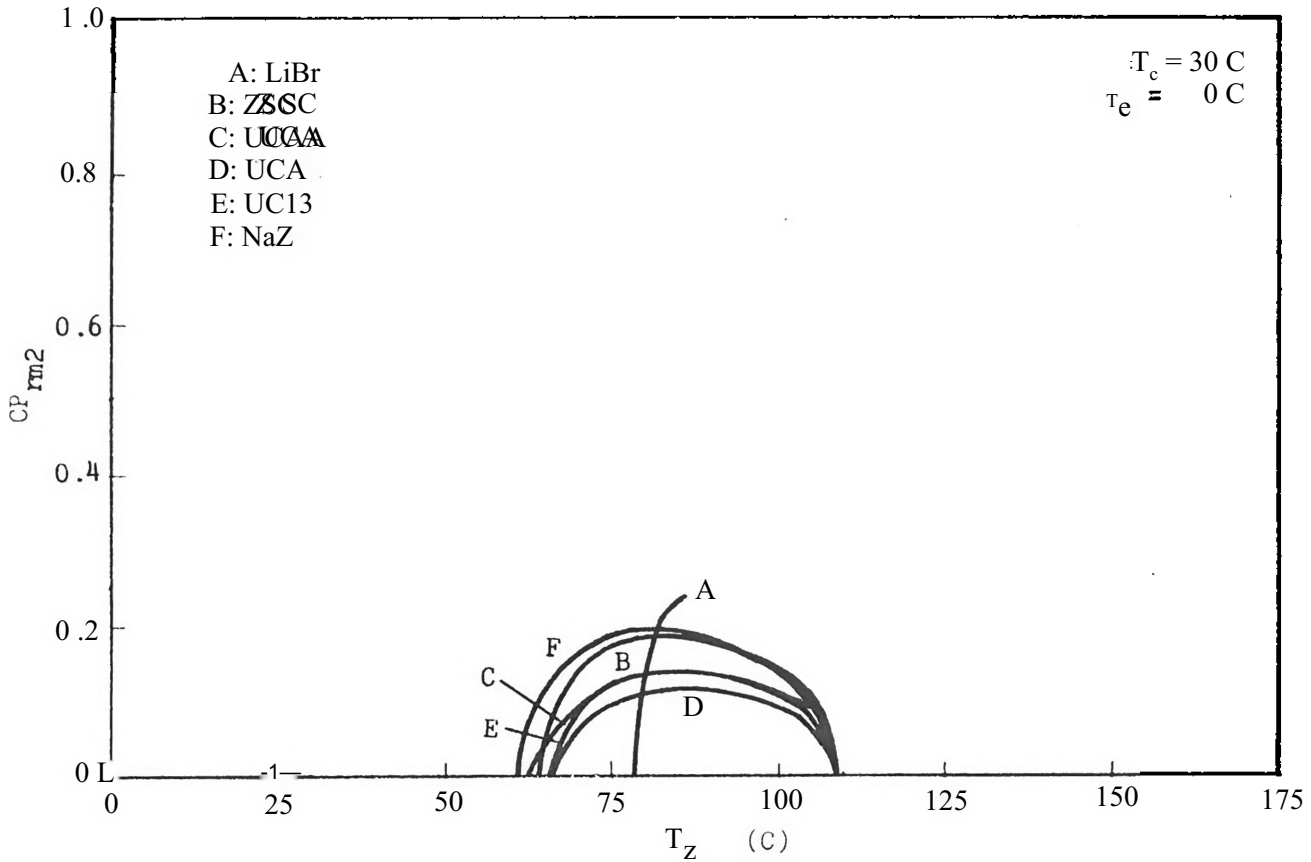

Fig. 28a Com parsion between the LiBr-water and z eoi ite-water refrigeration systems for a P-type solar collector.

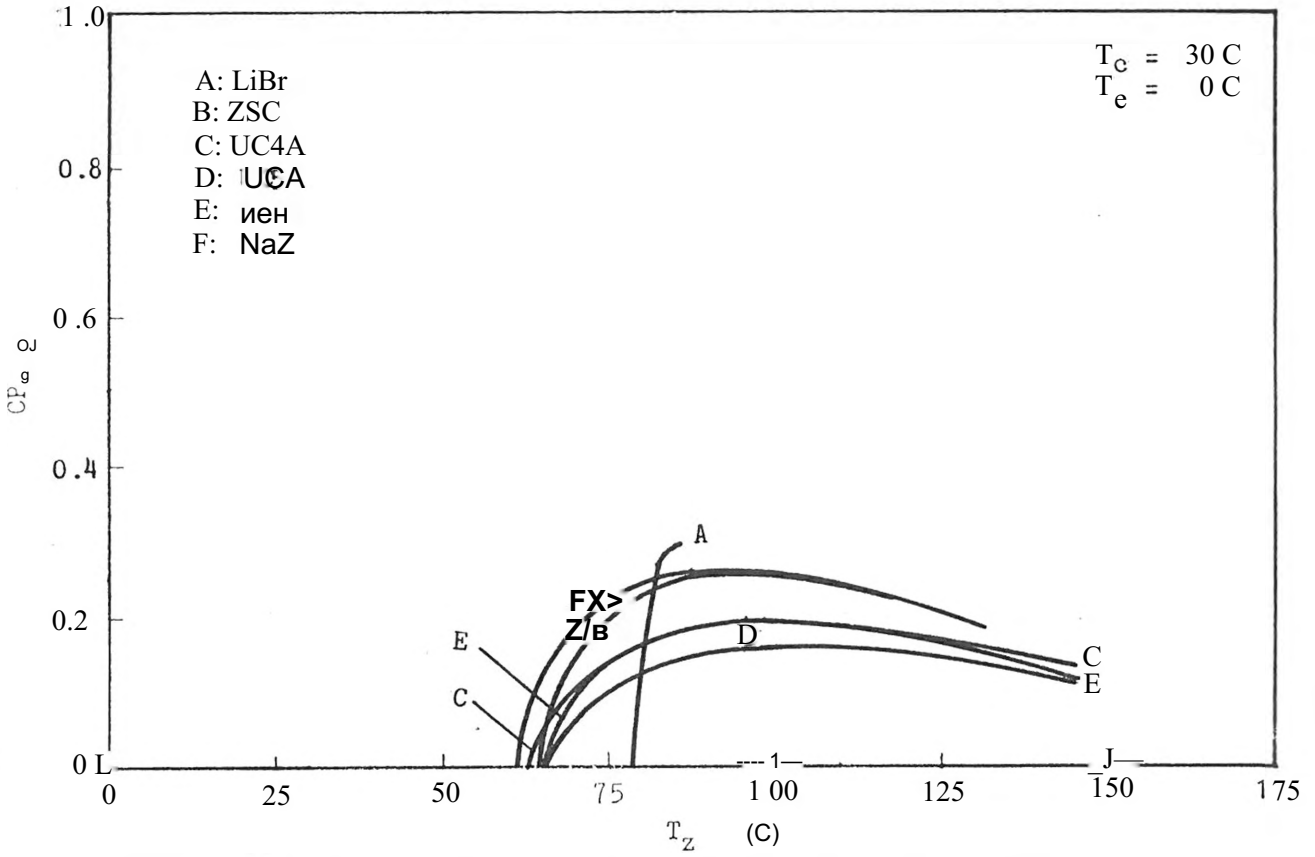

Fig. 28b Comparsion Between the LiBr-water. and zeolite-water refrigeration systems for a S-type solar collector.

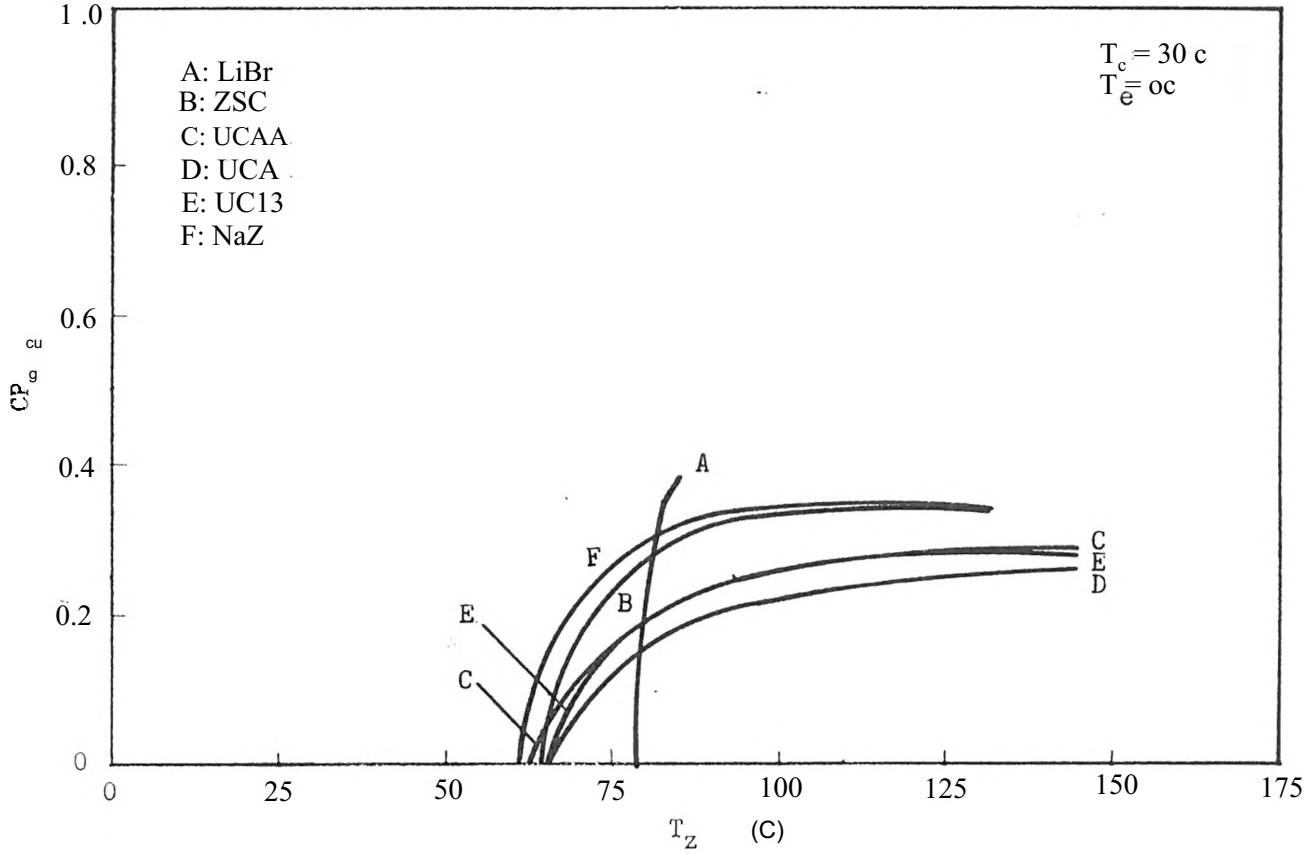

Fig. 28c Comparsion Between the LiBr-water and zeolite-water refrigeration systems for a V-type solar collector.

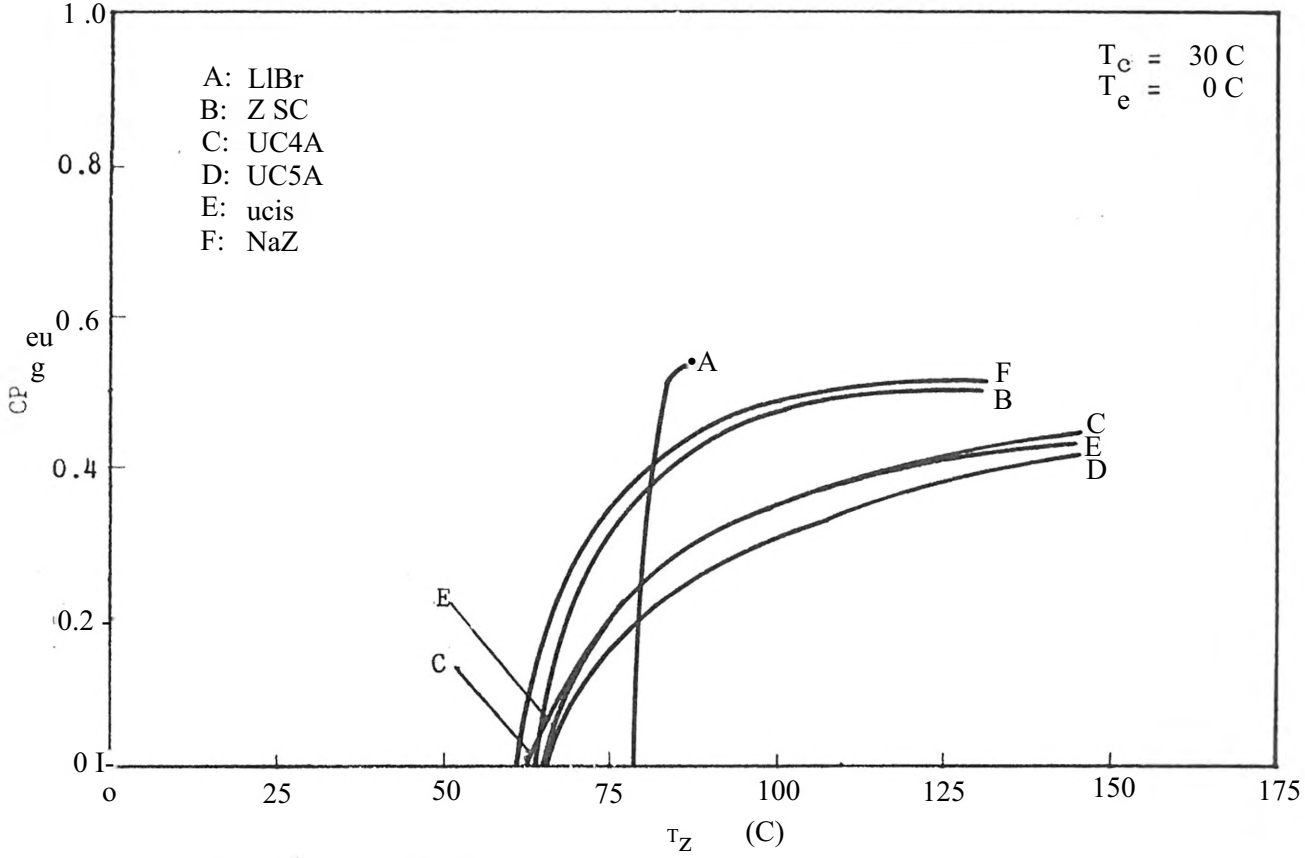

Fig. 28d Comparsion Between the LiBr-water and zeolite-water Refrigeration systems for a waste heat source.

CHAPTER V

CONCLUSIONS

Fran the results shewn in the previous chapter, several conclusions for the solar zeolite heat pump and refrigeration system can be summarized as follows:

1) The heat of absorption, ΔH, is only dependent on the slope of the constant mass concentration lines on the log P_v versus $1/T_Z$ graph. This means that points along a certain mass concentration line have the same value of heat of absorption. Also, This slope, m_z, can influence the desorption temperature. The higher the m_z value, the lower the desorption initiation temperature, and thus the higher the solar collector efficiency. Nevertheless, a high m_z value implies the high heat of absorption, ΔH« The high heat of absorption in turn reduces the system performance for both the heat pump and refrigeration systems.

2) The initiation desorption temperature of zeolite can be influenced by the zeolite pr operti es (m and C_z), and the condenser temperatur e. A low initiation desorption temperature

is preferred for the solar zeolite system since a high solar collector efficiency can be obtained.

3) The zeolite-water system has a slightly lower system performance than the LiBr-water system. However, the zeolite system has a wider heat-rejection temperature range. An inexpensive air cooling system can be used in the zeolite system. In contrast, the LiBr-water system requires water cooling equipment to control the LiBr temperature in summer to avoid crystallization problem.

4) The maximum mean heat pump system performance for a synthetic zeolite was found to be around θ'. 55-0.62 for the P-type solar collector; 0.65-0.78 for the S-type solar collector; 0.85-0.94 for V-type solar collector; and 1.20-1.30 for a waste heat source. The heat pump system performance for a natural zeolite was seen to be around 0.45-0.41 for the P-type sloar collector; 0.62-0.68 for the S-type solar collector; 0.82-0.90 for the V-type solar collector; and 1.30-1.38 for a waste heat source.

5) The maximum mean refrigeration system performance for a synthetic zeolite was around 0.20-0.24 for the P-type solar collector; 0.24-0.28 for the S-type solar collector; 0.28-0.34 for the V-type solar collector; and 0.42-0.48 for a waste heat source. The refrigeration system performance for a natural zeolite was

found to be around 0.18-0.23 for the P-type solar collector; 0.28-0.32 for the S-type solar collector; 0.36-0.40 for the V-type solar collector; and 0.55-0.60 for a waste heat source.

REFERENCES

1. Kreith, F. ,and Kreider, J. , Principles of Solar Engineering , Washington, McGraw-Hill, 197 8

2. "Patterns of Energy Consumption in the United States", Standford Research Institute Report, U. S. Gov't. Printing Off, Washington, January 1 972.

3. Prigmore, D. , and Barber, R. , "Cooling with the Sun's Heat" Solar Energy , 1 975, Vol. 17, pp. 185-1 92.

4. Epstein, M., Grolmes, M., Davidson, K. , and Kosar, D. , "Advanced Desiccant Dehumidif ication/Cooling Technology", ASME 5th Annual Technical Conference, 1983.

5. Johannsen, A. , "Design and Operation of a Liquid-Desiccant Type Solar Air Conditioning System", SUN II , 1979, Vol. 1, pp. 681-685.

6. Jurinak, J. J. , Mitchell, J. W. , and Beckman, W. A. , "Open Cycle Desiccant Air Conditioning as an Altermative to Vapor Can pression Cooling in Residential Applications", ASME 5th Annual Technical Conference, 1 983.

7. Alizadeh, S. , Bahar, F. , and Geoola, F. , "Design and Optimization of an Absorption Refrigeration System Operated by Solar Energy", Solar Energy , Vol. 22, 1979, PP 149-154.

8. Stoecker, W. F. , and Reed, L. D. , "Effect of Operating Temperatures on the Coefficient of Performance of Aqua-Ammonia Refrigerating Systems", ASHRAE Trans , Part 1, 1971, pp. 163-170

9. Bessler, W. F. , and Chen, C. N. , "Study on Parameter Variation for Solar Powered Lithium Bromide Absorption Cooling", Solar Cooling and Heating , 1 976, pp. 847

10. Huang, B. J. ,and Chang, T. Y. , "Design Analysis of Ammoni a-Water Absorption Refrigeration System", 1 97 8 Society of Autanative Engineering, Inc. Pro Intersic Energy Convers Eng. Conf. 13th, San Diego, Calif. Aug. , 1978, pp. 20-25

11. Wilur, J. , and Mitchell, E. , "Solar Absorption Air Conditioning Alternatives", Solar Energy , Vol. 17, 1975, pp. 193-199-

12. Peng, C. S. , and Howell, J. R. , "Analysis and Design of Hybrid

Doubl e-Absorpti on Cooling System for Low Grade Thermal Energy Application", Journal of Solar Energy Engineering , Vol. 103, Nov. 1981, p. 331

13. Vekatesh, A. , Sriramulu, V. , and Gupta, M. C. , "Theoretical and and Experimental Investigation of an Intermittent Solar Refrigerator", Sun II , Vol. 1, 1979, pp. 749-753.

14. Tchernev, D. , I. , "Solar Energy Application of Natural Zeolite" , Natural Zeolite and Its Use , Oxford, New York, Pergamon Press, 1978, pp. 479-484.

15. Meunier, F. , and Mischi er, B. , "Solar Cooling Through Cycles Using Microporous Solid Adsorbents", SUN II ,Vol. 1, 1 979, pp. 676-680.

16. Meunier, F. , Mischi er, B. , Guilleminot, J. J. , and M. H. Simonot, "On the Use of a Zeolite 13X-H20 Intermittent Cycle for the Application to Solar Climatization of Buildings", SUN II , Vol. 1, 1 979, pp. 739-743 .

17. Chang, S. C. , "Solar Zeolite Refrigeration System" , M.S. thesis University of Mississippi, Aug. 1984.

18. Shigeishi, R. A. , Langfors, C. H. , and Hollebone, B. R., "Solar Energy Storage Using Chemical Potential Changes Associated with Drying of Zeolite", Solar Energy , Vol. 23 , 1 979, pp. 489-495.

19. Shigeishi, R. A. , Langfors, C. H. , Hollebone, B. R. , and Gopal, R. , "The Rate of Solar Energy Storage and Retrieval in a Zeolite Water System", Solar Energy , Vol. 28, No. 5, 1 982, pp. 421-424.

20. Dubinin, M. M. , and Astakhov, V. A. , "Description of Adsorption Equilibriaot Vapors on Zeolites over Wide Ranges of Temperature and Pressure", Molecular Sieve Zeolite II , American Chemical Society, 1971.

21. Belton, G. and Ajami, F. , "Thermochemistry of Salt Hydrate", Report No. NSF/RANN/SE/GI 27976/TR/73/4 , University of Pennsylvania, Philadelphia, 1973

22. Union Carbide, " Molecular Sieves Water and Air Data Sheet", Adsorbent and catalyst , pp. F-43A-2, 4, 6